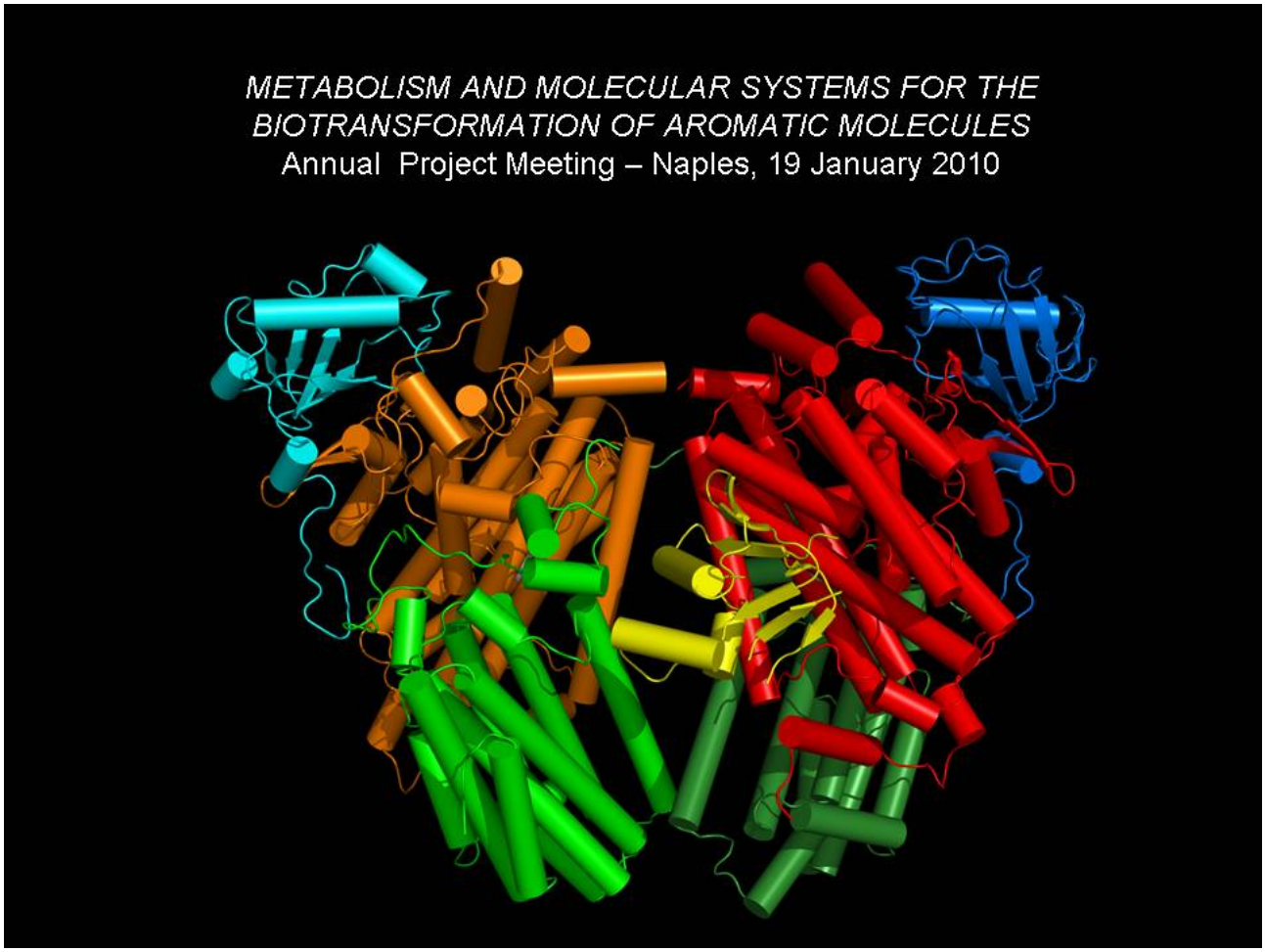

CONTENTS

Molecular characterization of genes involved in xenobiotic compounds degradation

Laura Bertini, Silvia Proietti, Carlo Caporale and Carla Caruso
Department of Agrobiology and Agrochemistry, University of Tuscia, Viterbo

Characterization of *P.* sp. OX1 *phe* operon was completed sequencing the last four genes (*phe*FGHI) of *meta* cleavage pathway coding for ADA, HOA, 4OD and 4OI enzymes. Homologous genes from *P.* sp. OX1 TOL pathway (*xyl*-likeQKIH) were also sequenced and sequence similarity studies were carried out. Recombinant ADA and HOA proteins from either *phe* or *xyl*-like operon were produced in order to reconstitute bifunctional aldolase/dehydrogenase enzyme. The regulation mechanism of *P.* sp. OX1 *phe* lower pathway was also investigated. 1.3 kb of the *phe* operon promoter (P_{phe}) were sequenced and subjected to functional studies. In order to identify new transcriptional regulator(s) involved in the control of the *phe* operon expression, Southwestern experiments were carried out. *P.* sp. OX1 crude protein extracts from cultures grown in the presence of phenol as the *phe* operon induction effector were analyzed using P_{phe} small fragments as a probe. Upon this growth condition, a new regulator, named XylR-like, was identified which belongs to the NtrC family of transcriptional activators. Xylr-like shows high sequence identity with TmbR from *P. putida* TMB (99%) and XylR from *P. putida* mt-2 (98%), whereas only 64% sequence identity with TouR from *P.* sp. OX1. Corresponding recombinant protein was produced and its specific interaction with UAS regions of P_{phe} was confirmed by Southwestern.

In bacteria, aerobic catabolic pathway for aromatic hydrocarbon degradation can schematically be divided into two major biochemical steps. Firstly, the *upper pathway* channels the hydrocarbons towards the formation of partially oxidized aromatic intermediates; then dihydroxylated aromatic molecules undergo ring cleavage and are further processed to give compounds that can enter the tricarboxylic acid (TCA) cycle (*lower pathway*). Bacteria belonging to the genus *Pseudomonas* are particularly versatile in their range of catabolic capabilities (1). The catabolic and regulatory genes , encoding the biodegradation of toluene and xylene and their oxidation products, have been extensively analyzed (2). The pWW0, isolated from *Pseudomonas putida* mt-2, was the first TOL plasmid to be identified (3) and a number of other TOL plasmids have been investigated in the last years although to a lesser extent (4, 5). *Pseudomonas sp.* OX1 is able to growth on toluene, *o*-xylene, 2,3 and 3,4 dimethylphenol and cresol as the sole carbon and energy source (6-9) due to the presence of two characteristic hydroxylating enzymes: the multienzymatic complexes of Toluene/*o*-xylene Monoxygenase (ToMO), coded by the *tou* operon, and Phenol Hydroxylase (PH), coded by a different catabolic operon induced by phenol (10-11). The final product of ToMO and PH activities (methyl substituted catechols) undergo a further degradation through the *meta*-pathway leading to intermediates of the TCA cycle.

Running title. *P.* sp. OX1 *phe* operon characterization and regulation

Keywords. *phe* operon, *tou* operon, *xyl*-like genes, aldolase/dehydrogenase bifunctional enzyme, transcriptional regulation

While both *upper* pathways that *P*. sp. OX1 use for the first steps of aromatic compound degradation are well characterised, less information are available for the *lower* pathway. The *P*. sp. OX1 gene cluster for PH displays a gene order similar to that of *Pseudomonas* sp. CF600 operon but the genetic organization of the *lower* pathway has not been elucidated so far.

The TOU pathway allows *P*. sp. OX1 to grow on *o*-xylene, but not on *meta* and *para* isomers. Nevertheless, it has been reported (12) the isolation of *P.* sp. OX1 mutants (M1) able to grow on the latter xylene isomers through the utilization of the TOL pathway that requires the progressive oxidation of a methyl group. In addition, revertants (R1) able to utilize all three xylene isomers for growth were isolated from M1 mutants (12). In such R1 mutants either the chromosomically encoded TOL or the *tou* pathways are expressed, whereas they are silenced by transposon-mediated genomic rearrangement in wild-type *P.* sp OX1 and M1 mutants, respectively.

In this work we report the full sequence of the last four genes of the *P*. sp. OX1 lower *meta*-pathway induced by phenol, that we called *phe* operon, and of the homologous genes from the TOL pathway. We also report the production of the recombinant bifunctional aldolase/dehydrogenase enzyme that catalyzes the final two steps of the *meta*-cleavage pathway for cathecol from both TOL and TOU pathways and the isolation of a new transcriptional regulator that could be involved in the regulation of the *phe* operon expression.

MATERIALS AND METHODS

Sequence of *P.* sp. OX1 *phe* and *xyl*-like lower *meta*-pathway genes. The cosmidic vector pFB3411 was used as template to complete the sequence of *P.* sp. OX1 *phe lower* pathway through primer walking procedure. The first primer was designed on the basis of the known 3' sequence of *phe*E gene (Di Donato, unpublished). New specific primers were designed from time to time on the basis of the newly determined sequence allowing to fully sequence *phe*FGHI genes. Corresponding *xyl*-likeQKIH genes were sequenced after cloning PCR amplified genes into pGEM®-T Easy vector (Promega). *xyl*-likeIH genes were amplified from genomic DNA using a forward primer (HOA2: 5'-ggccaggaagacatgatcg-3') mapping on the 3' region of *phe*G gene and a reverse primer (4OI1: 5'-tcagcgtctgaccttgctg-3') mapping on the 3' end of the homologous *xyl*H gene from *P. putida* mt-2. *xyl*-likeQK genes were PCR amplified using a forward primer (OEH1: 5'-ccggtcaaggccggtgattt-3') mapping on the 3' region of *phe*E gene and a reverse primer (g4ODrev: 5'-ggatgtcatgggcctgcag-3') mapping on the 5' region of *xyl*-likeI gene.

Expression of recombinant bifunctional enzyme. To produce ADA and HOA recombinant proteins, *phe*FG coding region was PCR amplified using BioTaq™ DNA polymerase (Bioline, London, UK) and the cosmidic vector pFB3411 as template. Gene sequence was engineered to introduce an *Nde* I site at the 5'-end and a *Bam*H I site at the 3'-end using the oligonucleotides NdeADAfor: 5'-ggaattc**catatg**aacaagaaactgaaagcg-3' and BamHOArev: 5'-cg**ggatcc**cgcggctgagggtacgg-3' as forward and reverse primer, respectively. Similarly, the same amplification strategy was used to amplify the coding region of *xyl*-likeQK genes from the genomic DNA of *P.* sp. OX1. The engineering was achieved using the oligonuleotides NdeADA: 5'-ggaattc**catatg**agcaagaaactgaaa-3' and BamHOA: 5'-cg**ggatcc**cgcggctgagggtacggt-3' as forward and reverse primer, respectively. In all primers the sequence of restriction sites is represented in bold. All primers have been synthesized by Eurofins MWG Operon. PCR was carried out on a Techne Thermal cycler model Progene (Princeton, NJ, USA) with the following program: initial denaturation at 95 °C for 2 min, amplification for 30 cycles of denaturation at 95 °C for 1 min, annealing at 65 °C (for *phe*FG) or 64 °C (for *xyl*-likeQK) for 1 min, extension at 72 °C for 30 sec. The amplified inserts were first subcloned in pGEM®-T Easy vector and inserted into *E. coli* strain DH5α, then fully sequenced to confirm the correct sequence. The engineered clones were then digested with *Nde* I and *Bam*H I, ligated into the same sites of the pET-22b(+) and inserted into *E. coli* strain BL21(DE3) for production of

recombinant proteins. Transformed cells were grown in LB medium containing 100 μg mL^{-1} ampicillin, at 37 °C to an absorbance of 0.6 at 600 nm. The protein expression was induced by the addition of 0.5 mM isopropyl β-D-1-thiogalactopyranoside (IPTG). Cells were harvested three hours after induction by centrifugation (8500 rpm, 4 °C, 15 min). Bacterial cell pellets containing recombinant ADA and HOA proteins were resuspended in 5 ml of 50 mM NaP, pH 7.5, containing 1 mM EDTA, 100 mM NaCl, 200 μg mL^{-1} lysozyme and a protease inhibitor cocktail. After incubation on ice for 30 min, the mixture was lyzed by sonication and treated with 100 μg of DNase at 37 °C for 60 min. The pellet, containing recombinant proteins, was recovered by centrifugation at 8500 rpm, 4 °C for 30 min and resuspended in 5 ml of 50 mM NaP, pH 7.5, containing 1 mM EDTA, 200 μg mL^{-1} lysozyme and 1 mg mL^{-1} sodium deoxycholate. The mixture was incubated on ice for 20 min and the pellet, recovered by centrifugation at 11400x*g*, 4 °C for 15 min, was resuspended in 5 ml of cold deionized water. After centrifugation at 15300x*g*, 4 °C for 30 min, the pellet was solubilized in 8 M urea. The suspension was centrifuged at 15300x*g* 4 °C for 10 min and the supernatant, containing denatured recombinant proteins was dialyzed three times against 500 ml of 100 mM MOPS, pH 7.5, containing 0.5 mM $MnCl_2$, 1 mM DTT and 10% (v/v) glycerol and then three times more against 500 ml of 50 mM NaP, pH 7.5 containing 10% (v/v) glycerol to allow proteins refolding. The dialysis was carried out at 4 °C, under stirring.

Sequence of *P.* sp. OX1 *phe* operon 5' upstream region and truncated version production. A *Bgl* II/*Bgl* II restriction fragment of pFB3411 spanning 6 kb from *orf*1 downstream P_{tou} promoter to *phe*N subunit of PH was subcloned into *Bam*H I site of pGEM®-7Zf vector and sequenced backwards starting from a specific primer designed on the known sequence of *phe*K subunit of PH. The sequence was extended for 1.3 kb upstream *phe*K subunit.

A 352 bp fragment of P_{phe} spanning positions -319/+32, was amplified by PCR introducing *Xho* I and *Bam*H I sites at the 5'- and at the 3'-end of the fragment, respectively, using the following forward and reverse primers: 5'-ccg**ctcgag**gcgatcacttctctttgc-3' (PheXho for) and 5'-cgc**ggatcc**ccctttatgtttgtgatcgg-3' (PheBam rev). The sequence of restriction sites is represented in bold. The amplified insert was digested with *Xho* I and *Bam*H I restriction enzymes and cloned into the same site of pGEM-7Zf(+) vector (Promega), then subjected to DNA sequencing of both strands to confirm the correct sequence. Two more fragments, one spanning the positions +32/-60 (Δ1 fragment) and the other spanning the positions -138/-226 (Δ3 fragment), were produced by PCR using the following primers: 5'-ctatatcccttcctctgg-3' (Phe Δ1 for), 5'-ccctttatgtttgtgatcgg-3' (Phe Δ1 rev), 5'-aatcggccgttgtcagtg-3' (Phe Δ3 for), 5'-cccggagcgttttttacc-3' (Phe Δ3 rev). Both forward primers were modified with a biotin molecule at the 5'-end with the aim to produce biotinilated fragments by PCR.

All primers have been synthesized by Eurofins MWG Operon. PCR was carried out on a Techne Thermal cycler model Progene with the following program: initial denaturation at 95 °C for 2 min, amplification for 30 cycles of denaturation at 95 °C for 1 min, annealing at 65 °C (for 352 bp fragment) or 52 °C (for Δ1 and Δ3 fragments) for 1 min, extension at 72 °C for 30 sec.

Total protein extract from *P.* sp. OX1 cultures. *P.* sp. OX1 was grown in M9-salts medium (13) containing 20 mM malate at 30 °C. When absorbance at 600 nm reached 0.2, phenol was added as inducer of *phe* operon expression to a final concentration of 4 mM. Induced culture was grown to an absorbance of 1.2 at 600 nm and then cells were harvested by centrifugation at 8000 rpm, 4 °C for 30 min. The pellet was resuspended in 50 mM Tris-HCl, pH 7.5 and the suspension was centrifuged at 8000 rpm, 4 °C for 10 min. Cells were resuspended in 50 mM Tris-HCl, pH 7.5 containing 2 mM EDTA, 150 mM NaCl, 200 μg mL^{-1} lysozyme and a protease inhibitor cocktail. The above buffer was added to the cell pellet in a ratio of 3 ml g^{-1} pellet. After incubation on ice for 30 min, the cells were disrupted by sonication and treated with 100 μg of DNase at 37 °C for 60 min. The supernatant was recovered by centrifugation at 8500 rpm, 4 °C for 30 min and protein concentration was determined according to the Bradford assay (14).

Southwestern analysis. Crude protein extracts from *P.* sp. OX1 cell culture induced by phenol were subjected to SDS-PAGE and transferred to nitrocellulose membrane by electroblotting. The proteins were renatured by

incubation of the membrane in 20 mM Tris-HCl, pH 7.5 containing 150 mM NaCl, 2.5 mM DTT, 2.5% (v/v) Nonidet P-40, 10% (v/v) glycerol and 3% (w/v) BSA, o.n. at 4 °C, under gentle shaking. The membrane was then washed twice with the binding buffer containing 10 mM Tris-HCl, pH 8.0, 50 mM NaCl, 1 mM DTT, 5% (v/v) glycerol and 0.125% (w/v) BSA. The hybridization with biotinylated Δ1 or Δ3 fragments was carried out adding 500 ng of each fragments into the binding buffer and it was extended for 6 hours, at 4 °C, under gentle shaking. The membrane was then washed twice with binding buffer and once with PBS 1x. The detection of the interaction was carried out using streptavidin horseradish peroxidase-conjugated immunoglobulin and positive bands were visualized using 4-chloro-1-naphthol (Sigma-Aldrich) as a chromogen.

The same protocol was used when purified recombinant transcriptional regulator XylR-like was analyzed with the same procedure.

Expression of recombinant transcriptional regulator XylR-like. *E. coli* strain BL21(DE3) transformed with pET-XylR-like was grown in LB medium containing ampicillin (100 μg mL^{-1}) at 37 °C to an absorbance of 0.5–0.6 at 600 nm. The protein expression was induced by the addition of 1 mM IPTG. Cells were harvested three hours after induction by centrifugation (9000 rpm, 4 °C, 10 min). Bacterial cell pellet containing recombinant protein was resuspended in 50 mM Tris–HCl, pH 8.0, containing 1 mM EDTA, 100 μg mL^{-1} lysozyme and a protease inhibitor cocktail. After incubation on ice for 15 min, the mixture was lyzed by sonication and treated with 100 mg of DNase at 37 °C for 60 min, afterwards the inclusion bodies were collected by centrifugation at 9 000 rpm, 4 °C for 30 min. The pellet, containing the inclusion bodies, was washed twice with 10 ml of 100 mM Tris, pH 8.0, 5 mM EDTA, 2 M urea, 3% Triton X-100 and twice with 10 ml of 100 mM Tris, pH 8.0, 5 mM EDTA to remove both urea and Triton X-100. The washed inclusion bodies were resuspended in 3 ml of 100 mM Tris–HCl, pH 8.0, containing 5 mM EDTA, 6 M guanidine and 30 mM dithiothreitol and fully reduced under nitrogen atmosphere at 37 °C for 1 h. After centrifugation at 9 000 rpm, 4 °C for 10 min, the supernatant was diluted into the refolding buffer (100 mM Tris–HCl, pH 8.0, containing 2 mM oxidised glutathione (GSSG), 3 mM reduced glutathione (GSH), 0.5M L-arginine and 5 mM EDTA), to a final protein concentration of 30 μg mL^{-1}, allowing the renaturation of recombinant XylR-like for two days at 15 °C. After renaturation, the samples were concentrated by ultrafiltration and protein concentration was determined according to the Bradford assay (14).

Results

Sequence of *Pseudomonas* sp. OX1 *phe*/*xyl*-like lower *meta*-pathway genes. The cosmidic vector pFB3411 that carries the complete *phe upper* and *lower* pathway (7) was used as a source of DNA for the complete elucidation of *Pseudomonas* sp. OX1 *phe lower* pathway. The pFB3411 vector contains a 22.4 kb *Eco*R I/*Eco*R I partial DNA fragment from *Pseudomonas* sp. OX1 cloned in pLAFR1, able to express all activities characteristic of a *lower meta*-pathway when transferred by conjugation into *P. putida* PaW340.

On the basis of the known 3'sequence of 2-oxopent-4-dienoate hydratase (OEH) coding gene (*phe*E) (Di Donato, unpublished), a specific primer was designed that allowed the elucidation of part of the following *phe*F gene coding for the aldehyde dehydrogenase acylating (ADA). On the basis of the newly determined sequence several specific primers were designed that allowed the complete elucidation of the *phe*FGHI genes, coding respectively for ADA, HOA (4-hydroxy-2-oxovalerate aldolase), 4OD (4-oxalocrotonate decarboxylase) and 4OI (4-oxalocrotonate isomerase), by primer walking. Since the overall gene organization of the *P.* sp. OX1 *phe lower* pathway was found to be similar with that of the phenol-induced *P.* sp. CF 600 *dmp* operon, we adopted the same gene nomenclature.

In order to compare homologous genes between TOU and TOL pathways, we also sequenced ADA, HOA, 4OD and 4OI coding genes from TOL pathway, which were named *xyl*-like genes (*xyl*-likeQ, *xyl*-likeK, *xyl*-likeI and *xyl*-likeH, respectively) due to the homology with pWW0 *xyl* genes from *Pseudomonas putida* mt-2. Specific

amplification of *xyl*-likeI and *xyl*-likeH genes was carried out designing a reverse primer mapping on the 3' end of the pWW0 *xyl*H gene since multiple alignment of known 4OI coding sequences from various bacterial strains showed that this region is the less conserved between homologous genes. As forward primer, an oligonucleotide mapping on the 3' region of *phe*G gene was used. For selective amplification of *xyl*-likeQ and *xyl*-likeK genes, a reverse primer mapping on the 5' region of *xyl*-likeI gene was designed and combined with a forward primer mapping on the 3' region of *phe*E gene. The amplicons were cloned into pGEM®-T Easy vector and fully sequenced. It is worthwhile to highlight that the amplification reactions produced amplicons only using genomic DNA as template; in fact, no amplification products were detected using pFB4311 vector as template. These results indicated that the primers pair used allow the specific amplification of *xyl*-like genes only.

Sequence similarity studies. Between all *P.* sp.OX1 lower *meta*-pathway genes, we focused our attention on *phe*F and *phe*G as well as on their homologues *xyl*-likeQ and *xyl*-likeK which constitute a bifunctional aldolase/dehydrogenase enzyme that catalyzes the final two steps of the *meta*-cleavage pathway. The *phe*F and *xyl*-likeQ genes consist both of 924 bp and their first codon is located 14 bp downstream of the stop codon of OEH coding gene; they codify for a putative protein of 307 amino acids with a calculated molecular mass of 32969.04 Da and a estimated pI of 5.17(*phe*F) and 32927 Da with a pI of 5.25 (*xyl*-likeQ), respectively. The *phe*G and *xyl*-likeK genes consist both of 1041 bp and their first codon is located 12 bp downstream of the stop codon of ADA coding gene; they codify for a putative protein of 346 amino acids with a calculated molecular mass of 37123.75 Da and a estimated pI of 5.54 (*phe*G) and 37118.72 Da with a pI of 5.54 (*xyl*-likeK), respectively.

On the basis of ADA, HOA, 4OD and 4OI nucleotide sequence of both *xyl*-like and *phe* clusters, sequence similarity studies were carried out. Sequences were aligned using ClustalW (15) and compared by determining their percentage of similarity. *phe* and *xyl*-like genes and corresponding proteins are highly similar to each other, sharing 99% identity; very high identity (96-99%) was also found with homologous proteins and genes from *P.* sp. S-47 and *P. stutzeri* AN10 whereas sequence identity fell down to 62-67% at nucletide level and 52-58% at amino acidic level when other strains were considered (Fig.1)

ad	CF600	mt-2	HS1	S-47	OX1 *phe*	OX1 *xyl*-like
AN10	66	64	66	99	97	98
OX1 *xyl*-like	67	64	66	97	99	
OX1 *phe*	66	64	66	97		
S-47	66	64	66			
HS1	86	91				
mt-2	85					

ADA	CF600	mt-2	HS1	S-47	OX1 *phe*	OX1 *xyl*-like
AN10	58	58	58	99	99	99
OX1 *xyl*-like	58	58	58	98	99	
OX1 *phe*	58	58	58	99		
S-47	58	58	58			
HS1	89	95				
mt-2	89					

ho	CF600	mt-2	HS1	S-47	OX1 *phe*	OX1 *xyl*-like
AN10	65	62	63	96	98	98
OX1 *xyl*-like	65	62	63	96	99	
OX1 *phe*	64	62	63	96		
S-47	64	63	63			
HS1	80	92				
mt-2	81					

HOA	CF600	mt-2	HS1	S-47	OX1 *phe*	OX1 *xyl*-like
AN10	53	55	52	99	99	99
OX1 *xyl*-like	53	55	52	99	99	
OX1 *phe*	53	55	52	99		
S-47	53	55	52			
HS1	83	92				
mt-2	87					

Fig. 1 Sequence similarity percentage between *ada* (panel A) and *hoa* (panel B) nucleotide (left) and protein (right) sequences from different *Pseudomonas* strain: *P.* sp. CF600 (Acc. n. X60835), *P. putida* mt-2 (Acc. n. M94186), *P. putida* HS1 (Acc. n. AF134348), *P.* sp. S-47 (Acc. n. AF320981), *P. stutzeri* AN10 (Acc. n. AF039534).

Expression of recombinant bifunctional enzyme. The coding region of *phe*FG genes was amplified from the cosmidic vector pFB3411 using specific oligonucleotide primers that introduced a *Nde* I restriction site at the 5'-end and a *Bam*H I site at the 3'-end of the sequence. Similarly, the same amplification strategy was used to amplify the

coding region of *xyl*-likeQK genes from the genomic DNA of *P.* sp. OX1. The engineered clones were ligated into *Nde* I and *Bam*H I sites of the pET-22b(+) expression vector and inserted into *E. coli* strain BL21(DE3) to produce recombinant proteins. The vectors containing the coding sequences corresponding to *phe*ADA and *phe*HOA and to *xyl*-likeADA and *xyl*-likeHOA were respectively named pET-*phe*ADA/HOA and pET-*xyl*-likeADA/HOA. The overexpression of recombinant proteins in transformed cells was analyzed by SDS–PAGE and the presence of two proteic bands of 33 and 37 kDa, in fair agreement with the predicted molecular mass from the deduced amino acid sequence of ADA (32969) and HOA (37124), respectively, were detected. The results shown in Fig.2 are relative to the expression of *xyl*-like ADA and HOA but identical results have been obtained for the overexpression of *phe* ADA and HOA (data not shown). The recombinant proteins were localized into the insoluble fraction obtained after sonication of cell pellets (Fig. 2, lane 2). Resuspension of the inclusion body fraction with 6 M urea allowed to solubilize most of the expressed proteins (Fig. 2, lane 3) which were then renatured by three dialysis steps against MOPS 100 mM (Fig. 2, lane 4).

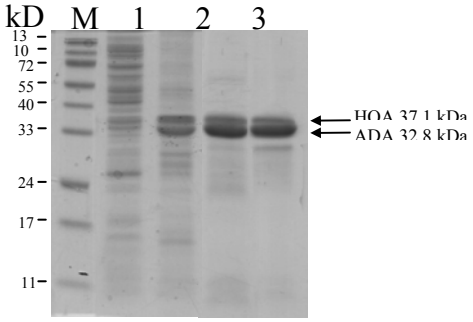

Fig. 2 SDS–PAGE analysis of total proteins from recombinant *E. coli* cultures containing pET-*xyl*-likeADA/HOA. Molecular weight markers (M); soluble (1) and insoluble (2) fraction after sonication; resuspended inclusion bodies (3); purified proteins after rinaturation (4).

Molecular characterization of 5' upstream region of *P.* sp. OX1 *phe* operon. To shed some light on regulation of *P.* sp. OX1 *phe* lower pathway, the promoter region of *phe* operon (P_{phe}) was characterized. On the basis of the known sequence of *phe*K subunit of PH multicomponent enzyme (10), a specific reverse primer was designed to extend the sequence backwards towards *phe* promoter region. The sequence was extended for 1.3 kb upstream *phe*K subunit. Characteristic σ^{54}-RNAP GG and GC binding motifs, centred at positions -12/-24, respectively, as well as the upstream activator sequences (UAS) located 100 to 200 bp upstream the -12/-24 region were identified. Two promoter deletions, one spanning the -12/-24 region (positions +32/-60, Δ1 fragment) and the other spanning the UAS (positions -138/-226, Δ3 fragment), were produced by PCR using a biotinylated forward primer. With the aim to identify new transcriptional regulators recognising the P_{phe} promoter, the biotinylated fragments were used as a probe in Southwestern experiments performed on crude protein extracts of *P.* sp. OX1 grown in the presence of phenol as the *phe* operon induction effector. A 72 kDa reaction band was detected using streptavidin-HRP antibody on both nitrocellulose membranes hybridized either with Δ1 or Δ3 fragment (Fig. 3).

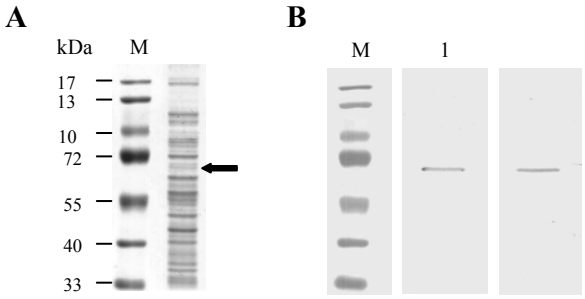

Fig. 3 Panel A: SDS-PAGE analysis of crude protein extracts of *P.* sp. OX1 grown in the presence of phenol (1). Panel B: Southwestern carried out on the same sample hybridized with biotinylated D1 (1) and D3 fragment (2). M: molecular weight markers. The protein band on SDS-PAGE detected with Southwestern is indicated by the arrow.

The protein band was analysed by LCMSMS after *in situ* tryptic digestion and the MASCOT search led to the identification of a regulator highly similar to TmbR (99%) from *P. putida* TMB (16) and to XylR (98%) from *P. putida* mt-2.

It belongs to NtrC family of transcriptional activators and shows only 64% sequence identity with TouR from *P.* sp. OX1. The gene coding this new transcriptional regulator was isolated from *P.* sp. OX1 genome using specific primers mapping on 5'- and 3'-ends of TmbR sequence. According to the high sequence similarity with XylR, the new transcriptional regulator was named XylR-like. The *xyl*R-like coding gene was subcloned into the pET-22b(+) expression vector (pET-XylR-like) and recombinant protein was produced.

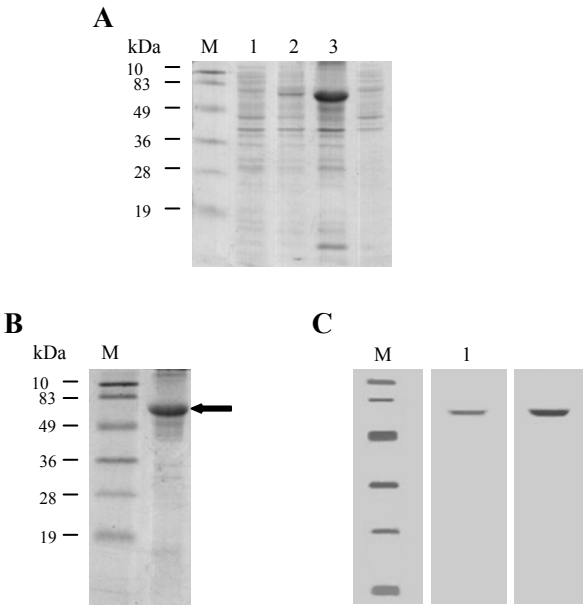

Fig. 4 Panel A: SDS-PAGE analysis of total proteins from recombinant *E. coli* cultures containing pET-XylR-like. Cell lysates from noninduced (1) and induced (2) *E. coli* cultures; insoluble (3) and soluble (4) fraction after sonication. Panel B: SDS-PAGE analysis of purified XylR-like after rinaturation (lane1). Panel C: Southwestern carried out on the same sample of panel B hybridized with biotinylated D1 (1) and D3 fragment (2). M: molecular weight markers. The protein band on SDS-PAGE detected with Southwestern is indicated by the arrow.

To confirm the ability of XylR-like to recognize the P_{phe} UAS regions, Southwestern analysis was carried out on recombinant regulator using Δ1 or Δ3 fragments as a probe. As shown in Fig. 4, specific reaction bands were detected using streptavidin-HRP antibody on both nitrocellulose membranes indicating that the recombinant protein is active.

Discussion

One of the central metabolic routes for the bacterial degradation of aromatic compounds is the *meta*-cleavage pathway for the catabolism of catechol and methyl-substituted catechols. This pathway operates in a number of different organisms, but the best studied examples are those found in pseudomonads. *P.* sp. OX1 can grow on *o*-xylene, 2,3- and 3,4-dimethylphenol, toluene and cresols degrading these compounds through a catabolic route that involves oxygenation reactions of the aromatic ring to form mono- and dimethylcatechols which are subsequently catabolized by a *meta*-cleavage pathway (6). The genes coding for the toluene and *o*-xylene catabolism are organized into two upper operons, one coding for ToMO (*tou* operon) and the other for Phenol Hydroxylase (PH) (*phe* operon). The *phe* operon is organized as the *P.* sp. CF600 *dmp* operon and contains the PH multicomponent genes followed by C2,3O and the *lower meta*-pathway genes. *P.* sp. OX1 is not able to utilize *m*- and *p*-xylene are for growth by, but they are cometabolized through *tou* pathway to intermediates unproductive for growth (7, 17). Nevertheless, *P.* sp. OX1 spontaneous mutant able to grow on *m*- and *p*-xylene through the TOL pathway was isolated (18). It is worthwhile to mention that the mutant was no longer able to grow on the xylene *ortho* isomer. In addition, a revertant was also isolated with the ability to grow on all three isomers (18).

In this work we focused our attention on the *lower meta*-pathway genes of both *tou/phe* and TOL pathways. In particular the last four

genes of both pathways, coding for ADA, HOA, 4OD and 4OI enzymes and named respectively *phe*FGHI and *xyl*-likeQKIH, were sequenced and sequence similarity studies were carried out. This group of genes is found in the same order in a number of pathways which involve extradiol cleavage of the aromatic ring, i.e. TOL pathway, *dmp* operon and *nah* operon (involved in naphthalene catabolism). This similar genetic organization suggests that the *meta*-pathway sequences share a common evolutionary origin and that the operons in which they reside have been formed in a modular manner by recombination between common sequences and the unrelated upstream gene(s). Nucleotide and deduced amino acid sequences of ADA and HOA coding genes of TOL plasmid pWW0 from *P*. putida mt-2, TOL plasmid pDK1 from *P*. putida HS-1, pVI150 plasmid (*dmp* operon) from *P*. sp. CF600, *nah* operon from *P*. *stutzeri* AN10, *xyl* operon from *P*. sp. S-47 were compared with the corresponding sequences of *phe* and *xyl*-like operons from *P.* sp. OX1. According with the hypothesis that all *xyl meta*-pathway operons, for example, could be derived from a common ancestor through a modular assembly, then it would be expected that the genes and proteins found in all *xyl* pathways would be more closely related to each other than to those in any other pathway. Surprisingly, *phe*FG and *xyl*-likeQK which share 99% identity, are more closely related to *nah*OM from *P*. *stutzeri* AN10 operon than to other *xyl*QK genes of TOL plasmid pWW0 and pDK1. Nevertheless, high sequence homology was found with corresponding *xyl*QK genes of *xyl* operon from *P*. sp. S-47. This result can be explained considering that *P*. sp. S-47 exhibits high nucleotide sequence homology with *P. putida* mt-2, except for the *xyl*JQK genes, which are more similar to the corresponding three genes from *P. stutzeri* AN10 (19).

The *P*. sp. OX1 gene cluster for phenol catabolism displays a gene order similar to that of *Pseudomonas* sp. CF600 *dmp* operon and its expression is under the control of a σ^{54}-dependent promoter. There are some evidence that the *tou* operon activator TouR is able to drive the expression of the *phe* operon (9), but whether TouR is the master regulator of the latter operon is still an open question. In this paper we report the isolation of a new regulator, xylR-like, expressed in *P*. sp. OX1 upon induction by phenol. We proved evidence that recombinant XylR-like binds tightly UAS regions of *phe* promoter. In the experimental condition used, TouR regulator, whose powerful effector is *o*-crosol, was not identified. Even if the similarity among the UAS of different σ^{54}-dependent promoters often allows cross-activation among heterologous regulatory circuits, it is worthwhile to highlight that XylR-like was identified under growth condition which induced preferentially *phe* operon instead of *tou* operon expression. Further experiments are still in progress in order to functionally characterize XylR-like and to address the question whether it plays a role in the expression regulation of *P*. sp. OX1 *phe* operon.

ACKNOWLEDGMENTS

This work was supported by grants from the Ministry of University and Research (PRIN/2007).

REFERENCES

1. **Williams, P. A., and J. R. Sayers**. 1994. The evolution of pathways for aromatic hydrocarbon oxidation in Pseudomonas. Biodegradation. **5:195-217**.
2. **Assinder, S. J., and P. A. Williams**. 1990. The TOL plasmids: determinants of the catabolism of toluene and xylenes. Adv. Microb. Physiol. **31: 1-69**.
3. **Williams, P. A., and K. Murray**. 1974. Metabolism of benzoate and the methylbenzoates by Pseudomonas arvilla mt-2: evidence for the exsistence of a TOL plasmid. J. Bacteriol. **120: 416-423**.
4. **Osborne, D. J., R. W. Pickup, and P. A. Williams**. 1988. The presence of two

complete homologous *meta* pathway operons on TOL plasmid pWW53. J. Bacteriol. **134: 2965-2975**.

5. **Keil, H., and P. A. Williams**. 1985. A new class of TOL plasmid deletion mutants in P. putida MT15 and their reversion by tandem gene amplification. J. Gen. Microbiol. **131: 1023-1033**.
6. **Baggi, G., P. Barbieri, E. Galli, and S. Tollari**. 1987. Isolation of a *Pseudomonas stutzeri* strain that degrades o-xylene. Appl. Environ. Microbiol. **53: 2129-2131**.
7. **Bertoni, G., E. Bolognese, F. Galli, and P. Barbieri**. 1996. Cloning of the genes for and characterization of the early stages of toluene catabolism in *Pseudomonas stutzeri* OX1. Appl. Environ. Microbiol. **62: 3704-3711**.
8. **Bertoni, G., M. Martino, E. Galli, and P. Barbieri**. 1998. Analysis of the gene cluster encoding toluene/o-xylene monooxygenase from *Pseudomonas stutzeri* OX1. Appl. Environ. Microbiol. **64: 3626-3632**.
9. **Arenghi, F. L., D. Berlanda, E. Galli, G. Sello, and P. Barbieri**. 2001. Organization and regulation of *meta* cleavage pathway gene for toluene and o-xylene derivative degradation in *Pseudomonas stutzeri* OX1. Appl. Environ. Microbiol. **67(7): 3304-3308**.
10. **Cafaro, V., V. Izzo, R. Scognamiglio, E. Notomista, P. Capasso, A. Casbarra, P. Pucci, and A. Di Donato**. 2004. Phenol hydroxylase and toluene/*o*-xylene monooxygenase from Pseudomonas stutzeri OX1: interplay between two enzymes. Appl. Environ. Microbiol. **70: 2211-2219**.
11. **Cafaro, V., R. Scognamiglio, A. Viggiani, V. Izzo, I. Passaro, E. Notomista, F. Dal Piaz, A. Amoresano, A. Casbarra, P. Pucci, and A. Di Donato**. 2002. Expression and purification of the recombinant subunits of toluene/*o*-xylene monooxygenase and reconstitution of the active complex. Eur. J. Biochem. **269: 5689-5699**.
12. **Bolognese, F., C. Di Lecce, E. Galli, and P. Barbieri**. 1999. Activation and inactivation of *Pseudomonas stutzeri* methylbenzene catabolism pathways mediated by a transposable element. Appl. Environ. Microbiol. **65(5):1876-1882**.
13. **Kahn, M., R. Kolter, C. M. Thomas, D. Figurski, R. Meyer, E. Remaut, and D. R. Helinski**. 1979. Plasmid cloning vehicles derived from plasmid ColE1, F, RK6 and RK2. Methods Enzymol. **68:268-280**.
14. **Bradford, M. M**. 1976. A rapid sensitive method for the quantification of microgram quantities of protein utilizing the principle of protein–dye binding. Anal. Biochem. **72:248–25.**
15. **Thompson, J.D., D.G. Higgins, and T.J. Gibson**. 1994. CLUSTALW: improving the sensitivity of progressive multiple sequence alignment through sequence weighting, position specific gap penalties and weight matrix choice. Nucleic Acids Res. **22:4673–4680**.
16. **Favaro, R., C. Bernasconi, N. Passini, G. Bertoni, G. Bestetti, E. Galli, and G. Dehò**. 1996. Organisation of the *tmb* catabolic operons of *Pseudomonas putida* TMB and evolutionary relationship with the *xyl* operons of the TOL plasmid pWWO. Gene **182: 189-193**.
17. **Barbieri, P., L. Palladino, P. Di Gennaro, and E. Galli**. 1993. Alternative pathways for *o*-xylene or *m*-xylene and *p*-xylene degradation in a *Pseudomonas stutzeri* strain. Biodegradation. **4:71-80**.
18. **Di Lecce, C., M. Accarino, F. Bolognese, E. Galli. and P. Barbieri**. 1997. Isolation and metabolic characterization of a *Pseudomonas stutzeri* mutant able to grow on the three isomers of xylene. Appl. Environ. Microbiol. **63:3279-3281**.
19. **Park, D. W., L. Kyoung, C. Jong-Chan, K. Toshiaki, and K. Chi-Kyung**. 2004. Genetic structure of xyl gene cluster responsible for complete degradation of (4-chloro)benzoate from Pseudomonas sp. S-47. Journal of microbiology and biotechnology. **14(3): 483-489**.

ToMO -A mutants: From an *in-silico* Design Approach to Functional Characterization

Luca Bianchi, Enrico Caruso, Viviana Orlandi, Marco Lanfranchi, Gabriella Fanali, Stefano Banfi, Mauro Fasano, and Paola Barbieri
Department of Structural and Functional Biology – University of Insubria – Varese

Toluene/*o*-xylene monooxygenase (ToMO) is a NADH/O_2-dependent non-heme diiron enzyme, isolated from *Pseudomonas* sp. OX1, able to catalyze the introduction of the OH group on the aromatic ring of toluene and o-xylene. Recently, the structure of the ToMO-H has been solved by X-ray crystallography.
On the basis of *in-silico* docking approach, we designed two new mutants in the A subunit, D211A and D211A/E214G, that should have a different spectrum of substrates with respect to the wild type. These two mutants have been constructed by site directed mutagenesis of the ToMO gene cluster previously cloned in pMZ1256. During the screening of the mutant clones we also isolated another mutant, D211A/E214G/D217K. These mutants were used in biotransformation assays of toluene and nitrobenzene for a preliminary functional characterization. As regards the biotransformation of toluene, all the mutants were less efficient than the wild type, and, among them, D211A/E214G/D217K was the best performant. Nitrobenzene was transformed by all the mutants with an efficiency higher than that of the wild type.

Toluene/*o*-xylene monooxygenase (ToMO) was cloned from the chromosome of *Pseudomonas sp.* OX1 (1). ToMO is an enzymatic complex composed by six different subunits $(ABE)_2CDF$ coded by the *touABCDEF* genes. This organization is similar to that observed for several enzymatic complexes involved in the monooxygenation of aromatic compounds. $(ABE)_2$ constitutes the hydroxylase subcomplex (ToMO-H), C and F are members of an electron transport chain from NADH to the center of reaction; D subunit is an uncharacterized effector protein (2). The structure of the ToMO-H has been solved by X-ray crystallography to 2.3 Å resolution (3). The structural data showed a large hydrophobic pocket in the A subunit, where the diiron center, whose structure resembles that predicted for oxidized methane monooxygenase hydroxylase (MMOH) and toluene 4-monooxygenase hydroxylase (T4MOH), is placed.

The Fe-Fe distance of 3.0 Å is identical to that of MMOH. The structure of oxidized ToMOH was determined from crystals grown in the presence of 1.5 mM NaN3. Within the ToMOH A-subunit lies a large channel of ~30–35 Å in length and 6–10 Å in width that connects the diiron center to the surface of the protein. Starting at the diiron center, the channel traverses a four-helix bundle and extends toward the surface through a space created by the interface of helix motifs. At the surface of the protein, amino acid side chains create a fork in the channel, the arms of which lead to two adjacent openings. The channel diameter of 6–10 Å is large enough to accommodate aromatic substrates or products as they move toward or away from the active site. Crystals soaked with the product analogue 4-bromophenol, chosen to facilitate

---

Running title. Biotransformations of ToMO-A mutants

Keywords. toluene/*o*-xylene mono-oxygenase; site direct mutagenesis; biotransformations

identification of the hydroxyl group, contained 3 molecules in the channel. The 4-bromophenol molecules are positioned in such a way that the hydroxyl moieties are directed toward the surface; their orientations in the channel appear to be determined by a combination of both hydrogen bonding interactions between the bromophenol hydroxyl groups with the protein and by π-stacking interactions between the bromine atom, protein side chains, and adjacent bromophenol phenyl rings. Although it is unknown whether the channel can direct the orientation of substrate molecules as they try to gain access to the active site pocket, or how such substrate steering might be accomplished, the positioning of the bromophenol molecules suggests that a mechanism of this kind exists.

ToMO could be engineered to produce oxidized compounds with pharmaceutical, industrial and biotechnological value. Dihydroxy-nitroaromatics are relevant in the pharmaceutical industry. Nitrocatechol (NC) derivatives have been shown to be selective inhibitors of catechol-*o*-methyltransferase and may be used in the treatment of Parkinson disease (4, 5, 6). 4-NC and 3-NC were recently found to be competitive inhibitors of nitric oxide synthase and may be new leads for innovative, nitrocatechol-based, pharmacophores of potential therapeutic interest (7). 3-NC is also essential as a building block for the production of some antihypertensive pharmaceuticals such as flesinoxan (8, 9). Monohydroxylated derivatives of many aromatic compounds could be precursors of molecules currently produced by traditional chemical synthesis; increase and optimization of industrial biotransformation processes are aligned to "green chemistry" philosophy.

In this work, our goals was to design and construct TouA mutants endowed with a spectrum of substrates different than that of the wild type (wt).

MATERIALS AND METHODS

***In-silico* analyses.** PyMol (http://www.pymol.org; DeLano W.L., 2002) and SPDBV (10) software were used to design ToMO-H mutants. *In-silico* docking assays were performed with AutoDock 4.0 and Autogrid 4.0 (11, 12, 13).

Molecular and Biochemical methods. Selected mutants were produced by Finzymes Phusion® Site-Directed Mutagenesis Kit. As template for mutagenesis we used pMZ1256, a pGEM3Z derivative containing the *touABCDEF* cluster cloned in *E. coli* JM 109 strain (*recA1 hsdR17 thi* Δ*lac-proAB*) (F' *traD36 proAB lacI*^{q}ZΔM15) (2). *E. coli* was transformed with plasmid DNA by electroporation. Protein total content determination was performed by BCA1 kit (Sigma Aldrich).

Chemicals. Toluene (Riedel), nitrobenzene (Fluka), *o*-cresol, *m*-cresol, *p*-cresol, *o*-nitrophenol, *m*-nitrophenol, *p*-nitrophenol, aniline, anisole, benzophenone, biphenile, indole (Fluka), quinoline, trans-stilbene, 1,2,3-trimehtoxybenzene, 2,2,4-trimethylpentane (isooctane) were purchased from Sigma Aldrich. All chemicals were of the highest purity available.

Biotransformation assays and product analyses. Recombinant *E. coli* JM109 strains were grown in Luria Broth (LB) medium supplemented with ampicillin (50 μg/ml), at 37°C to O.D.600nm of 0.6. After the induction of ToMO expression with isopropyl-b-D-thiogalactopyranoside (IPTG) for 30 minutes, the cells were washed in phosphate buffer (PB) and resuspended in PB at O.D. 600nm of 2.0. Glucose was added to cellular suspension to final concentration of 1 mM. Toluene was supplied in the vapour phase; in these conditions toluene final concentration in aqueous phase was about 5 mM, the maximum achievable in this system. Nitrobenzene (NB) was added to cellular suspension to final concentration of 1 mM. Samples were collected at fixed times and filtered through 0,2 μm HPLC compatible filters. Samples were analyzed by reversed phase HPLC equipped with C18 Agilent column for the analyses of toluene and cresols and with C8 Ascentis column for nitrobenzene. Mobile phase: H_2O:methanole 2:8. Detection (λ): 214 nm for toluene and cresols; 240 nm for nitroaromatics.

Results and discussion

In a previous work (14) a TouA mutant isolated by saturation mutagenesis, E214G/D312N/M399V, was found able to oxidize nitroaromatics substrates with an efficiency higher than that of wt ToMO. TouA positions D312 and M399 did not appeared to play an important role in catalysis whereas E214G was found responsible for the enhanced rate of oxidation of the nitroaromatics. TouA variants E214G, E214A, E214V oxidized *o*-nitrophenol and formed 3-nitrocatechol respectively 2.1-, 1.6-, and 1.2-fold faster than the wt ToMO, whereas variant E214W formed 3-nitrocatechol 3-fold slower. The mutants with R groups roughly equivalent in size to glutamate, E214Q and E214F, oxidized *o*-nitrophenol at the same rate. These results suggested that position E214 is a gate amino acid that controls the rate of nitroaromatic oxidation.

Our 3D structure analysis confirmed the hypothesis that E214, situated more than 10 Å away from the diiron center, is potentially involved in regulating the flow of molecules into the active site. Particularly, two residues located at the channel entrance, E214 and D211, seem to be able to block the transit of molecules toward the reaction center through hindrance (Fig 1a). As position 211 is located in an alpha helix region, we chose to replace the aspartate with an alanine because of its small hindrance and high alpha propensivity. *In-silico* 3D analysis of D211A and E214G/D211A substitutions confirmed the preliminary observation (Fig 1 b). E214G/D211A molecular surface representation showed the wide cavity caused by the fusion of the two openings.

By a preliminary *in-silico* docking approach, performed using Monte Carlo – Simulated Annealing algorithm, we tested the ability of many aromatic compounds, including molecules larger than toluene, to get through the opening created introducing the cited mutations. The free energy docking values obtained by simulations on nitrobenzene, quinoline, anisole, aniline, biphenile, benzophenone, trans-stilbene, and 1,2,3-trimethoxybenzene, were compatible with a transient interactions across the opening in which the molecules were able to accommodate. On the bases of these results we hypothesized that the mutants should allow a better transit of some potential substrates and thus they could display a spectrum of substrates different than that of the wt (Fig 2).

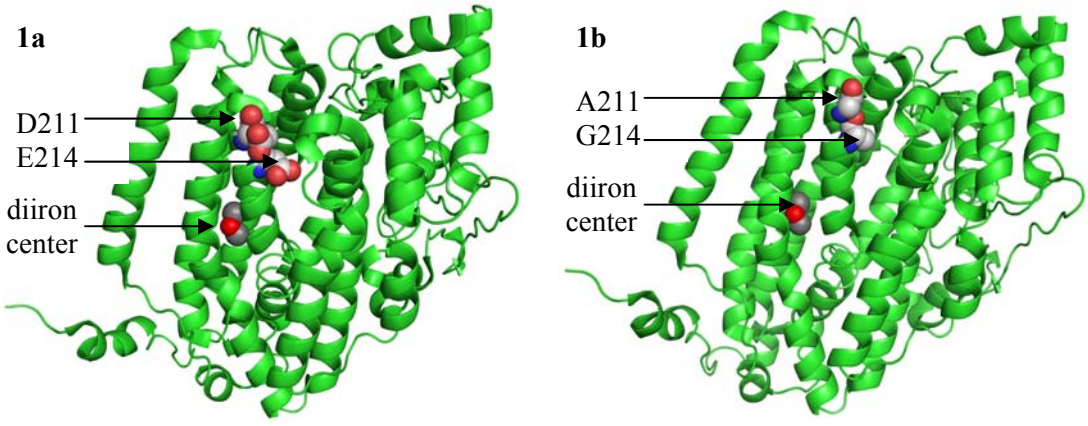

Fig. 1. Ribbon representation of TouA subunit. Diiron center is located in a wide hydrophobic pocket. At channel opening level, D211 and E214 residues (wt) (a) show more hindrance than that the A211 and G214 residues **(**b**)**.

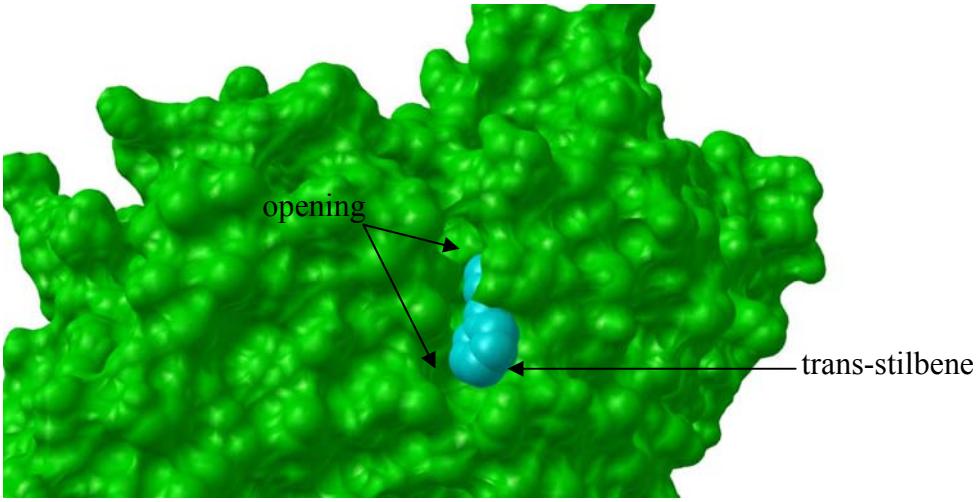

Fig. 2. Docking simulation performed using Monte Carlo- Simulated Annealing algorithm on D211A/E214G mutant using trans-stilbene

The D211A and D211A/E214G mutants were constructed by site direct mutagenesis and found functional as regards the oxidation of indole to indigo. DNA sequencing confirmed the presence of the desired mutations and moreover allowed to isolate an interesting unexpected triple mutant (D211A/E214G/D217K).

A protocol developed in our laboratory was used to evaluate the efficiency of the mutants in the biotransformations of toluene and nitrobenzene.

This preliminary characterization revealed that, when toluene was supplied in the vapour phase, D211A, D211A/E214G and D211A/E214G/D217 mutants were less efficient than the wild type in cresols production, and, among them, D211A/E214G/D217 was the best performing. (Fig 3).

As expected (15), the efficiency of E214G was comparable with that of the wt. Preliminary experiments were also performed using a different biotransformation protocol supplying toluene dissolved in an isooctane organic phase. In these conditions E214G produced an amount of cresols 5-6 times greater than the wt (Fig 4).

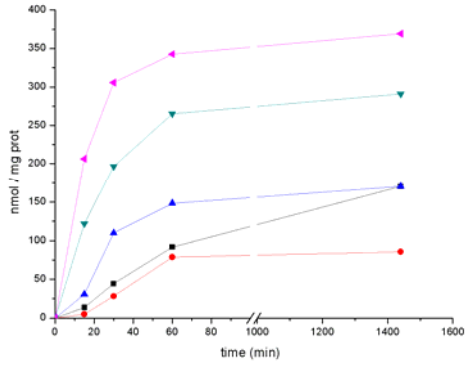

Fig. 3. Biotransformation of toluene by wt (◀), D211A (■), D211A/E214G (●), D211A/E214G/D217K (▲) and E214G (▼). Data are expressed as nmol of product/mg of protein.

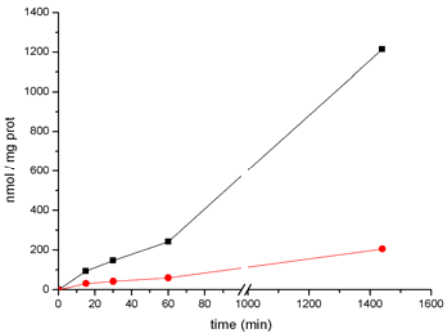

Fig. 4. Biotransformation of toluene in biphasic system by wt (●) and E214G (■). Data are expressed as nmol of product/mg of protein

Nitrobenzene transformations were performed in aqueous system. An HPLC signal compatible with a product more oxidized than the substrate was observed, but its retention time didn't match to any nitrophenol isomer; analyses are under way in order to identify the biotranformation product. However, nitrobenzene was transformed by all the mutants with an efficiency higher than that of the wt (Fig 5). Apparently, D211A transformed the highest amount of nitrobenzene after 24 hours of reaction. Exploratory assays on the others substrates, previously tested *in-silico*, showed that D211A and D211A/E214G mutants display a different range of substrates with respect to the wt. No significant differences where instead observed when the mutants were compared with E214G (Table 1).

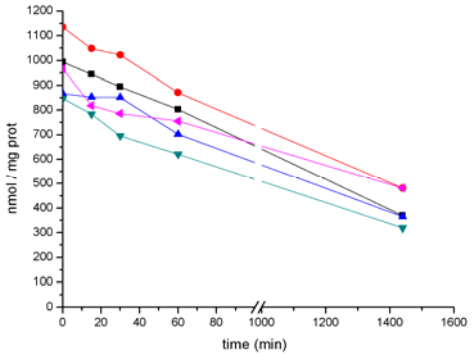

Fig. 5: Biotransformation (decrease) of nitrobenzene by wt (◄), D211A (■), D211A/E214G (●), D211A/E214G/D217K (▲) and E214G (▼). Data are expressed as nmol of substrate/mg of protein.

Table 1. *Qualitative results of exploratory biotransformation assays. Data were obtained by HPLC analysis*

SUBSTRATE	wt	E214G	D211A	D211A/E214G
Toluene	+	+	+	+
Nitrobenzene	-	+	+	+
Aniline	-	+	+	+
Anisole	+	+	+	+
Biphenile	+	+	-	+
Benzophenone	-	-	-	-
Quinoline	+	+	+	+
Trans-stilbene	-	-	-	-
1,2,3-trimethoxybenzene	-	-	-	-

Conclusions

In-silico approach and docking analyses allowed to realized some potentially interesting TouA mutants. Theoretical data showed that mutants D211A, D211A/E214G, and D211A/E214G/D217K should have a different spectrum of substrates with respect to the wt. In particular, in these mutants, all the molecules tested in *in silico* assays and larger than the natural substrate should easily get to the active site. All the three mutants oxidize nitrobenzene with an efficiency higher than that of the wt, however nitrobenzene biotransformation product needs to be chemically characterized by gas chromatography-mass spectrometry analysis (GC-MS). The different results obtained testing two different protocols for the biotransformation of toluene suggest that the operative conditions are very important for

the process. As regards, biphasic systems allowed the production of a greater amount of cresols. Preliminary data concerning the other aromatic compounds are partially in contrast with the *in-silico* predictions; however, as different results may be obtained using different biotransformation protocols, it will be necessary optimize transformation systems and conditions for each molecule.

ACKNOWLEDGMENTS

This work was supported by grants from the Ministry of University and Research (PRIN/2007). We also thank Dr. Guido Sello (Department of Organic and Industrial Chemistry, University of Milan) for his useful suggestions.

REFERENCES

1. **Bertoni G., F. Bolognese, E. Galli, and P. Barbieri**. 1996. Cloning of the Genes for and Characterization of the Early Stages of Toluene and *o*-Xylene Catabolism in *Pseudomonas stutzeri* OX1. Appl. Environ. Microbiol. **62**: 3704–3711.
2. **Bertoni G., M. Martino, E. Galli, and P. Barbieri**. 1998. Analysis of the Gene Cluster Encoding Toluene/*o*-Xylene Monooxygenase from *Pseudomonas stutzeri* OX1. Appl. Environ. Microbiol. **64** p. 3626–3632.
3. **Sazinsky M. H., J. Bard, A. Di Donato, and S. J. Lippard.**. 2004. Crystal structure of the toluene/*o*-xylene monooxygenase hydroxylase from Pseudomonas stutzeri OX1. Insight into the substrate specificity, substrate channeling and active site tuning of multicomponent monooxygense Appl. J Biol Chem. (2004) **279**:30600-10.
4. **Borgulya J., H. Bruderer, K. Bernauer, G. Zuercher and M. Da Prada**.1989. Catechol-*o*-methyltransferase-inhibiting pyrocatechol derivatives: synthesis and structure-activity studies. Helvetica Chim. Acta **72**: 952–968.
5. **Learmonth D. A. and A. P. Freitas**. 2002. Chemical synthesis and characterization of conjugates of a novel catechol-*o*-methyltransferase inhibitor. Bioconjug. Chem. **13**: 1112–1118.
6. **Learmonth D. A., M. A. Vieira-Coelho, J. Benes, P. C. Alves, N. Borges, A. P. Freitas and P. Soares-da-Silva**. 2002. Synthesis of 1-(3,4-dihydroxy-5-nitrophenyl) 2-phenyl-ethanone and derivatives as potent and long acting peripheral inhibitors of catechol*o*-methyltransferase. J. Med. Chem. **45**: 685–695
7. **Palumbo A., A. Napolitano and M. d'Ischia**. 2002. Nitrocatechols versus nitrocatecholamines as novel competitive inhibitors of neuronal nitric oxide synthase: lack of the aminoethyl side chain determines loss of tetrahydrobiopterin-antagonizing properties. Bioorg. Med. Chem. Lett. **12**: 13–16.
8. **Ennis M. D. and N. B. Ghazal**. 1992. The Synthesis of (+)- and (−)- Flesinoxan: application of enzymatic resolution methodology. Tetrahedron Lett. **33**: 6287–6290
9. **Krab-Husken L**.. 2002. Production of Catechols: Microbiology and Technology. Wageningen University, Netherlands
10. **Guex, N.**.1996. Swiss-PdbViewer: a new fast and easy to use PDB viewer for the Macintosh.
11. **Goodsell D. S. and A. J. Olson**. 1990. Automated docking of substrates to proteins by simulated annealing. Proteins: Structure, Function and Genetics. **8**:195-202.
12. **Morris G. M., D. S. Goodsell, R. S. Halliday, R. Huey, W. E. Hart, R. K. Belew and A. J. Olson**. 1998. Automated Docking Using a Lamarckian Genetic Algorithm and Empirical Binding Free Energy Function J. Comp. Chem. **19**: 1639-1662.
13. **Huey R., G.M. Morris, A.J. Olson and D.S. Goodsell**. 2007. A semiempirical free energy force field with charge-based

desolvation. J. Comp. Chem. **28**: 1145-1152.

14. **Vardar G., and T.K. Wood.** 2005. Alpha-Subunit Positions Methionine 180 and Glutamate 214 of *Pseudomonas stutzeri* OX1 Toluene-*o*-Xylene. J. of Bacteriology **187**:1511-1514

15. **Vardar G, K. Ryu, T. K. Wood**. 2004. Protein engineering of toluene-*o*-xylene monooxygenase from *Pseudomonas stutzeri* OX1 for oxidizing nitrobenzene to 3-nitrocatechol, 4-nitrocatechol, and nitrohydroquinone. Journal of Biotechnology. **115**: 145-156

Development of regulated multienzymatic biocatalysts expressing oxidoreductive enzymes

Patrizia Di Gennaro[1], Erika Mapelli[1], Silvana Bernasconi[2], Guido Sello[2]
[1]Dipartimento di Scienze dell'Ambiente e del Territorio, Università di Milano-Bicocca, p.za della Scienza 1, 20126 Milano [2]Dipartimento di Chimica Organica e Industriale, Università degli Studi di Milano, via Venezian 21, 20133 Milano

The aim of this work was the construction of recombinant strains containing two enzymatic activities mutually expressed, through the development of regulated system for the production of functionalized epoxides in one-pot biocatalysis reactions. Two biocatalysts were developed, based on different hosts, such as *P. putida* and *E. coli*. The former was constructed in *P. putida* PaW340, where styrene monooxygenase expression (SMO, from *P. fluorescens* ST strain) is controlled by the autoinducible promoter P_{ToMO} and by the regulator TouR of *P. stutzeri* OX1, while naphthalene dihydrodiol dehydrogenase (DDH, from *Pseudomonas fluorescens* N3 strain) was cloned into pVLT31 vector under the control of P*tac* promoter, inducible by isopropyl β-D-1-thiogalactopyranoside (IPTG). The latter, constructed in *E. coli* JM109, is based on the expression of SMO in pVLT33 vector under the control of P*tac* promoter, inducible by IPTG, while DDH was cloned into pMW61 vector under the control of P*nar* promoter, inducible in anaerobic conditions and in the presence of nitrates.

Each activity was tested in bioconversion experiments with reference substrates, respectively styrene for SMO and cinnamyl alcohol for DDH. Moreover, bioconversion experiments were performed by the two subsequent enzymatic steps.

Biocatalysis has the potential to attain an outstanding role in the future development of chemical synthesis. Enzyme selectivity and mild reaction conditions have an intrinsic appeal for chemists, that can exploit these characteristics to perform more efficient and greener syntheses. However, several improvements are still needed to turn the use of enzymes into a routine task; among them, an increase of available activities, a better understanding of enzyme mechanisms, and a more efficient management of catalysts. [1-7]

In this regard, the possibility of introducing more than one enzymatic activity in a single cell to build a multifunction catalyst is certainly appealing. In this way, the execution of reaction sequences without intermediate separation could demonstrate highly efficient: it will remind cellular anabolic/catabolic pathways. To add another similarity, it could be interesting to simulate the activity control present in cell, using regulators, or similar machinery, to activate/deactivate enzymes. Still far from this objective, we considered the possibility of producing regulated whole cell biocatalysts expressing two enzymatic activities in mutually exclusive form.

The selection of the activities to consider was directed by our in-house pool of enzymes; also with a look to the final products of the biocatalysis we selected a monooxygenase (SMO) and a dehydrogenase (NDDH), so we could have prepared functionalized epoxides. SMO is a styrene monooxygenase from *P.fluorescens* ST [8] that transforms styrene into the corresponding enantiopure epoxide; NDDH is a dihydrodiol

---

Running title. Regulated multienzymatic biocatalysts

Keywords. Biocatalysts, whole cell, multienzymatic, one-pot

dehydrogenase from *P.fluorescens* N3 [9] that transforms naphthalene dihydrodiol into dihydroxy naphthalene(Figure1).

The genes expressing these activities are usually inserted into plasmids where they are under the control of promoters and regulators. In addition, when using whole cell biocatalysts plasmids are inserted into host cells that should be compatible with the expression systems. To build alternatively activated systems the controlling structures should be mutually exclusive. We selected three expression systems and two host strains (*E.coli* JM109 and *P.putida* PaW340). The first expression system relies on the P*tac* promoter [10] inducible by IPTG and compatible with both *E.coli* and *P.putida*; the second uses the autoinducible promoter P_{ToMO} and the regulator TouR of *P. stutzeri* OX1 [11] and is compatible with *P.putida* only; the third is based on the P*nar* promoter [12], inducible in anaerobic conditions and in the presence of nitrates and compatible with *E.coli* only.

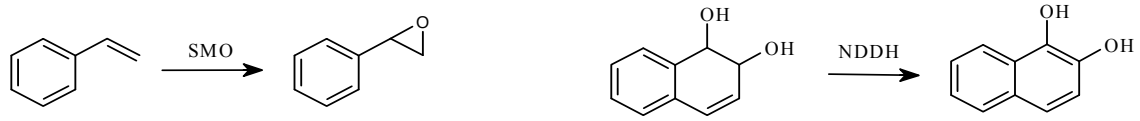

Figure 1: Reactions catalyzed by Stirene Monooxygenase SMO and Naphthalene Dihydrodiol Dehydrogenase NDDH.

MATERIAL AND METHODS

Bacterial strains and plasmids. The bacterial strains and plasmids used in this work are listed in the original papers.

***Pseudomonas putida* PaW340 (pKPT-SmoTouR + pVLT3128)**: the host strain is *P. putida* PaW340. SMO was cloned in pKGB4N vector under the control of the autoinducible promoter P_{ToMO} and of the regulator TouR from *P. stutzeri* OX1, thus it shows the gratuitous activation effect depending on the growth phase. NDDH was cloned into pVLT31 vector under the control of P*tac* promoter, inducible by IPTG.

***Escherichia coli* JM109 (pVLT33-Smo + pLG2228)**: the host strain is *E. coli* JM109. SMO was cloned in pVLT33 vector under the control of P*tac* promoter, inducible by IPTG. NDDH was cloned in pMW61 vector under the control of P*nar* promoter, inducile in anaerobic conditions and in the presence of nitrates.

Culture conditions in flask. *E. coli* and *P. putida* strains were routinely grown in Luria-Bertani broth at 37 and 30° C, respectively. Ampicillin and kanamycin were used in selective media at concentrations of 100 and 50 μg/ml, respectively.

For testing experiments of auto-induction, the *P. putida* PaW340 recombinant strains were cultured in 500 mL Erlenmeyer flasks containing 100 mL of M9 medium [13] supplemented with 20 mM malate. The cells grown in flask destined for bioconversion experiments were first washed twice in M9 medium and then treated as described below. At the end of the growth, the cells were collected, washed twice, and stored at – 20° C for further use in bioconversion experiments. The exhaustion of glucose was monitored by the glucose oxidase-peroxidase assay performed with the Accu-Check Kit (Roche).

Bioconversion conditions and monitoring

Bioconversion cultures. When needed the required amount of cells was unfrozen by shaking at 30 °C for 1 hour in M9 medium containing glucose (0.2% w/v). Then, the culture cell density was adjusted at the required value by addition of M9 medium; finally, glucose (initial concentration 0.2% w/v; similar amounts added when needed) and the substrate were added and the transformation was performed in a flask (usually 250 mL containing 50 mL of culture) at 30 °C on a horizontal shaker .

In both biocatalyst production and bioconversion the culture media were sterilized at 131°C, 10 min.; or by filtration on 45 μm Millipore filters; all equipments are autoclaved. Cell density was measured using a Shimadzu photometer at 600 nm. Glucose was monitored using enzyme sticks (Glukur Test) from Roche.

Bioconversion analysis. Substrate and product were monitored analysing the water phase by HPLC, Hitachi-Merck, UV–visible detector at 220 nm, reverse phase column C18 (Hibar LICHROSORB 50334, 10µm, 25 cm), H_2O:CH_3CN 1: 1 eluent, 1 mL/min flow, Hitachi D2500 integrator.

The absolute (S)-configuration of biocatalytically prepared (S)-styrene oxide (proven via comparison with commercially available, enantiopure (S)-styrene oxide (Aldrich)) was used as the reference for all epoxides and the configuration accordingly presumed. Enantiomeric excesses were measured using a Chrompack ChiralDex-CB column.

Optical rotation were obtained in $CHCl_3$ or CH_3OH using JASCO P-1030 polarimeter.

^{1}H-NMR spectra were obtained in $CDCl_3$ or CD_3OD (Merck) using Bruker AC-300 and Bruker AC-200 instruments. Thin-layer chromatography was carried out on silica gel plates (60 F_{254}, Merck): spots were detected visually by ultraviolet irradiation (254 nm) or using cerium-molibdic solution as stainer. All products were chromatographated over silica gel (*n*-hexane/ethyl acetate in different ratio as required).

Chemicals. All the chemicals are from Acros, CarloErbaReagents, Sigma Aldrich, Oxoid, or Fluka. TLC plates (Alugram SL G/UV254) are from Merck.

Results

This work consists in the preparation of the above mentioned biocatalysts together with their test in bioconversion experiments.

The first biocatalyst is *P. putida* PaW340 (pKPT-SmoTouR + pVLT3128) that contains two plasmids expressing the SMO and the NDDH activities. They are sketched in Fig. 2.

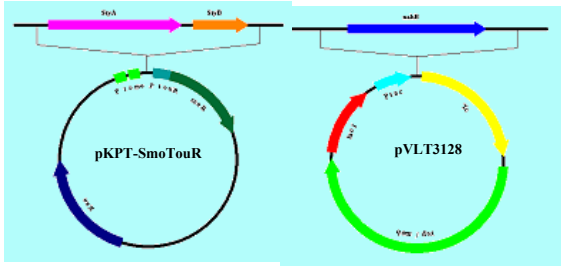

Figure 2. Construction of the pKPT-SmoTouR and pVLT3128 plasmids used to transform *P. putida* PaW340

The promoter pTOMO and the regulator Tour activate the expression of the SMO genes (StyA and StyB) when the carbon source is exhausted, giving origin to a gratuitous induction. This implies that the protein production begins when the cell growth is near to the end. It is important to monitor the catalyst activity to select the cell at their maximum activity. This was done using the indole test that produces indigo (blue color) from indole in the presence of an oxygenase activity. As shown in Figure 3, the highest activity came out after 6 hrs. from the start of the event.

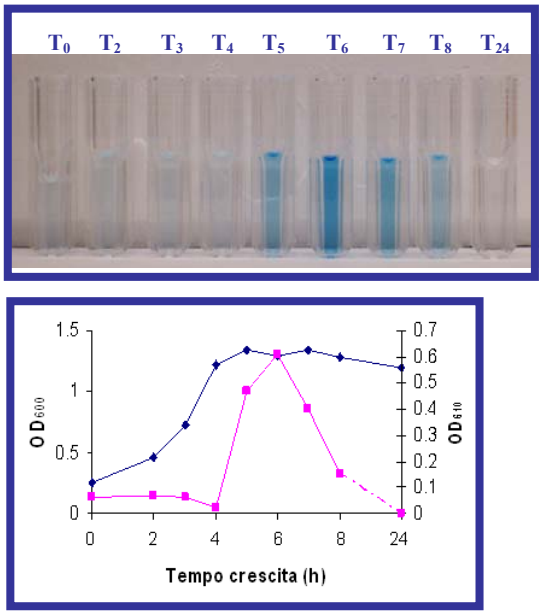

Figure 3. SMO activity measured by indigo production (Absorbance at 610 nm) from indole after gratuitous induction in *P. putida* PaW430 (pKPT-SmoTouR+ pVLT3128).

The promoter Ptac is activated by IPTG; also in this case an experiment to check the time of maximum activity was performed, using naphthalene dihydrodiol as test substrate (brown-black colour). Here, the time is not as critical as in the SMO case. (Figure 4)

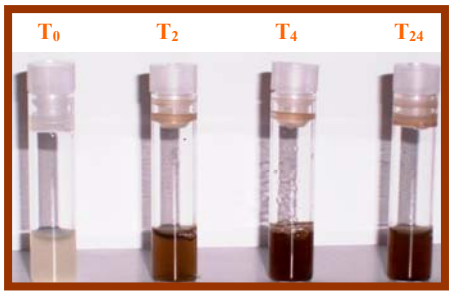

Figure 4. NDDH activity measured by the 1,2-dihydroxynaphthalene production (brown color formation) from naphthalene dihydrodiol after induction with IPTG in *P. putida* PaW430 (pKPT-SmoTouR + pVLT3128).

The second biocatalyst is *E. coli* JM109 (pVLT33-Smo + pLG2228) that contains two other plasmids expressing the SMO and the NDDH activities. They are sketched in Figure 5. Here, the SMO genes are under Ptac control, thus induced by IPTG. As shown in Figure 6, the highest activity came out after 8 hrs. from the start of the event.

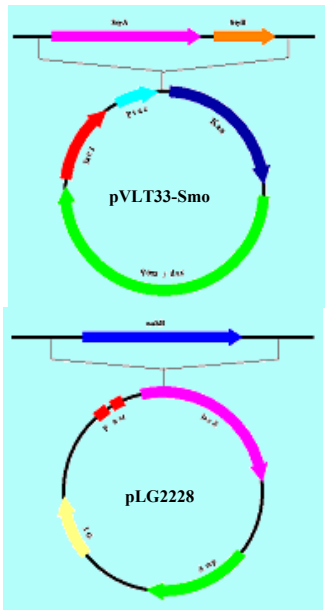

Figure 5. Construction of the pVLT33-Smo and pLG2228 plasmids used to transform *E. coli* JM109.

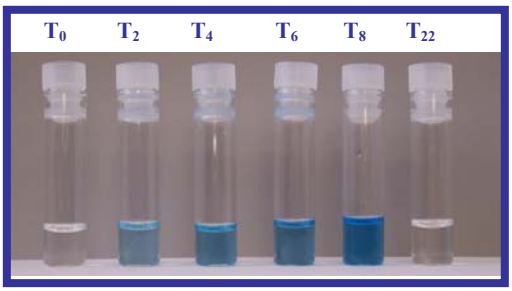

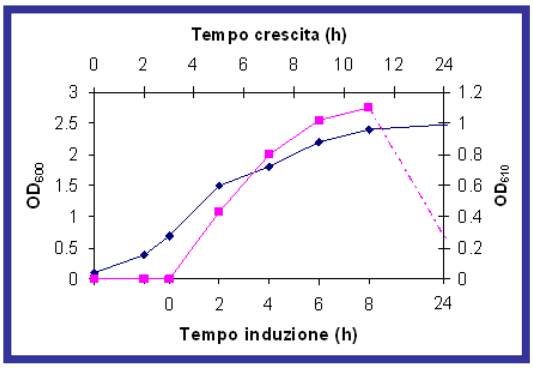

Figure 6. SMO actvity measured by indigo production (Absorbance at 610 nm) from indole after IPTG induction in *E. coli* JM109 (pVLT33-Smo + pLG2228).

In contrast, NDDH is under the control of Pnar promoter that is activated in anaerobic conditions in the presence of nitrates. In presence of oxygen that promoter is strongly repressed and cannot work. It is assumed that

the participation of different small proteins causes the rearrangement in active form of the promoter. (Figure 7)

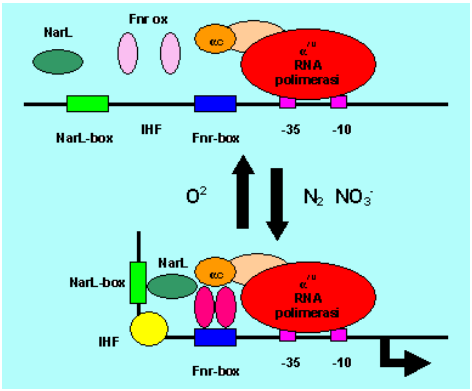

Figure 7. Scheme of the nitrate reductase Pnar Promoter activation in presence of nitrate and anaerobic conditions.

Here, the activity of NDDH is badly expressed, as demonstrated by Figure 8, that reports the activity test.

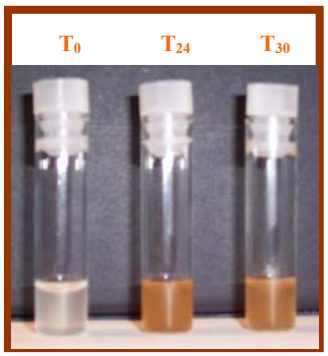

Figure 8. NDDH activity measured by the 1,2-dihydroxynaphthalene production (brown color formation) from naphthalene dihydrodiol after induction with nitrate and in anaerobic conditions in *E. coli* JM109 (pVLT33-Smo + pLG2228).

This result is probably due to the negative effect on *E. coli* of the anaerobic conditions.

These same results are clearly shown by the reaction trends of the single steps transformations. In Figure 9 we can see that the epoxide preparation has comparable rate in both catalysts whilst the first is much more effective in the alcohol oxidation.

The last experiments concerned the execution of the two step sequences; here, the selected substrate was cinnamic alcohol that is easily oxidized by both enzymes. In order to perform the two steps (Figure 9), it is important to remember that the product of NDDH (cinnamic acid) is not recognized by SMO.

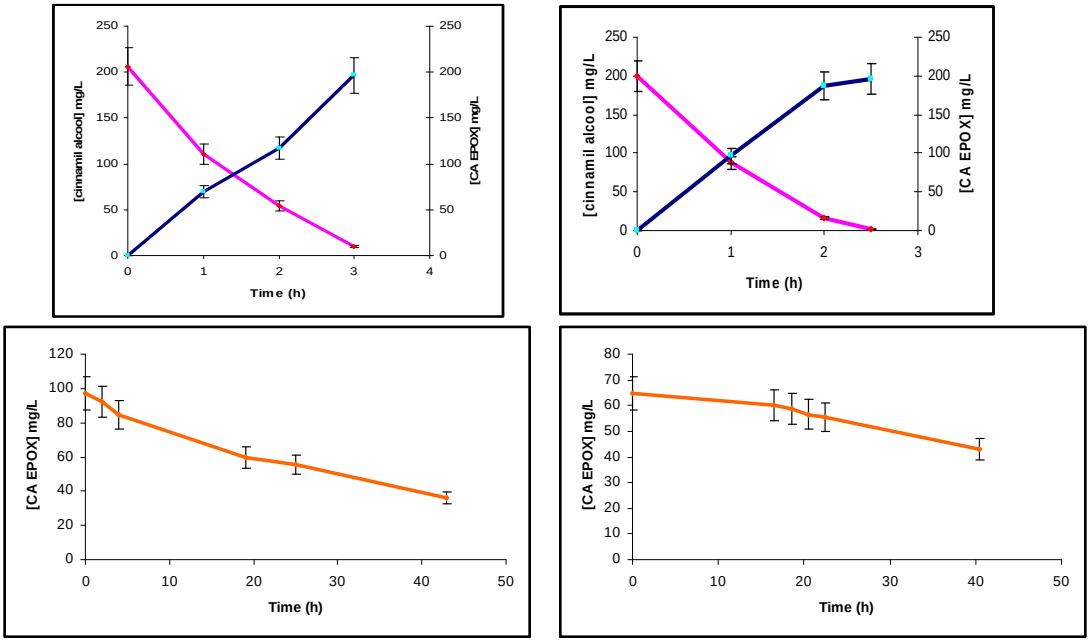

Figure 9. Bioconversion of the cinnamylalcohol in the two sequential steps with *P. putida* PaW430 (pKPT-SmoTouR+ pVLT3128): SMO activity measured as cinnamylepoxide production and NDDH activity measured as cinnamylepoxide consumption.

As a consequence, we need to activate NDDH only when all the alcohol has been transformed into the epoxide. Thus, we activated the SMO synthesis first; then, after a dilution, NDDH production was started. This was possible because the two expression systems in both catalysts are mutually exclusive.

The result exactly reproduces the result obtained by the single step experiments.

Discussion

In this work, we developed two biocatalysts expressing two enzymatic activities each. The expression systems were realized to be mutually exclusive and, thus, they can be activated at will. The first expression system is gratuitously activated; at the exhaustion of the carbon source; the second one when anaerobic conditions are established.

The two biocatalysts were functioning and bioconversion experiments were performed by the two subsequent enzymatic steps. For this reason, cells were grown activating SMO expression, then their catalytic activity was exploited, and finally they were inducted to obtain DDH expression, because it uses as substrate the product formed during the first reaction. To verify the applicability and to compare the two biocatalysts the one-pot multienzymatic reaction with cinnamyl alcohol was chosen as an example: SMO catalyses the conversion of cinnamyl alcohol to the corresponding epoxide, while DDH oxidises the last one to epoxide of cinnamic acid. The activity obtained from the two systems expressing the styrene monooxygenase, measured as production of the epoxide of cinnamyl alcohol, is comparable and it is about 65 mg L^{-1} OD^{-1} h^{-1}. Therefore, the gratuitous induction system (P_{ToMO}) can be a new alternative in biocatalysis processes, because expensive external inducers are not required. On the contrary, the activity obtained from the two systems expressing naphthalene dihydrodiol dehydrogenase and measured as consumption of cinnamyl epoxide, showed a higher efficiency of P*tac* promoter (63 % in 48h) than P*nar* promoter (34% in 48h).

ACKNOWLEDGMENTS

This work was supported by grants from the Ministry of University and Research (PRIN/2007 - Study of regulatory and catalytic systems for the development of bioconversion and biodegradation processes) and from Università degli Studi di Milano.

REFERENCES

1. **Chen G., Fournier R.L., Varanasi S.** 1997. Experimental demonstration of pH control for a sequential two-step enzymic reaction. Enz. Microbiol. Technol. **21**:491-495.
2. **Kihumbu D., Stillger T., Hummel W., Liese A.** 2002. Enzymatic synthesis of all stereoisomers of 1-phenylpropane-1,2-diol. Tetrahedron: Asymmetry. **13**:1069-1072.
3. a) **Glueck S.M., Fabian W.M.F., Faber K., Mayer S.F.** 2004. Biocatalytic asymmetric rearrangement of a methylene-interrupted bis-epoxide: Simultaneous control of four asymmetric centers through a biomimetic reaction cascade. Chem. Eur. J. **10**:3467-3478. b) **Larissegger-Schnell B., Kroutil W., Faber K.** 2005. Chemo-enzymatic synthesis of (R)- and (S)-2-hydroxy-4-phenylbutanoic acid via enantio-complementary deracemization of (±)-2-hydroxy-4-phenyl-3-butenoic acid using a racemase-lipase two-enzyme system. Synlett. 1936-1938.
4. **Hecquet L., Bolte J., Demuynck C.** 1996. Enzymic synthesis of "natural-labeled" 6-deoxy-L-sorbose precursor of an important food flavor. Tetrahedron. **52**:8223-8232.
5. **Guerard C., Alphand V., Archelas A., Demuynck C., Hecquet L., Furstoss R., Bolte J.** 1999. Transketolase-mediated synthesis of 4-deoxy-D-fructose 6-phosphate by epoxide-hydrolase-catalysed resolution of 1,1-diethoxy-3,4-epoxybutane. Eur. J. Org. Chem. 3399-3402.
6. **Zimmermann F.T., Schneider A., Schoerken U., Sprenger G.A., Fessner W.-D.** 1999. Efficient multi-enzymatic synthesis of D-xylulose 5-phosphate. Tetrahedron: Asymmetry. **10**:1643-1646.
7. **Bestetti G., Di Gennaro P., Galli E., Leoni B., Pelizzoni F., Sello G**., **Bianchi**

D. 1994. Bioconversion of substituted naphthalenes to the corresponding salicylic acids. Appl. Micr. Biotech. **40**:791-793.

8. **Di Gennaro P., Colmegna A., Galli E., Sello G., Pelizzoni F., Bestetti G.** (1999). A new biocatalyst for production of optically pure aryl epoxides by styrene monooxygenase from *Pseudomonas fluorescens* ST. Appl. Environ. Microbiol. 65: 2794-2797.
9. **Di Gennaro P., Galli E., Albini G., Pelizzoni F., Sello G., Bestetti G.** (1997). Production of substituted naphthalene dihydrodiols by engineered Escherichia coli containing the cloned the cloned naphthalene 1,2-dioxygenase gene from *Pseudomonas fluorescens* N3. Res. Microbiol. 148: 355-364.
10. **De Lorenzo V., Eltis L., Kessler B., Timmis K.N.** (1993). Analysis of *Pseudomonas* gene products using lacI^q/Ptrp-lac plasmids and trasposons that confer conditional phenotypes. Gene. 23: 17-24.
11. **Arenghi F.L.D., Berlanda D., Galli E., Sello G., Barbieri P.** (2001). Organization and regulation of meta cleavage pathway gene for toluene and *o*-xylene derivative degradation in *Pseudomonas stutzeri* OX1. Appl. Environ. Microbiol. 67: 3304-3308.
12. **Walker M.S. and De Moss J.A.** (1992). Role of alternative promoter elements in transcription from the *nar* promoter of *Escherichia coli.* J. Bacteriol. 178: 3971-3973.
13. **Sambrook J. and Russel D.** (2000). Molecular cloning: a laboratory manual. Cold Spring Harbor Laboratory Press, Cold Spring Harbor.

Study on the one-pot multienzymatic production of organic compounds

Patrizia Di Gennaro[2], Guido Sello[1], Silvana Bernasconi[1]
[1]Dipartimento di Chimica Organica e Industriale, Università degli Studi di Milano, via Venenzian 21, Milano. [2]Dipartimento di Scienze dell'Ambiente e del Territorio, Università di Milano-Bicocca, p.za della Scienza 1, 20126.

Some enzymatic activities that could potentially allow the preparation of special compounds have been selected. All of them show oxidoreductive actions, but with very different selectivity. Two recombinant strains (*E.coli* JM109 (pTAB19), that expresses a monooxygenase activity (SMO) from *P.fluorescens* ST, and *E.coli* JM109 (pVL2028), that expresses a dehydrogenase activity (NDDH) from *P.fluorescens* N3), and a wild strain (*E.coli* JM109, that expresses a reductase activity (ECAKR)), have been selected, whilst among commercial enzymes an alcohol dehydrogenase (LBADH) from *Lactobacillus brevis* has been chosen. The study has concerned the test of the single activities on different substrates and the analysis of some reaction sequences (mainly formed by two steps). The results permitted the validation of the approach potential, the high flexibility of the biocatalysts, and the possibility of producing many compounds, using simple and efficient procedures.

In the framework of our ongoing interest in biocatalysis we have studied the possibility of preparing organic compounds by multienzymatic synthesis. [1-7] The enzyme activities were selected from our biocatalyst pool and from commercial enzymes. We selected four enzymes that can perform the transformations sketched in Figure 1.

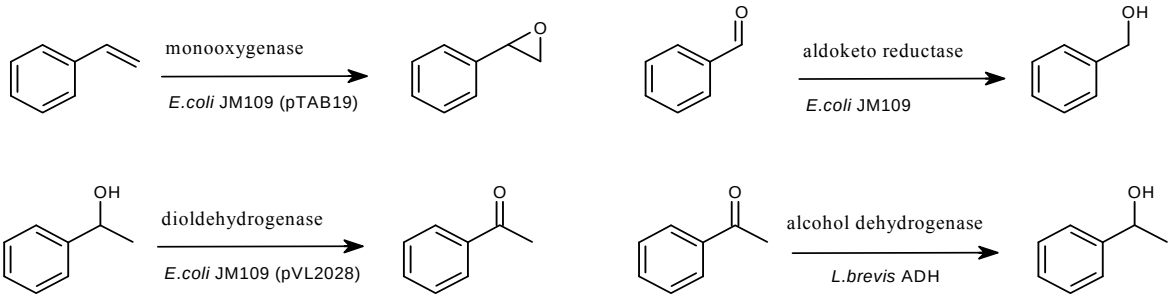

Fig. 1. Biotransformations performed by different biocatalysts

All of them are oxidoreductive reactions; but, they have different characteristics, concerning both substrate specificity and processing schemes. The first biocatalyst is an *E.coli* strain expressing styrene monooxygenase from *P.fluorescens* ST (SMO). This activity showed good versatility and exceptional stereoselectivity; it is thus appropriate to be used in chemical synthesis. [8] The second biocatalyst is also an *E.coli* strain, this one expresses a dihydrodioldehydrogenase (NDDH), involved in the transformation of naphthalene dihydrodiol into the corresponding dihydroxy naphthalene. It has been used in the oxidation of alcohols into ketones or carboxylic acids, showing a broad range of accepted substrates. [9]. The third biocatalyst is a wild type *E.coli* strain that shows an interesting and highly chemoselective potential in reducing aldehydes into the corresponding primary alcohols (ECAKR). [10] The last biocatalyst

Running title. Multienzymatic syntheses
Keywords. Organic compounds, synthesis, multienzymatic, one-pot

is a commercial alcohol dehydrogenase in pure form (LBADH). It is particularly well suited for the oxidation/reduction of methyl ketones: in contrast to whole cell biocatalysts, it requires a method for cofactor regeneration. [11]

Our main objective is the test of the possibility to perform several enzymatic reactions in sequence in order to obtain multifunctionalized structures without needing any intermediate separation or purification. This can be obtained because enzymes are highly selective and the reaction conditions are mild. As will be evident in the Results section, the same reactions should be very difficult to perform using chemical catalysts without interferences.

The selection of the substrates has been carried out taking into account both the compounds. Our monooxygenase needs an aromatic ring conjugated to the double bond, thus limiting the structural diversity. In contrast, the alcohol oxidases are all much more versatile. As a consequence we selected aromatic compounds searching for different structural variety in the rest of the molecule.

Another parameter has been considered; it concerns the possibility to change both the order and the direction of the transformations. For example, is it possible to use the SMO and the NDDH just mixing the cells with the substrates? Or, what does it happen when adding a new cell biocatalyst to an enzyme in solution? To answer to these and other questions we selected some sequences and some substrates and performed both single transformations and two-step sequences. In Figure 2 the selected reactions are reported.

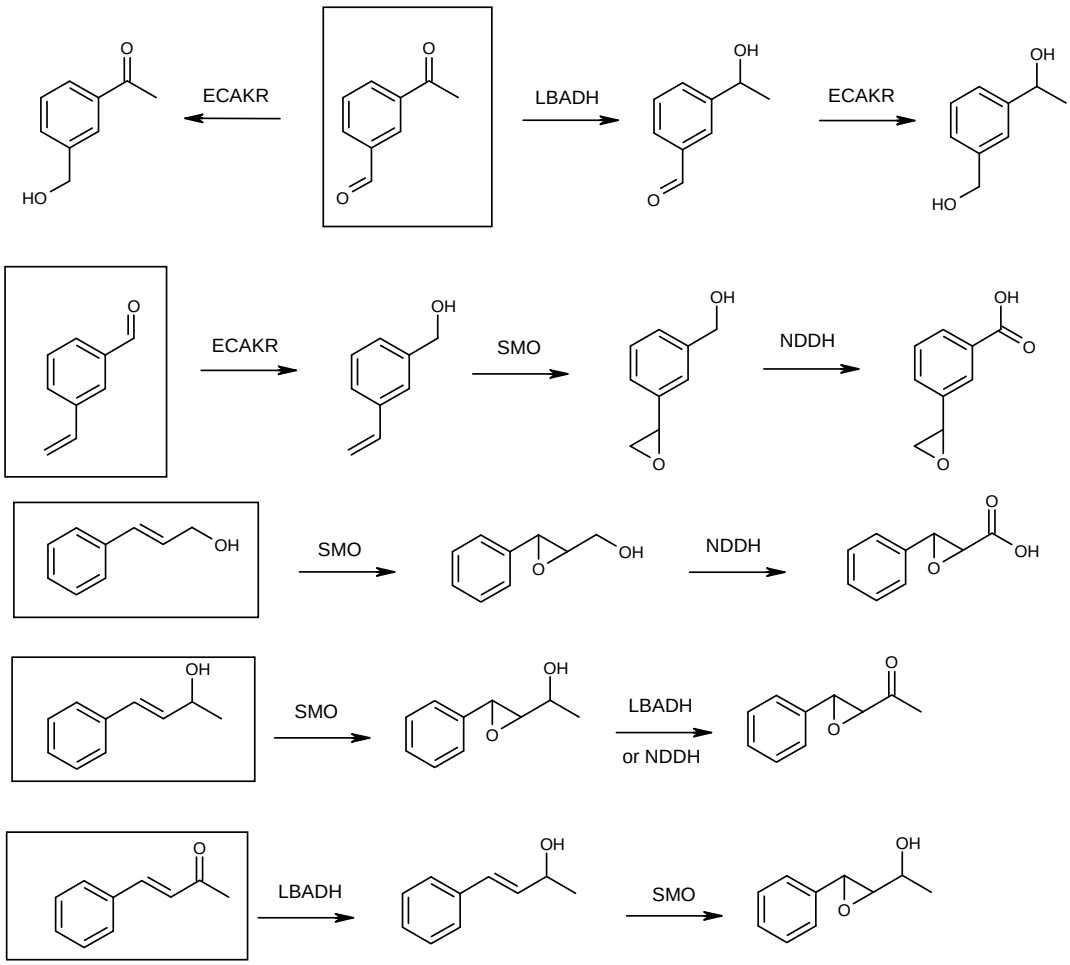

Fig. 2. Summary of selected transformations

achieved knowledge about the enzyme activities and the need to prepare interesting

MATERIALS AND METHODS

Cell biocatalyst growth conditions in flask. A single colony of one *E. coli* JM109 culture was grown overnight at 30°C in a 100 mL flask containing 20 mL of LB (Luria-Bertani) [15] medium, containing the needed antibiotic (kanamycin or ampicillin at final concentrations: 50 or 100 μg/mL).

Then, 10 mL of the culture were centrifuged (10000 rpm, 4 °C, 10 minutes), cell collected, and added to 100 mL of M9 [15] medium, in a 500 mL flask, containing the needed antibiotic and IPTG (Isopropyl-α-D-thiogalactopyranoside) 1 mM; glucose (0.2% w/v) and thiamine (0.05mM) were added; the culture was grown overnight at 30°C. Cells were immediately frozen at -20 °C.

Bioconversion cultures. When needed the required amount of cells was unfrozen by shaking at 30 °C for 1 hour in M9 medium containing glucose (0.2% w/v). Then, the culture cell density was adjusted at the required value by addition of M9 medium; finally, glucose (initial concentration 0.2% w/v; similar amounts added when needed) and the substrate were added and the transformation was performed in a flask (usually 250 mL containing 50 mL of culture) at 30 °C on a horizontal shaker .

In both biocatalyst production and bioconversion the culture media were sterilized at 131°C, 10 min.; or by filtration on 45 μm Millipore filters; all equipments are autoclaved. Cell density was measured using a Shimadzu photometer at 600 nm. Glucose was monitored using enzyme sticks (Glukur Test) from Roche.

Bioconversion analysis. Substrate and product were monitored analysing the water phase by HPLC, Hitachi-Merck, UV–visible detector at 220 nm, reverse phase column C18 (Hibar LICHROSORB 50334, 10μm, 25 cm), H_2O:CH_3CN 1: 1 eluent, 1 mL/min flow, Hitachi D2500 integrator.

The absolute (S)-configuration of biocatalytically prepared (S)-styrene oxide (proven via comparison with commercially available, enantiopure (S)-styrene oxide (Aldrich)) was used as the reference for all epoxides and the configuration accordingly presumed. Enantiomeric excesses were measured using a Chrompack ChiralDex-CB column.

Optical rotation were obtained in $CHCl_3$ or CH_3OH using JASCO P-1030 polarimeter.

^{1}H-NMR spectra were obtained in $CDCl_3$ or CD_3OD (Merck) using Bruker AC-300 and Bruker AC-200 instruments. Thin-layer chromatography was carried out on silica gel plates (60 F_{254}, Merck): spots were detected visually by ultraviolet irradiation (254 nm) or using cerium-molibdic solution as stainer. All products were chromatographated over silica gel (*n*-hexane/ethyl acetate in different ratio as required).

Chemicals. All the chemicals were from Acros, CarloErbaReagents, Sigma Aldrich, Oxoid, or Fluka. TLC plates (Alugram SL G/UV254) are from Merck.

Results

We had four biocatalysts available; thus, several combinations were possible. Initially, we limited to two the number of steps in order to check if the possibility of performing one-pot transformations was rational. The first selected sequence uses SMO and NDDH as enzymatic activities; the first choice we made concerned the substrate of the reactions and, if needed, the order of the addition of the catalysts. We knew that only styrene-type double bonds are transformed by SMO and that no withdrawing group should be present. In addition, we knew that NDDH can oxidize primary and secondary alcoholic groups giving organic acids or ketones, respectively. With these premises the first selected substrate was cinnamyl alcohol that can be transformed into the corresponding cinnamic acid epoxide (Figure 3). However, in this case

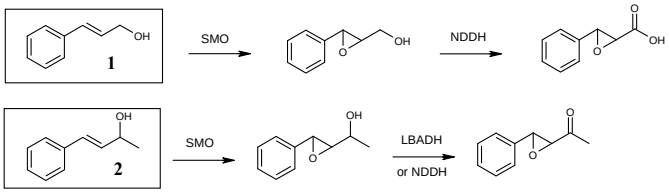

Fig. 3. Reaction sequence: SMO, then NDDH or LBADH

the only possible order is the use of SMO followed by NDDH, because the reverse order would have formed cinnamic acid that we knew is not a substrate of SMO. More, the second catalyst can be added only after the end of the first transformation.

A second selected substrate was 4-phenylbut-3-en-2-ol that is very similar to compound **1** but that contains a secondary alcoholic group. Also in this case the order is strictly that shown in the Figure.

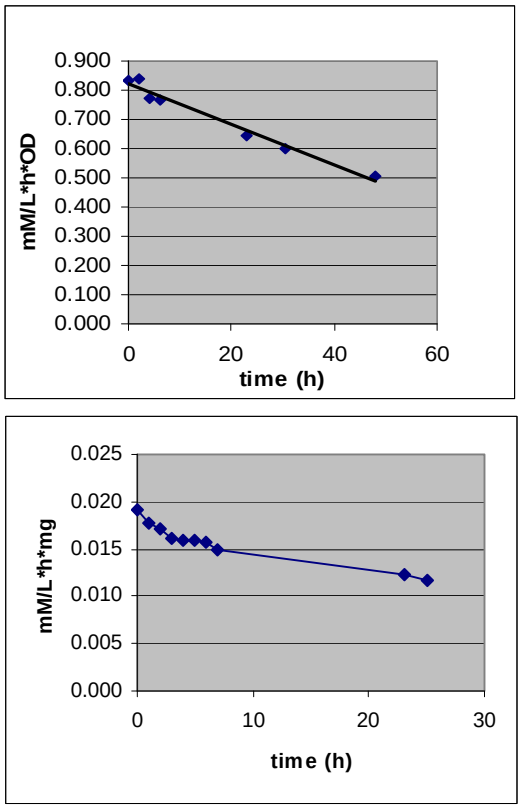

Fig. 4. HPLC analyses using either NNDH (upper panel) or LBADH (lower panel)

The first single step was initially controlled giving the expected product in short time for both compounds. In contrast the second step, involving the NDDH, showed long reaction time and low overall yield. This happens because the structure of the epoxide intermediates is not well recognized by the enzyme. The HPLC analyses reported in Figure 4 show the experimental results. Even using LBADH to perform the second step for compound **2** did not improve the reaction.

When the sequences were tested the results were in complete agreement with those of the separated single steps.

A second two step sequence was then considered. In this case the order of the enzyme use was changed together with the starting substrate. In fact, using 4-phenyl-but-3-en-2-one and LBADH it is possible to prepare the corresponding alcohol that can be then transformed into the epoxy alcohol. (Figure 5)

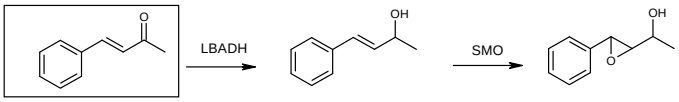

Fig. 5. Reaction sequence: LBADH, then SMO

The single step reactions showed that both steps are feasible: the first reached a 75% equilibrium in less than 1 hour, and the second gave a complete conversion in few hours. When combined the simultaneous presence of the two activities allowed for an even better result; in fact, as the product of the first step was consumed by SMO the first reaction proceeded further to give a 95% overall conversion. In this case, because the first substrate does not react with SMO, the two catalysts can be simultaneously present.

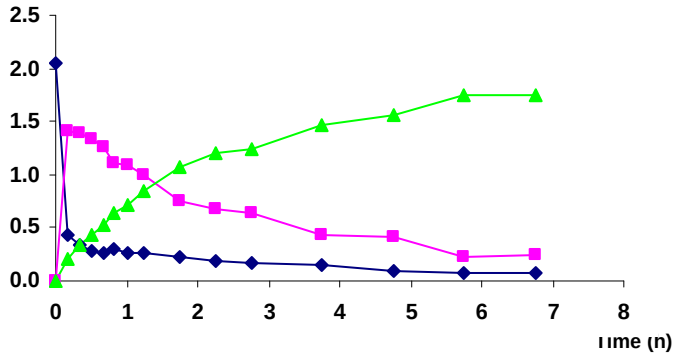

Fig. 6. HPLC analysis: ◆ketone decrease, ■alcohol increase and decrease, ▲epoxyalcohol increase

In order to test the possibility to perform the sequence SMO – NDDH we selected a new substrate: 3-vinyl benzaldehyde. In principle, this compound should react with SMO to give 3-epoxybenzaldehyde and with NDDH to give 3-epoxybenzoic acid. Also in this case we firstly tested the single step transformations and even here we expected that 3-vinylbenzoic acid is not a good substrate for SMO. Unexpectedly, the

reaction of **3** with SMO gave 3-epoxybenzyl alcohol as the only product. In fact, in the host strain *E.coli* JM109 it is present an aldoketoreductase that can rapidly and selectively reduce aldehydes to the corresponding alcohols. This reaction is so fast that we could not see any trace of the aldehyde at any reaction time. Nevertheless, the reaction of compound **4** with NDDH gave the expected product as the only product. We thus realized a three step sequence using three enzymes: ECAKR, SMO and NDDH. We also verified the possibility of preparing both the epoxy alcohol and the epoxy acid, both in enantiopure form. (Figure 7) The reaction rates were quite appreciable: ECAKR performed its transformation in less than 1 hour, SMO needed less than 6 hours and NDDH needed 12 hours; thus, in less than 24 hours we got the final product. [12]

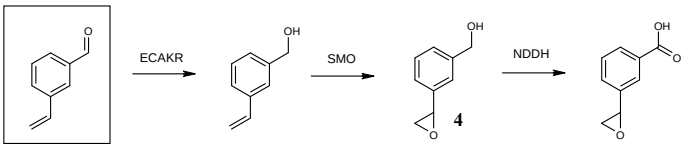

Fig. 7. Reaction sequence: ECAKR, then SMO, then NDDH

The last sequence was suggested by the experience with the enzymes already used. In fact, we learned that using ECAKR we can selectively reduce aldehydes, while using LBADH we can selectively reduce ketones. To test this point we selected 3-acetylbenzaldehyde that contains both a methylketone group and an aldehyde. In this sequence, both orders, ECAKR – LBADH and LBADH – ECAKR, were feasible. The separated single steps worked optimally giving exclusively the corresponding alcohols. A different result came out when performing the second step. In fact, whilst ECAKR could efficiently reduce the remaining aldehyde to the alcohol, LBADH could not do the same. This caused the necessity to use the order LBADH – ECAKR only. The final result was the nearly complete conversion of **5** into **6**.

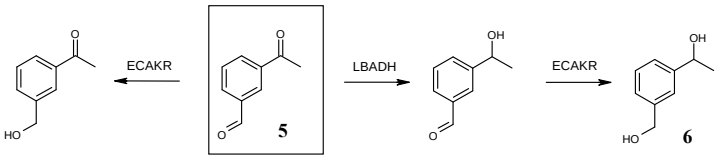

Fig. 8. Reaction sequence: LBADH, then ECAKR. The alternative order stops after the first reaction

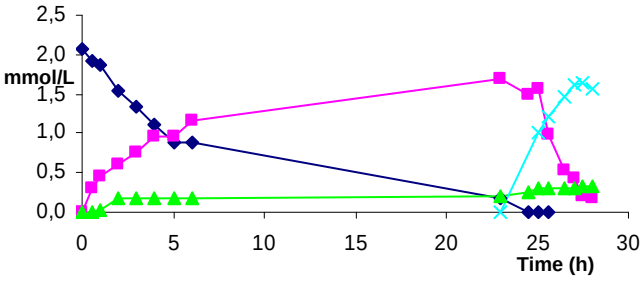

Fig. 9. HPLC analysis: ◆ketone decrease, ■alcohol increase and decrease, **X** epoxyalcohol increase, ▲side product,

Discussion

The replacement of chemical catalysts with biocatalysts is an interesting target of research. The potential benefits are evident: cleaner reactions in milder conditions, with a look to a large use of water as the solvent. In addition, the selectivity and the similar reaction conditions that are natural in the use of biocatalysts could permit a better use of multistep, one-pot reactions. As a general goal it is possible to imagine a complete substitution of chemical catalysts with biocatalysts, arriving at the simulation of cell synthesis style: series of concatenated reactions in the same container at the right time.

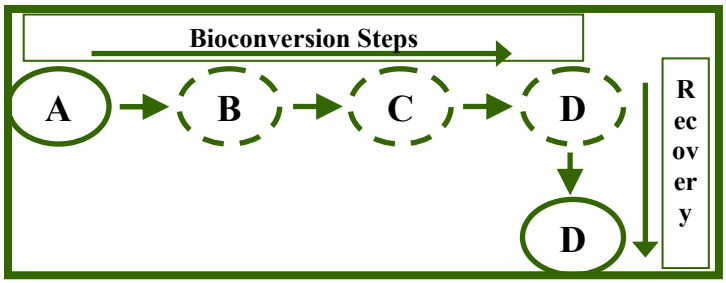

But, several developments are still necessary. They mainly concern two fundamental aspects: enzymes with specific catalytic activities and broadening of enzyme recognition power. In this work we investigated the possibility to use both whole cell and pure enzyme catalysts. Besides selecting the catalysts with the correct reactivity and their corresponding substrates, we would also like to control the possible interferences between them. Just to mention one, it could have been possible that the pure enzyme was limited in its action by the presence of a cell culture.

Our results clearly show that, at least for the selected catalysts, there is a complete independence of action. In fact, when used both in single step reactions and in sequences the yield and rate are comparable. In addition, in one case we could demonstrate that the presence of a second transformation using the product of the first reaction as substrate allows a better final result, shifting the final yield from 75% to 95%.

Overall, the results are convincing and we will continue in this study following two directions: the selection of new enzymatic activities and the preparation of longer reaction sequences. It is clear that more attention should be put in the optimization of the processes in order to improve the total yield.

ACKNOWLEDGMENTS

This work was supported by grants from the Ministry of University and Research (PRIN/2007 - Study of regulatory and catalytic systems for the development of bioconversion and biodegradation processes) and from Università degli Studi di Milano.

REFERENCES

1. **Chen G., Fournier R.L., Varanasi S.** 1997. Experimental demonstration of pH control for a sequential two-step enzymic reaction. Enz. Microbiol. Technol. **21**:491-495.
2. **Kihumbu D., Stillger T., Hummel W., Liese A.** 2002. Enzymatic synthesis of all stereoisomers of 1-phenylpropane-1,2-diol. Tetrahedron: Asymmetry. **13**:1069-1072.
3. a) **Glueck S.M., Fabian W.M.F., Faber K., Mayer S.F.** 2004. Biocatalytic asymmetric rearrangement of a methylene-interrupted bis-epoxide: Simultaneous control of four asymmetric centers through a biomimetic reaction cascade. Chem. Eur. J. **10**:3467-3478. b) **Larissegger-Schnell B., Kroutil W., Faber K.** 2005. Chemo-enzymatic synthesis of (R)- and (S)-2-hydroxy-4-phenylbutanoic acid via enantio-complementary deracemization of (±)-2-hydroxy-4-phenyl-3-butenoic acid using a racemase-lipase two-enzyme system. Synlett. 1936-1938.
4. **Hecquet L., Bolte J., Demuynck C.** 1996. Enzymic synthesis of "natural-labeled" 6-deoxy-L-sorbose precursor of an important food flavor. Tetrahedron. **52**:8223-8232.
5. **Guerard C., Alphand V., Archelas A., Demuynck C., Hecquet L., Furstoss R., Bolte J.** 1999. Transketolase-mediated synthesis of 4-deoxy-D-fructose 6-phosphate by epoxide-hydrolase-catalysed resolution of 1,1-diethoxy-3,4-epoxybutane. Eur. J. Org. Chem. 3399-3402.

6. **Zimmermann F.T., Schneider A., Schoerken U., Sprenger G.A., Fessner W.-D.** 1999. Efficient multi-enzymatic synthesis of D-xylulose 5-phosphate. Tetrahedron: Asymmetry. **10**:1643-1646.
7. **Bestetti G., Di Gennaro P., Galli E., Leoni B., Pelizzoni F., Sello G**., **Bianchi D.** 1994. Bioconversion of substituted naphthalenes to the corresponding salicylic acids. Appl. Micr. Biotech. **40**:791-793.
8. **Bernasconi S., Orsini F., Sello G., Di Gennaro P.** 2004. Bacterial monooxygenase-mediated preparation of nonracemic chiral oxiranes: study of the effects of substituent nature and position. Tetrahedron:Asymmetry **15**:1603-1606.
9. **Sello, G.; Bernasconi, S.; Orsini, F.; Mattavelli, P.; Di Gennaro, P.; Bestetti, G.** 2008. Biocatalyst expressing cis-naphthalene dihydrodiol dehydrogenase from Pseudomonas fluorescens N3 catalyzes alcohol and 1,2-diol dehydrogenase reactions. J. Mol. Cat. B: Enzymatic. **52-53**:67-73
10. **Weckbecker A., Hummel W.** 2004. Improved synthesis of chiral alcohols with Escherichia coli cells co-expressing pyridine nucleotide transhydrogenase, NADP+-dependent alcohol dehydrogenase and NAD+-dependent formate dehydrogenase. Biotechnol Lett **26**:1739-1744
11. **Wenfang L., Ping W.** 2007. Cofactor regeneration for sustainable enzymatic biosynthesis. Biotechnol. Adv. **25:**369-384
12. **Sello G., Bernasconi S., Orsini F., Di Gennaro P.** 2009. Multienzymatic preparation of (-)-[3-(oxiran-2-yl)phenyl]methanol and (-)-3-(oxiran-2-yl)benzoic acid. Tetrahedron: Asymmetry, **20**:563-565.

The catalytic potential of recombinant bacterial multicomponent monooxygenases ToMO and PH for the synthesis of antioxidant tyrosol and hydroxytyrosol in the strain *E.coli*/JM109

Viviana Izzo, Eugenio Notomista, Roberta Scognamiglio, Luca Troncone, Giuliana Donadio and Alberto Di Donato

Dipartimento di Biologia Strutturale e Funzionale, Università di Napoli Federico II, Via Cinthia, I-80126 Napoli and CEINGE-Biotecnologie Avanzate S.c.ar.l., Napoli.

Phenolic compounds present in olive oil such as tyrosol and hydroxytyrosol have been shown to provide beneficial cardiovascular effects probably due to the presence of the ortho-diphenolic group in their molecular structure. As a consequence, dietary supplements containing phenolic antioxidants from olive oil are today a major interest for pharmaceutical and food industries.

Among biocatalysts, bacterial multicomponent monooxygenases are of primary interest due to their ability to catalyze a variety of complex oxidations, including monohydroxylation and dihydroxylation reactions of phenolic compounds. In this work we have developed in the strain of *E.coli* JM109 a recombinant system based on the contemporary presence of a variant of ToMO and of PH monooxygenase systems, for the bioconversion of 2-phenylethanol in both tyrosol and hydroxytyrosol.

Olive oil is the main fat source in the Mediterranean diet and a growing experimental evidence has been accumulated in the last decades highlighting a significative connection between the regular incorporation in the diet of this natural products on one hand and health benefits such as a lower incidence of coronary heart disease and of certain cancers on the other (1-7).

Antioxidant molecules fulfill their biological role *in vivo* preserving the integrity of olives from the oxidation associated to the high temperatures and ultraviolet radiations of the Mediterranean climate (3).

Among natural phenolic compounds found in olive fruits and virgin olive oil, hydroxytyrosol is certainly one of the more attractive due to several properties such as its antibacterial activity, scavenging of free radicals, protection against oxidative DNA damage and LDL oxidation, prevention of platelet aggregation and inhibition of 5- and 12-lipooxygenases (1, 8-12).

As this *o*-diphenol is not commercially available, a lot of attention has been recently devoted to develop methods aimed at obtaining this compound either from natural sources like vegetative waters (6, 7) or through chemical synthesis (13-16). However, both these methodologies show several limitations: chemical synthesis may lead in fact to high yield of hydroxytyrosol but involves at the same time the use of toxic reagents. Furthermore, the compounds synthesized usually require further purification to get rid of any possible contamination of either toxic reagents or byproducts formed during the reaction.

The extraction of hydroxytyrosol from olive mill wastewaters, on the other hand, can be an expensive procedure that does not always result in good yield of the desired product (17-19, 8).

To overcome these drawbacks related to the production of hydroxytyrosol, much attention has been dedicated in the last years to the development of bioconversions which make use of the metabolic versatility of either purified enzymes or whole microorganisms to

Running title. Biotransformation of antioxidants

Keywords. Bioconversion, mono-oxygenase, mutagenesis, antioxidant

perform enzymatic syntheses of industrial interest (20-22). In this perspective, the utilization of Bacterial Multicomponent Monooxygenases (BMMs) (23) is of particular interest given the fact that these enzymes catalyze a variety of complex oxidations, including monohydroxylation and dihydroxylation reactions of aromatic compounds. Oxygenase biocatalysts are already used in the chemical industry to obtain additives for agriculture, synthones, drugs and plastics and, due to their catalytic properties, these multicomponent enzymes, either wild type or engineered, could represent a valid biosynthetic tool to set up bioconversions of different aromatic compounds for the production of phenolic antioxidants.

Among others, the multienzymatic systems ToMO (toluene *o*-xylene monooxygenase) and PH (phenol hydroxylase) from *Pseudomonas sp.* OX1 have been extensively studied for the analysis of the molecular determinants responsible for their regioselectivity in the hydroxylation reaction (24-27). Moreover, a computational model was recently developed that quantitatively predicts the effects on regioselectivity of mutations in the active site pocket of the hydroxylase moiety of ToMO (28), thus allowing the rational design of variants of the enzyme to be used in biosynthesis and bioremediation procedures.

The main aim of the present work has been to investigate the use of ToMO and PH enzymatic systems for the bioconversion of 2-phenylethanol (40-41), a cheap and comercially available substrate, to tyrosol and hydroxytyrosol (Fig.1). To this purpose several variants of this multicomponent monooxygenase were tested for their ability to convert 2-phenylethanol in tyrosol. ToMO variant E103G-F176S was then subcloned with a copy of the *ph* gene cluster in a single vector to develop a cell-based system of *E.coli* expressing both enzymatic activities and endowed with the ability to perform a first and a second hydroxylation reaction on the aromatic ring of 2-phenylethanol to obtain tyrosol and hydroxytyrosol, respectively.

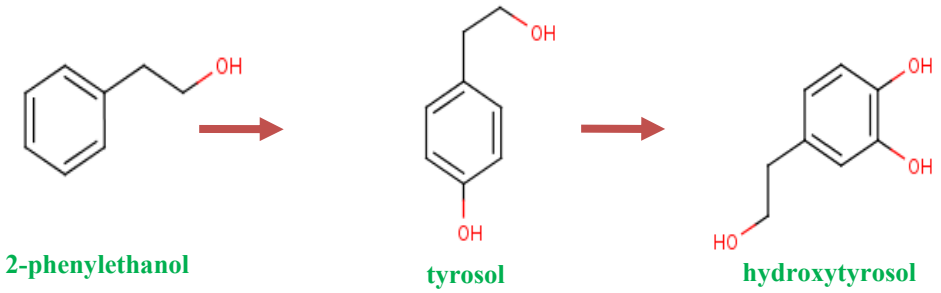

Figure 1: Strategy for the biosynthesis of hydroxytyrosol starting from 2-phenylethanol.

MATERIALS AND METHODS

Materials.. Bacterial cultures, plasmid purifications, and transformations were performed according to the procedures of Sambrook et al. (29).

ToMO A mutagenesis and construction of expression vectors. Plasmids for the expression of ToMO complexes with mutated ToMOA subunits were prepared by site-directed mutagenesis of plasmid pTOU as previously described (26). For simultaneous expression in *E.coli* of PH and E103G/F176S ToMO variant, the DNA sequence coding for the PH complex was excised from plasmid pGEM-3Z/*ph* using *SalI* and *XbaI* restriction endonucleases, while the sequence coding for the ToMO mutant was cut off using *XbaI* and *KpnI*. Both fragments were purified by agarose gel electrophoresis, ligated with the pGEM-3Z vector previously cut with *SalI* and *KpnI*, and used to transform JM109

competent cells. The resulting recombinant plasmid was designated pGEM-3Z/RS1S. It should be noted that vector pGEM-3Z/RS1S allow transcription of ToMO and PH open reading frames into a single mRNA under control of the *lac* promoter of the pGEM-3Z vector.

Whole-cell assays. The assays were performed as described previously (26) using *E. coli* JM109 cells transformed with plasmids of interest. The recombinant strains were routinely grown in Luria-Bertani medium (30) supplemented with 100 μg/ml ampicillin at 37°C to an optical density at 600 nm (OD_{600}) of ~0.6. Expression of the recombinant protein was induced with 0.1 mM isopropyl-β-D-thiogalactopyranoside at 37°C in the presence of 0.2 mM $Fe(NH_4)_2(SO_4)_2$. One hour after induction, cells were collected by centrifugation and suspended in M9 minimal medium containing 0.4% glucose. The hydroxylase activity of cells was measured with phenol as the substrate by monitoring the production of catechol in continuous coupled assays with recombinant C2,3O from *P. stutzeri* OX1, as described previously (26). Specific activity was expressed as mU/OD_{600}, one milliunit being defined as the amount of catalyst that oxidized 1 nmol of phenol per min at 25°C.

The determination of apparent kinetic parameters for 2-phenylethanol and tyrosol was carried out by two different discontinuous assays. Tyrosol produced from hydroxylation of 2-phenylethanol was estimated by the Folin-Ciocalteu reagent (30). For the calculation of the k_{cat} values, amounts of proteins were calculated as described previously (26). All the ToMO mutant enzymes showed expression levels similar to that of the wild-type enzyme.

Identification of reaction products. Reaction products were identified with a HPLC system equipped with a Waters 1525 binary pump coupled to a Waters 2996 photodiode array detector. Mono- and dihydroxylated products were separated using an Ultrasphere C_{18} reverse-phase column (4.6 by 250 mm; pore size, 80 Å), and the absorbance of the eluate at 254 for 2-phenylethanol, 275 for tyrosol and 280 nm for hydroxytyrosol was monitored. The products were identified by comparing their HPLC retention times and UV-visible spectra with those of standard solutions. The amount of each product was determined by comparing the area of the peak with the areas obtained using known concentrations of standards. For a more detailed identification of the reaction products, a NMR analysis was performed in collaboration with dr. A. Pezzella at the Department of Organic Chemistry and Biochemistry of the University Federico II of Naples.

Determination of apparent kinetic parameters. Apparent kinetic parameters were calculated with the program GraphPad Prism (GraphPad Software).

Modeling of substrates and intermediates into the active site of ToMO A. Substrates and reaction intermediates were docked into the active site of ToMO A by using the Monte Carlo energy minimization strategy. The ZMM-MVM molecular modeling package (ZMM Software Inc. [**http://www.zmmsoft.com**]) was used for all calculations. This software allows conformational searches using generalized coordinates such as torsion and bond angles instead of conventional Cartesian coordinates. Substrate and intermediate structures were prepared using the PyMOL software (DeLano Scientific LLC). Geometry was optimized using the Zl module of ZMM. Partial charges were attributed using the complete neglect of differential overlap method in the HyperChem software (HyperCube Inc. [**http://www.hyper.com**]).

The X-ray structure of the ToMO A-thioglycolate complex (PDB code 1T0Q) was used to build the models of the ToMO A-substrate and ToMO A-intermediate complexes. The docking procedure is described in detail in the supplemental material of reference 28.

Results

ToMOA variants for the bioconversion of 2phenylethanol to tyrosol. *E.coli*, strain JM109 transformed with either pGEM3Z-*ph* or pBZ1260, expressing PH and ToMo enzymatic systems respectively, were grown and induced as described in Materials and Methods. Cells were then resuspended in M9-G and incubated with either 2-phenylethanol or tyrosol at a final concentration of 5 mM. After a 14 h incubation cells were collected by centrifugation and supernatants were analyzed on HPLC as described in Materials and Methods. Identification of products was

performed by NMR and showed that ToMO was mostly active on 2-phenylethanol while PH was not. On the other hand PH was able to convert tyrosol in hydroxytyrosol whereas no product was evident after having incubated PH expressing cells with the meta isomer produced in the reaction of ToMO with 2-phenylethanol. Thus it was evident that, while PH was already a good candidate for the biosynthesis of hydroxytyrosol from 2-phenylethanol, site directed mutagenesis had to be performed in order to change the regiospecificity of ToMO on 2-phenylethanol (Fig.2).

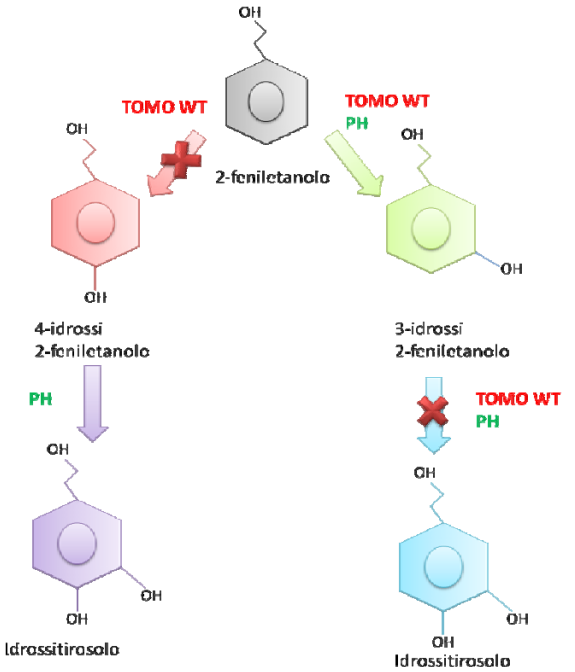

Figure 2: Scheme showing the different regioselectivity of ToMO and PH towards 2-phenylethanol and tyrosol.

In a previous paper we described a modeling strategy allowing to predict quantitatively the regioselectivity of ToMO mutants on alkylbenzenes (28). The strategy was based on a simple kinetic model (Fig. 3A-B): the substrate binds into the active site in different orientations generating productive and unproductive enzyme/substrate complexes; the three possible productive complexes are in equilibrium both with the unproductive complexes and with the three transition states leading to the *o*-, *m*-, and *p*-substituted phenols. According to this kinetic model the regioselectivity of a ToMO variant depends exclusively on the relative stability of the three different transition states. In agreement with this assumption we were able to predict the relative abundance of the products by docking of the putative high energy intermediates into the active site (28).

Here we show that our strategy can help also to design ToMO mutants able to hydroxylate efficiently and with high regioselectivity any desired substituted benzene. According to the kinetic model, the catalytic efficiency and in particular the apparent k_{cat} value of a ToMO mutant would depend both on the absolute stability of the transition state(s) and on the relative abundance of the productive and unproductive enzyme/substrate complexes (Fig. 3B).

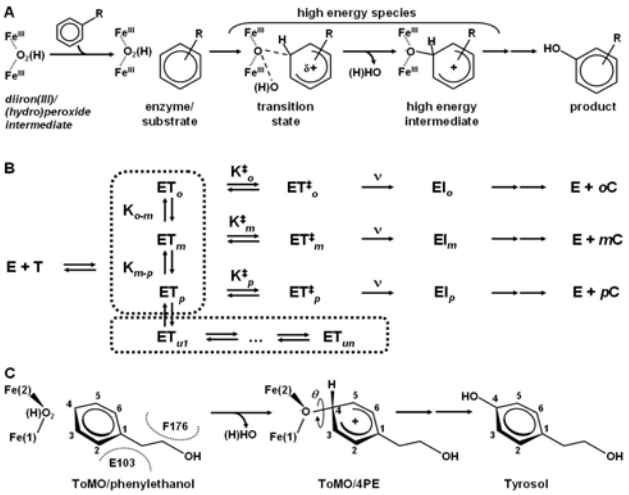

Figure 3: Kinetic model describing the regioselectivity of the hydroxylation reaction catalyzed by ToMO. ***A***) Hypothetical enzyme/substrate intermediates during the hydroxylation of an aromatic substrate in the active site of ToMOA; ***B***) Distribution and kinetic constants relative to productive and unproductive enzyme/transition state complexes; ***C***) Modeling of the 4-hydroxyphenylethanol intermediate in the active site of ToMOA.

This means that a ToMO variant will catalyze efficiently the hydroxylation of a substituted benzene to a desired substituted phenol (i) if the high energy intermediate corresponding to the desired phenol fits well to the active site, (ii) if it fits better to the active site than any other possible high energy intermediate and (iii) if the substrate is oriented productively for catalysis in a high percentage of the ToMO/substrate complexes.

Hence, we docked into the active site of wild type ToMO the three high energy intermediates for the hydroxylation of phenylethanol to 2-, 3, and 4-hydroxyphenylethanol (hereafter indicated 2PE, 3PE and 4PE, respectively). All the high energy intermediates showed considerable deviations from the ideal geometry (data not shown) in agreement with the finding that wild type ToMO is a bed catalyst for phenylethanol hydroxylation. The highest deviation from the ideal orientation was observed in the case of the intermediate 2PE and the lowest for the intermediate 3PE, in agreement with the finding that wild type ToMO produces more than 95% of 3-hydroxyphenylethanol.

The analysis of the ToMO/4PE complex showed that too close van der Waals contacts between the side chain of Phe-176 and the hydroxyethyl moiety of 4PE were responsible for the bad positioning of this intermediate and hence for the low production of 4-hydroxyphenylethanol (tyrosol) (Fig.3C). Therefore we repeated the analysis on six mutants with smaller residues at position 176 (Ile, Leu, Val, Thr, Ser, and Ala). Moreover, as Phe-176 side-chain is closely packed to Glu-103 side-chain and the mutant (E103G)-ToMO is one of the most effective catalysts for the para hydroxylation of toluene we also modeled the six double mutants (E103G, F176X)-ToMO were X is again Ile, Leu, Val, Thr, Ser, or Ala (Fig.3C). The comparison between the parameters measured by docking the intermediates 3PE and 4PE (data not shown) shows that all the mutations at position 176, both alone and in combination with mutation E103G, should improve selectively the binding of the intermediate 4PE.

ToMO variants were realized by means of site directed mutagenesis using a PCR-based methodology. Kinetic parameters on tyrosol were determined as described in the Material and Methods section, and results are presented in Table 1 (errors are within 10%).

Mutant	K_m	k_{cat} sec^{-1}	K_s $\mu M\ sec^{-1}$
F16T	662	0,14	$0,2*10^{-3}$
F176L	276	0,0 8	$0,29*10^{-3}$
F176I	392	0,028	$0,07*10^{-3}$
E103GF176T	1045	0,72	$0,69*10^{-3}$
E103GF176L	362	0,18	$0,5*10^{-3}$
E103GF176I	759	0,48	$0,62*10^{-3}$
E103GF176S	557	0,5	$0,9*10^{-3}$
E103GF176A	404	0,06	$0,14*10^{-3}$
E103GF176V	435	0,149	$0,3*10^{-3}$

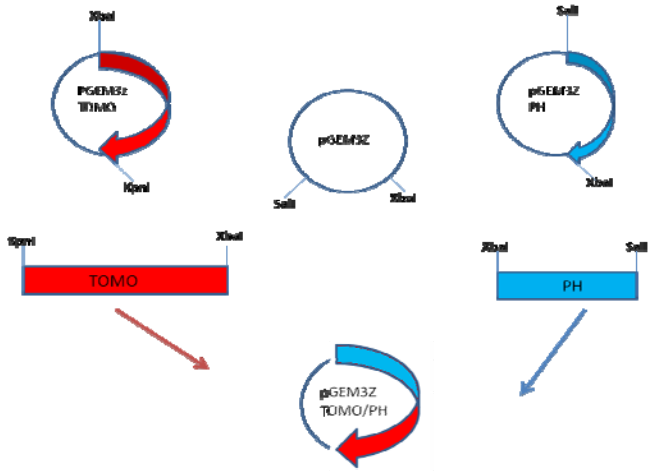

Figure 4: Cloning strategy to overexpress both ToMO and PH systems from the pGEM3Z expression vector

Cloning of ToMOA variant and of PH in a single vector for bioconversion of 2-phenylethanol in hydroxytyrosol. The strategy used to subclone in a unique expression vector ToMOA variant E103G-

F176S with a copy of the *ph* gene cluster is described in the Material and Methods section and is shown in Fig.4.

The plasmid obtained was used to transform competent cells of *E.coli*, strain JM109, which were used in a biotransformation assay of 2-phenylethanol. HPLC analysis of the supernatant obtained after 14 hours of incubation shows the presence in the growth medium of both tyrosol and hydroxytyrosol, showing that the contemporary presence of the two monooxygenase systems allows for the complete procedure of biosynthesis to occur. Data to calculate the yield of this process are still under investigation.

Discussion

In this work we investigated the use of recombinant multicomponent monooxygenase systems ToMO (toluene *o*-xylene monooxygenase) and PH (phenol hydroxylase) for the biosynthesis in a recombinant strain of *E.coli* of tyrosol and hydroxytyrosol from 2-phenylethanol, a cheap and commercially available substrate. Due to the inability of ToMO *wt* to convert 2-phenylethanol in 4-hydroxyphenylethanol (tyrosol), we developed a new computational model to design several ToMO variants to overcome this problem and we identified in the residue Phe-176 a major steric hindrance for the correct positioning of the reaction intermediate leading to tyrosol production (indicated as 4PE). The data obtained show that all the mutations at position 176, both alone and in combination with mutation E103G, allow the ToMO multicomponent system to produce exclusively tyrosol from 2-phenylethanol. Moreover, as shown in Table 1, variants bearing also mutation E103G, which does not affect the regioselectivity of the hydroxylation reaction on 2-phenylethanol, are more effective on this substrate if compared to the corresponding single mutants in position Phe176-X.

From a kinetic point of view, the high values of K_M and the relatively low values of k_{cat} suggest that more mutations are probably necessary to improve this first step of hydroxylation on 2-phenylethanol. To this purpose future mutations might be performed in a different region of the enzyme and more specifically in the entry channel of the active site. The data show that Ks values are comparable among the double mutants, the most effective catalyst being variant E103G/F176S. This latter was consequently chosen to be subcloned with the *ph* gene cluster to allow complete biosynthesis of hydroxytyrosol from 2-phenylethanol. Future experiments are now aimed at optimizing the yield of hydroxytyrosol obtained by this recombinant system in the strain of *E.coli* JM109.

ACKNOWLEDGMENTS

This work was supported by grants from the Ministry of University and Research (PRIN/2007).

REFERENCES

1. **Owen RW. Giacosa A., Hull WE., Haubner R., Würtele G., Spiegelhalder B., Bartsch H.** 2000. Olive-oil consumption and health: the possible role of antioxidants. Lancet Oncol. **1**:107-112.
2. **Rietjens SJ., Bast A., and Haenen GRMM. 2007.** New insights into controversies on the antioxidant potential of the olive oil antioxidant hydroxytyrosol. J. Agric. Food Chem. **55**: 7609-7614.
3. **Visioli F., Poli A., Galli C.** 2002. Antioxidant and other biological activities of phenols from olives and olive oil. Med. Res. Rev. **22**: 65-75.
4. **Waterman E., Lockwood B.** 2007. Active components and clinical applications of olive oil. Altern. Med. Rev. **12**: 331-342.

5. **Visioli F., Bellomo G., Galli C. 1998.** Free radical-scavenging properties of olive oil polyphenols. Biochem. Biophys. Res. Commun. **247**: 60-64.
6. **Ranalli A., Lucera L., Contento S.** 2003**.** Antioxidizing potency of phenol compounds in olive oil mill waste waters. J. Agric. Food Chem. **51**: 7636-7641.
7. **Capasso R., Cristinzio G., Evidente A., Scognamiglio F.** 1992. Isolation, spectroscopy and selective phytotoxic effects of polyphenols from vegetable waste waters. Phytochemistry. **12**: 4125-4128.
8. **Espin JC., Soler-Rivas C., Cantos E., Tomas-Barberan FA., Wichers HJ.** 2001. Synthesis of the antioxidant hydroxytyrosol using tyrosinase as biocatalyst. J. Agric. Food Chem. **49**: 1187-1193.
9. **De la Puerta R., Ruiz Gutierrez V., Hoult JR.** 1999. Inhibition of leukocyte 5-lipoxygenase by phenolics from virgin olive oil. Biochem Pharmacol. **57**: 445-9.
10. **Deiana M., Aruoma OI., Bianchi ML., Spencer JP., Kaur H., Halliwell B., Aeschbach R., Banni S., Dessi MA., Corongiu FP.** 1999. Inhibition of peroxynitrite dependent DNA base modification and tyrosine nitration by the extra virgin olive oil-derived antioxidant hydroxytyrosol. Free Radic Biol Med. **26**:762-769.
11. **Salami M., Galli C., De Angelis L., Visioli F.** 1995. Formation of F2-isoprostanes in oxidized low density lipoprotein: inhibitory effect of hydroxytyrosol. Pharmacol. Res. **31**: 275-279.
12. **Petroni A., Blasevich M., Salami M., Papini N., Montedoro GF., Galli C.** 1995. Inhibition of platelet aggregation and eicosanoid production by phenolic components of olive oil. Thromb Res. **78**: 151-160.
13. **Baraldi PG., Simoni D., Manfredini S., Menziani E.** 1983. Preparation of 3,4-dihydroxy-1-benzeneethanol: a reinvestigation. Liebigs Ann. Chem. **83**: 684-686.
14. **Azabou S., Najjar W., Ghorbel A., Sayadi S.** 2007. Mild photochemical synthesis of the antioxidant hydroxytyrosol via conversion of tyrosol. J Agric Food Chem. **55**: 4877-4882.
15. **Bernini R., Mincione E., Barontini M., Crisante F.** 2008. Convenient synthesis of hydroxytyrosol and its lipophilic derivatives from tyrosol or homovanillyl alcohol. J Agric Food Chem. **56**: 8897-8904.
16. **Capasso R., Evidente A., Avolio S., Solla F.** 1999. A highly convenient synthesis of hydroxytyrosol and its recovery from agricultural waste waters. J Agric Food Chem. **47**: 1745-1748.
17. **Sayadi S., Ellouz R.** 1995. Roles of Lignin Peroxidase and Manganese Peroxidase from Phanerochaete chrysosporium in the Decolorization of Olive Mill Wastewaters. Appl Environ Microbiol. **61**: 1098-1103.
18. **Hamdi H.** 1993. Future prospects and constraints of olive mill wastewaters use and treatment: a review. Bioprocess Eng. **8**: 209–214.
19. **Dordick JS., Khmelnitsky YL., Sergeeva MV.** 1998. The evolution of biotransformation technologies. Curr.Opin. Microbiol. **1**: 311-318.
20. **Ishige T., Honda K., Shimizu S.** 2005. Whole organism biocatalysis. Curr. Opin. Chem. Biol. **9**: 174–180.
21. **Straathof AJ., Panke S., Schmid A.** 2002. The production of fine chemicals by biotransformations. Curr Opin Biotechnol. **13**: 548-56.
22. **Bouallagui Z., Sayadi S.** 2006. Production of high hydroxytyrosol yields via tyrosol conversion by Pseudomonas aeruginosa immobilized resting cells, J. Agric. Food Chem. **54**: 9906-9911.
23. **Harayama S., Timmis KN.** 1992. Aerobic degradation of aromatic hydrocarbons by bacteria. In: Sigel H, Sigel A (eds) Metal ions in biological

systems. Marcel Dekker, New York. **28**: 99-156.

24. **Cafaro V., Izzo V., Scognamiglio R., Notomista E., Capasso P., Casbarra A., Pucci P., Di Donato A.** 2004. Phenol hydroxylase and toluene/o-xylene monooxygenase from Pseudomonas stutzeri OX1: interplay between two enzymes. Appl Environ Microbiol. **70**: 2211-9.
25. **Sazinsky MH., Bard J., Di Donato A., Lippard SJ.** 2004. Crystal structure of the toluene/o-xylene monooxygenase hydroxylase from Pseudomonas stutzeri OX1. Insight into the substrate specificity, substrate channeling, and active site tuning of multicomponent monooxygenases. J Biol Chem. **279**: 30600-10.
26. **Cafaro V., Notomista E., Capasso P., Di Donato A.** 2005. Regiospecificity of two multicomponent monooxygenases from Pseudomonas stutzeri OX1: molecular basis for catabolic adaptation of this microorganism to methylated aromatic compounds. Appl Environ Microbiol. **71**: 4736-4743.
27. **Cafaro V., Notomista E., Capasso P., Di Donato A.** 2005. Mutation of glutamic acid 103 of toluene o-xylene monooxygenase as a means to control the catabolic efficiency of a recombinant upper pathway for degradation of methylated aromatic compounds. Appl Environ Microbiol. **71**: 4744-50.
28. **Notomista E., Cafaro V., Bozza G., Di Donato A.** 2009. Molecular determinants of the regioselectivity of toluene/o-xylene monooxygenase from Pseudomonas sp. strain OX1. Appl Environ Microbiol. **75**: 823-36.
29. **Sambrook J., Fitsch EF., Maniatis T.** 1989. *Molecular Cloning: A Laboratory Manual.* Cold Spring Harbor, Cold Spring Harbor Press.
30. **Singleton VL., Orthofer R., Lamuela-Raventós RM.** 1999. Analysis of total phenols and other oxidation substrates and antioxidants by means of Folin-Ciocalteu reagent. Methods Enzymol. **299**: 152–177.

Novosphingobium sp. PP1Y has adapted to use the aromatic fraction of fuels oils as the sole carbon and energy source

Eugenio Notomista[1,2], Francesca Pennacchio[1], Valeria Cafaro[1], Viviana Izzo[1,2], Luca Troncone[1], Mario Varcamonti[1], and Alberto Di Donato[1,3]

[1]Dipartimento di Biologia Strutturale e Funzionale, Università di Napoli Federico II, Complesso Universitario di Monte S. Angelo, Via Cinthia 4- 80126 Naples, Italy; [2]Facoltà di Scienze Biotecnologiche, Università di Napoli Federico II and [3]CEINGE-Biotecnologie Avanzate S.c.ar.l., Naples, Italy.

Strain *Novosphingobium* sp. PP1Y, isolated from a surface seawater sample collected from a closed bay in the harbor of Pozzuoli (Naples, Italy), uses fuel oils as the sole carbon and energy source. Like other Sphingomonads this bacterium shows a "planktonic/sessile dimorphism" growing both in a sessile form made up of aggregated cells (flocks) and a planktonic form (free cells). Moreover, it forms a biofilm layer on several types of solid and liquid hydrophobic surfaces including polystyrene, polypropylene and diesel-oil. While growing on diesel oil and in orbital shaking, strain PP1Y emulsifies the oil phase to small drops coated by a layer of extracellular material and bacterial cells.

Strain PP1Y is not able to grow on pure linear alkanes, cyclic alkanes and alkane mixtures but is able to grow on a surprisingly wide range of aromatic compounds including mono, bi, tri and tetracyclic aromatic hydrocarbons and heterocyclic compounds. The peculiar features of strain PP1Y suggest that it has adapted to efficiently grow at the water/fuel oil interface using the aromatic fraction of the fuel oils as the sole carbon and energy source.

Aromatic compounds are among the most widespread and dangerous pollutants. Several polycyclic aromatic hydrocarbons (PAH), like naphthalene and phenanthrene, are very toxic for aquatic organisms (4, 6, 13), whereas, benzene, chrysene, benzo[a]anthracene, benzo[a]pyrene and aromatic amines are carcinogenic and represent a direct risk for human health (2, 20). Coal, petroleum and their derivatives are the main sources of aromatic compounds released into the environment. Depending on the oilfield, petroleum can contain from about 20% to more than 40% aromatic hydrocarbons (1, 8, 10, 25).

Gasoline contains up to 25% mono- and up to 10% poly-cyclic aromatic hydrocarbons (19). Diesel-oil, on the contrary, contains a larger amount of PAHs – up to 20% – and only 5-6% alkylbenzenes (11). These aromatic fractions are extremely complex including tens if not hundreds of molecules belonging to (poly)alkyl-benzenes, PAHs, (poly)alkyl-PAHs, naphthenes (i.e. polycyclic compounds with fused aromatic and saturated rings) and heterocyclic compounds containing nitrogen, sulfur or oxygen.

Fuel spills do not occur only during accidents involving oil tankers but daily during fuel transfers thus generating widespread hydrocarbon pollution. Likely, this explains why hydrocarbon degrading bacterial strains are so largely diffused in the environment. The so-called "obligate hydrocarbonoclastic bacteria", like *Alkanivorax*, *Marinobacter* and *Oleispira* (27), are among the most effective oil degraders. However, these bacteria degrade prevalently if not exclusively the saturated fraction of petroleum and oil fuels. The most

Running title. Growth of *Novosphingobium* sp. PP1Y on fuel oils.

Keywords. Bioremediation, *Novosphingobium*, Sphingomonadales, fuel oil, polycyclic aromatic hydrocarbon.

effective degraders of aromatic compounds belong to Sphingomonads (Gram-), Pseudomonads (Gram-), and Mycobacteria (Gram+) (17, 23). Sphingomonads are unusual alpha-proteobacteria which contain glycosphingolipids instead of the more common lipopolysaccharides in the outer membrane (9). This peculiarity makes their cell surface more hydrophobic than that of other Gram- strains and this is considered one of the reasons why several Sphingomonads have developed the ability to degrade mono and polycyclic aromatic compounds (17, 23). Some interesting examples are *Novosphingobium aromaticivorans*, which can use alkyl-benzenes as the sole carbon and energy sources (3), *Novosphingobium pentaromativorans* US6-1^T, which degrades PAHs with 3-5 rings (22), *Sphingomonas paucimobilis* EPA505, which degrades several polycyclic compounds (24), and *Sphingomonas wittichii* RW1^T, which can grow using dibenzofuran and dibenzo-*p*-dioxin and co-metabolizes mono and dichloro-derivatives of these toxic aromatic compounds (26).

We report the characterization of strain *Novosphingobium* sp. PP1Y a bacterium isolated from a surface seawater sample collected from a bay for the docking of small boats in the harbor of Pozzuoli (Naples, Italy). The strain PP1Y not only uses a surprisingly large number of mono and polycyclic aromatic compounds as the sole carbon and energy sources but shows a very interesting and effective adaptation to grow on complex mixtures of aromatic compounds dissolved in oil phases like diesel-oil and gasoline.

MATERIALS AND METHODS

Materials. All the chemicals, including saturated and aromatic hydrocarbons, were from Sigma and were of the best available purity. Car diesel oil and gasoline were from Agip, Exxon and Q8.

Culture Media. Luria Bertrani (LB) broth was prepared according to Sambrook et al. (18). Sea-Salts medium contained the indicated amount (0.5-5%, w:v) of sea salts (Sigma-Aldrich) and 1 g/l NH_4Cl. M9 medium contained 7 g/l Na_2HPO_4, 3 g/l KH_2PO_4, 1 g/l NH_4Cl, and 0.5 g/l NaCl. pH was adjusted to 6.9. After autoclaving 5 ml of a *trace element solution* were added to 1 l of cooled M9. *Trace element solution* contained: 30.1 g/l $MgSO_4$, 27.3 g/l $FeSO_4$ x $7H_2O$, 5.4 g/l MgO, 1.0 g/l $CaCO_3$, 0.72 g/l $ZnSO_4$ x 7 H_2O, 0.56 g/l $MnSO_4$ x H_2O, 0.125 g/l $CuSO_4$ x 5 H_2O, 0.14 g/l $CoSO_4$ x 7 H_2O, 0.03 g/l H_3BO_3, 0.004 g/l $NiCl_2$ x 6 H_2O, 0.006 g/l Na_2MoO_4 x 2 H_2O, and 25.6 ml/l HCl (36%). Potassium phosphate minimal medium (PPMM) contained 20 mM potassium phosphate at pH 6.9, 1 g/l NH_4Cl and the indicated amount of NaCl (0-5%, w:v). The *trace element solution* was added as described for the M9 medium.

Phenanthrene-Agar plates. 20 ml of liquid M9-agar (1%) were added to a Petri plate and allowed to solidify. 20 mg of phenanthrene were dissolved in 0.6 ml of methanol and added to 5 ml of liquid M9-agar (1%). The resulting milky solution was spread on the M9-agar layer and allowed to solidify.

Isolation of Strain PP1Y. Seawater samples were collected inside the harbor of Pozzuoli (Naples, Italy). All samples were collected at the surface and close to oil stains. Phenanthrene crystals were added to seawater samples. After two-three weeks of incubation at 25°C some samples showed the appearance of turbidity and/or brown/yellow color which are indications of microorganisms growth. These samples were used to inoculate M9 containing phenanthrene as the sole source of carbon and energy. After two/three weeks of incubation turbid and/or colored cultures were used to inoculate fresh medium containing PAHs as the sole carbon source. After three-four rounds of enrichment, aliquots were spread on agar plates containing phenanthrene as the sole carbon source. Several yellow colonies surrounded by clear halos were observed on plates. Strain PP1Y was isolated starting from one of these colonies and purified through four plating cycles on LB.

Strain PP1Y has been deposited at the DSMZ-Deutsche Sammlung von Mikro-organismen und Zellkulturen GmbH (Inhoffenstr. 7 B38124 Braunschweig, Germany) with identification code DSM 19530 (patent pending ITMI20081407).

Identification of Strain PP1Y. To identify strain PP1Y, 16S rDNA gene was sequenced at BMR Genomics (Padova, Italy, http://www.bmr-

genomics.it). The sequence was compared with sequences available in the GenBank database using the BLAST search system.

Optimal salt concentration, pH and temperature for growth of PP1Y. In order to find out the optimum salt concentration, 10 µl aliquots of a culture grown in LB (about 1 $O.D._{600nm}$) were inoculated in 10 ml of PPMM containing 5 g/l of tryptone, 2,5 g/l of yeast extract, and NaCl from 0% to 5% (w/v) or in 10 ml of Sea-Salts medium (0.5-5%, w/v) containing 5 g/l of tryptone, 2,5 g/l of yeast extract, and incubated at 30 °C. The optimal pH was determined using PPMM containing 5 g/l of tryptone, 2,5 g/l of yeast extract, and 10 mM NaCl. The pH of the solutions was adjusted at the desired value (5.5-8.5). The optimum temperature was determined by inoculating cells of strain PP1Y in LB medium and incubating the cultures at different temperatures. Growth was monitored by measuring the optical density at 600 nm.

Growth on fuel oils. Growth on diesel-oil, gasoline and paraffin-dissolved gasoline as the sole source of carbon and energy was performed using PPMM containing 10-250 mM NaCl or Sea-Salts medium (0.5%-2%). Cultures were incubated at 30 °C under orbital shaking. Bacterial growth was followed by measurement of absorbance at 600 nm or by measuring total proteins, carbohydrates and DNA of the cultures as described below.

Growth on single hydrocarbons. Utilization of individual aromatic compounds as growth substrates was determined by supplementing 10 ml of PPMM containing 10 mM NaCl with 8 mg of an aromatic compound in liquid or crystalline form (depending on the hydrocarbon) or with 8 mg of the pure aromatic compound dissolved in 400 µl of *n*-dodecane (C_{12}), *n*-tetradecane (C_{14}), low viscosity paraffin (LVP) or high viscosity paraffin (HVP). The final concentration of the liquid aromatic hydrocarbons (0.8 g per liter of culture) was 7.5 mM in the case of xylenes and ethylbenzene and 6.6 mM in the case of propylbenzene and ethyltoluenes. For each aromatic substrate several cultures were incubated in 50 ml polypropylene tubes at 30 °C under orbital shaking. At increasing times the cultures were freeze-dried and the dried material was washed twice with 5 ml of hexane and twice with 5 ml of water-saturated diethyl ether/methanol/water = 8:3:1 (v/v/v) to remove oils, lipids and salts (5). The washed material was dried under nitrogen and dissolved in 5 ml of 20 mM H_2SO_4 containing 10% ethanol.

The protein content was assayed with the Bradford reagent (Sigma), using bovine serum albumin as standard. The total carbohydrate content was assayed by the phenol/H_2SO_4 method (7) using glucose as standard. The DNA content was assayed with ethidium bromide using plasmid pGEM-3Z (Promega) as standard. The samples were diluted in Tris acetate 0.1 M pH 8 containing 10 mM EDTA and mixed with an ethidium bromide solution (Sigma) in a ratio 10000:1 (v/v) according to the manufacturer instructions. The fluorescence of the samples was measured using a Chemidoc XRS densitometer (BioRad).

Phase contrast microscopy. An Olympus BX-51 phase contrast microscope equipped with a DP-70 camera was used to obtain images of flocks, oil drops and mucilaginous sheets. Except when specifically indicated samples were not fixed or stained.

Nucleotide sequence accession numbers. The 16S rRNA gene sequence has been deposited in GenBank under accession number GU244504.

Results

Isolation of strain PP1Y. Strain PP1Y was isolated through a standard enrichment procedure using PAHs from a seawater sample collected at the sea surface. Small amounts of liquid cultures, deposited on M9-Agar plates containing phenanthrene as the sole carbon source, formed light yellow colonies surrounded by a clear halo in about 5-7 days at 25°C (data not shown). The appearance of a clear halo in the milky layer of phenanthrene crystals is an indication that the colonies are able to degrade phenanthrene causing dissolution of crystals. Plated on phenanthrene-M9-Agar plates strain PP1Y was able to decolorize almost completely the plate in about one week (data not shown).

Analysis of 16S rDNA gene and identification of strain PP1Y. A fragment of the 16S rDNA gene obtained by PCR using universal primers was sequenced and the sequence was used to search the GenBank database. 96-99% sequence identity was found with the rDNA sequences of several *Novosphingobium* strains, whereas, 92-97%

sequence identity was found with the rDNA sequences of several *Sphingomonas*, *Sphingobium* and *Sphingopixis* strains (data not shown).

Strain PP1Y is closely related to *N. pentaromativorans* US6-1^T (2 differences in a 1481 bases-long alignment) a strain isolated in Korea and able to degrade PAH with 3-5 rings. Therefore on the basis of the 16S rRNA sequence, strain PP1Y can be considered a new strain of *N. pentaromativorans*. However, strains PP1Y and US6-1^T differ in several relevant physiological features including optimal salinity, metabolic properties, motility and "planktonic/sessile dimorphism" – as described in the following sections – thus suggesting that strain PP1Y could be a new *Novosphingobium* species rather than a new strain of *N. pentaromativorans*.

Phenotypic characterization of strain PP1Y. The strain yields positive results in the assays for citrate assimilation, β-galactosidase, urease, and arginine-dihydrolase activities. In the same tests strain US6-1^T yields negative results (22). Moreover, the lipidic constitution of the strain is more similar to that of *Novosphingobium subarcticum* JCM10398^T than to that of *Novosphingobium pentaromativorans* US6-1^T (22) (data not shown).

Novosphingobium sp. PP1Y is able to grow at NaCl concentrations ranging from 0% to 4% (w:v). Highest growth rates can be measured at NaCl concentrations between 0.5% and 1.5% (w:v). Growth is very slow at NaCl concentrations above 5%. These features suggest that strain PP1Y is able to grow either in seawater or in brackish water, like river estuaries and costal lagoons and that these environments could be the main ecological niche of strain PP1Y.

It is interesting to note that the behavior of strain US6-1^T is very different. In fact, the highest growth rate for this strain is observed at 2.5% NaCl. Moreover, the strain is not able to grow at NaCl concentrations below 1% (22).

Strain PP1Y is able to grow in a wide range of temperatures (from about 18°C to 42°C) and of pH values (from 5 to about 7.5). Highest growth rate is observed at 32-34°C and pH 6.0-7.0 in rich media and at 29-30°C in minimal media.

Morphological analysis of strain PP1Y. Cells of *Novosphingobium* sp. PP1Y, observed by phase contrast microscopy, appear as short rods. They can be motile (likely flagellate) or non- motile (data not shown). Non-motile cells can form aggregates of different dimensions from 50-100 μm to macroscopic "flocks" 1-10 mm long. The number and dimension of flocks is influenced by several parameters including shaking, temperature and growth substrates. For example, formation of flocks is favored by slow shaking, by high temperature (34°-38°C), by the presence of casaminoacids and mediums with high phosphate concentrations like M9. Dried and stained with methylene blue, flocks show the presence of bunches of cells trapped inside a blue-stained matrix (data not shown). A similar behavior has already been described for some other Sphingomonads which show the so-called "planktonic/sessile dimorphism" (15). These dimorphic strains can exist in a sessile form made up of aggregated cells joined by polysaccharidic extracellular material, and a planktonic form of free cells. About 5% of the free cells are motile, possessing a single polar flagellum (15). It is interesting to note that no planktonic/sessile dimorphism has been described for *Novosphingobium pentaromativorans* US6-1^T.

Flocks formed by strain PP1Y posses also some peculiar features. They adsorb hydrophobic and/or cationic dyes like methylene blue and Red Sudan III (not shown), and adhere to hydrophobic surfaces as plastic polymers (for example polypropylene and polystyrene). Moreover, *Novosphingobium* sp. PP1Y forms a biofilm on several types of hydrophobic surfaces. A yellow biofilm layer is formed by *Novosphingobium* sp. PP1Y cultured in

polystyrene Petri plates containing liquid reach medium in about 24 h. After about 48-72 h the plates contain a homogeneous gelatinous layer 3-4 mm thick (not shown). The biofilm, detached from the plates by vigorous shaking, forms gelatinous sheets. Formation of biofilm is observed also on polypropylene surfaces, and, more surprisingly, at the boundary between a liquid aqueous phase and an oil phase.

Growth on fuels. *Novosphingobium* sp. PP1Y is able to use diesel-oil and gasoline as the sole carbon and energy source (data not shown). Diesel-oil is well tolerated – at least up to a ratio 1:1 water:diesel-oil (v/v) – whereas gasoline is more toxic. The highest concentration allowing growth of the strain was found to be 50:1 water:gasoline (v/v). This is likely due to the fact that gasoline is a light fraction of petroleum and contains low molecular weight, hydrosoluble hydrocarbons like hexane and cyclohexane which damage cell membranes and proteins (16, 21). In fact, gasoline diluted 3-5 fold (v/v) in LVP – a mixture of medium and long chain alkanes which can reduce partitioning of small hydrocarbon to the water phase – is less toxic than pure gasoline and allows to obtain higher growth rates and higher cell densities (not shown).

During growth under orbital shaking in biphasic systems water/diesel-oil and water/(gasoline-paraffin) *Novosphingobium sp.* PP1Y provokes emulsification of the oil phase which spreads in small drops with a diameter ≤ 1 mm. When shaking is stopped drops stratify at the surface but do not join together to form a homogeneous oil phase. Analysis of the diesel-oil drops by phase contrast microscopy reveals that each drop is coated by bacterial cells at a density roughly increasing with the incubation time (Fig. 1B-D). Under UV light drops appear enlightened from the inside by an intense blue fluorescence typical of PAHs (Fig. 1B-C). This finding confirms that cell-coated drops contain diesel-oil. Several drops show irregularities or disruption of the coating (Fig. 1E), likely due to collisions with other drops or with the test tube, which suggests the existence of a layer of extracellular material. Moreover, in aged cultures "super-aggregates" were detected formed by two or more coated drops clearly glued by strongly refractive material (Fig. 1F). These finding suggest that *Novosphingobium sp.* PP1Y has developed a "mechanical" emulsification strategy based on the physical entrapment of small quantities of oil phase.

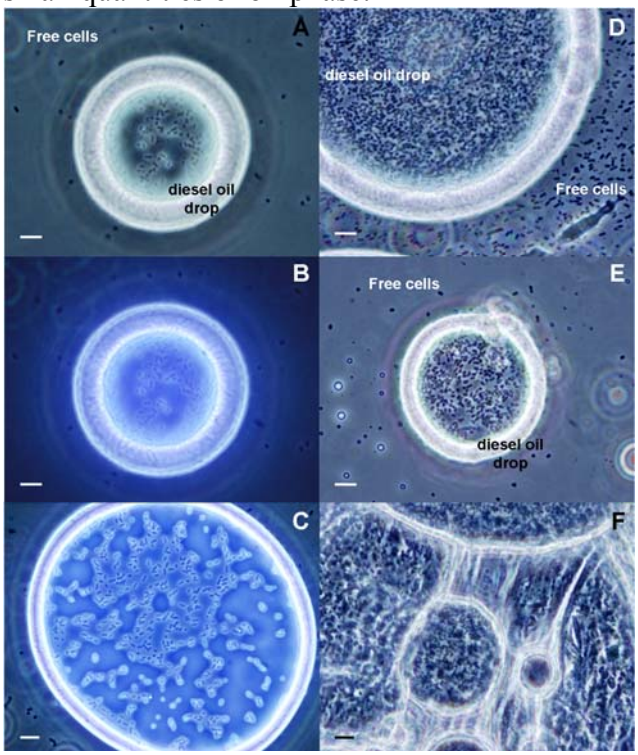

Fig. 1. Phase contrast microscopy analysis of coated diesel-oil drops. A) and B) Coated diesel-oil drop after 2 days of incubation observed using visible light only or UV/visible light, respectively. C) Coated diesel-oil drop after 2 days of incubation observed using UV/visible light. D) Coated diesel-oil drop after 10 days of incubation. E) Diesel-oil drop with damaged coating. F) Super-aggregates of coated drops. Bar = 10 μm.

Growth on single hydrocarbons. *Novosphingobium sp.* PP1Y is not able to grow on pure linear alkanes, like hexane, *n*-decane, C_{12}, C_{14}, *n*-pentadecane, on pure cyclic alkanes, like cyclohexane, and on alkane mixtures like LVP and HVP. On the contrary, it is able to grow on a surprisingly

wide range of aromatic hydrocarbons (Table 1). Except benzene and 1,2,3-trimethylbenzene, *Novosphingobium sp.* PP1Y is able to grow on all mono and bicyclic aromatic hydrocarbons commonly found in petroleum-derived fuels (Table 1). Except isopropylbenzene, and butylbenzene, all liquid aromatic hydrocarbons (Table 1) are good growth substrates, allowing to obtain cultures with $O.D._{600nm}$ values ≥ 0.5 in less than 4-7 days (not shown). Moreover these aromatic hydrocarbons sustain similar growth efficiency if provided either in pure form or dissolved in C_{12}, C_{14}, LVP, or HVP at 0.5%-2.0% (w/v) as shown in Fig. 2A-B for *p*-xylene. Biphenyl, naphthalene, phenanthrene and the dimethylnaphthalenes which are solid at room temperature allow similar growth rates only in oil-dissolved form (Fig. 2C-D). Pure crystals of these hydrocarbons yield a much slower growth likely due to their low water solubility (less than 1.5 mg/l in the case of phenanthrene) (not shown).

Oil-dissolved anthracene, pyrene, chrysene, benz[a]anthracene, and fluoranthene allow slower growth (incubation times > 7-10 days) and lower growth efficiencies (Fig. 2F shows the case of pyrene). The slow growth could be attributed to the lower bio-availability of these PAHs which not only have water solubility 100-10000 lower than that of naphthalene (table 1) but have also low solubility in liquid paraffins.

Table 1. Growth of strain PP1Y in biphasic cultures containing gasoline, diesel-oil or a single aromatic hydrocarbon in C_{14} (2%, w/v).

	Hydrocarbon[a]	**Solubility in water (mg/l)**	**Log K_{ow}**	**Growth**[b]
	diesel-oil			F,C,T
	gasoline			F,T
monocyclic aromatic	*benzene*	1760	2.13	-
	toluene	515	2.69	F,c
	o-xylene	178	2.8-3.1	F,c
	m-xylene	161	3.2	F,c
	p-xylene	162	3.15	F,c
	ethylbenzene	152	3.15	f,c,s
	2-ethyltoluene	93	3.53	F,c
	3-ethyltoluene	94	3.88	f,c,s
	4-ethyltoluene	95	3.90	F,c,s
	propylbenzene	60	3.6	S
	isopropylbenzene	61	3.66	S(*slow*)
	1,2,3-trimethylbenzene	75	3.66	-
	1,2,4-trimethylbenzene	58	3.65	F,c
	1,3,5-trimethylbenzene	48	3.42	F,c
	butylbenzene	50	4.4	c/S(*slow*)
naphthenes	*indan*[c]	109	3.33	f
	tetrahydronaphthalene	47	3.5-3.8	S
	acenaphthene	4	3.92	S
	fluorene	2	4.18	f,c(*slow*)
polycyclic	naphthalene	32	3.36	F,c
	1-methylnaphthalene	28	3.87	F,c
	2-methylnaphthalene	25	3.86	F,c
	1,2-dimethylnaphthalene	15	4.31	F,c

	1,3-dimethylnaphthalene	8	4.6	F,c
	1,7-dimethylnaphthalene		4.44	f,c,T
	2,3-dimethylnaphthalene	3	4.6	F,c
	2,6-dimethylnaphthalene	2	4.31	F,c
	2,7-dimethylnaphthalene			F,c
	biphenyl	7.5	4.09	F,c
	phenanthrene	1.3	4.57	F,c,T
	fluoranthene	0.26	5.22	c
	pyrene	0.13	4.88	S
	anthracene[d]	0.07	4.5	c,s(*slow*)
	benzo[a]anthracene[d]	0.014	5.91	c,s(*slow*)
	chrysene[d]	0.002	5.86	c,s(*slow*)
hetero cyclic	dibenzofuran	10	4.17	S
	carbazol	1.8	3.72	S
	dibenzothiophene	1.47	4.38	S

[a] Aromatic hydrocarbons that are liquid at room temperature are reported in italics.
[b] F = amorphous flocks and/or free cells (≥ 0.5 $O.D._{600nm}$); f = amorphous flocks and/or free cells (<0.5 $O.D._{600nm}$); C = emulsion containing coated oil drops (high cell density); c = emulsion containing coated oil drops (low cell density); T = biofilm on the polypropylene tube; S = formation of mucilage containing sheets visible by the naked eye; s = formation of sheets; - = no growth.
[c] Indan was used at 1% (w/v).
[d] Due to their low solubility in paraffins, anthracene, benz[a]anthracene and chrysene were used as saturated solutions in C_{14}.

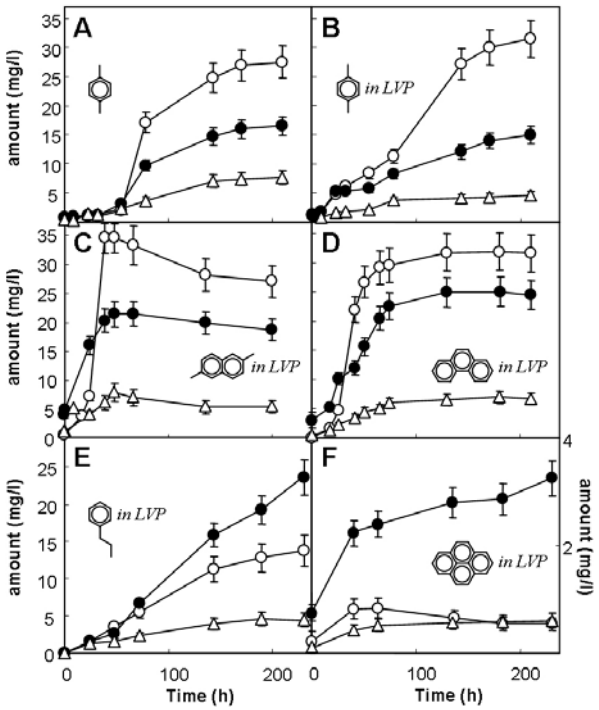

Fig. 2. Composition of cultures grown using single aromatic hydrocarbons. Empty circles, total proteins; filled circles, total carbohydrates; empty triangles, total DNA.

Discussion

Sphingomonads able to degrade aromatic hydrocarbons have been frequently isolated from soil or fresh water, seawater and wastewater sediments (3, 12, 14, 22). On the contrary, strain *Novosphingobium* sp. PP1Y described in this paper has been isolated from sea surface. Adaptation of this strain to grow at the water/oil interface led it to develop several peculiar features which make it very well suited for the use in *in situ* bioremediations interventions. In fact, the presence of several aromatic hydrocarbons in complex mixtures improves its growth and degradation capabilities rather impairing them. Diesel-oil and gasoline, which are among the most complex hydrocarbon mixtures, are the best growth substrates. The ability of strain *Novosphingobium* sp. PP1Y to spontaneously form biofilm on several surfaces could allow the adhesion of cells to soil, sand and mud particles thus reducing its washing out by atmospheric agents. This feature could reduce the necessity to

frequently re-inoculate the strain in the materials under treatment. Moreover, its ability to form emulsions reduces the need to use detergents which are often required in bioremediation treatments and its capacity to encapsulate oil drops and to preferentially remove the aromatic fraction may avoid the dispersion of toxic aromatic hydrocarbons in the environment. Finally, the ability of the microorganism to grow in a wide range of pH, temperature and salinity values allows for the use of *Novosphingobium* sp. PP1Y in a variety of environments, including costal lagoons and river estuarines.

ACKNOWLEDGMENTS

This work was supported by grants from the Ministry of University and Research (PRIN/2007).

REFERENCES

1. **Atlas, R. M.** 1975. Effects of temperature and crude oil composition on petroleum biodegradation. Appl Microbiol. **30:**396-403.
2. **Baird, W. M., L. A. Hooven, and B. Mahadevan.** 2005. Carcinogenic polycyclic aromatic hydrocarbon-DNA adducts and mechanism of action. Environ Mol Mutagen. **45:**106-14.
3. **Balkwill, D. L., G. R. Drake, R. H. Reeves, J. K. Fredrickson, D. C. White, D. B. Ringelberg, D. P. Chandler, M. F. Romine, D. W. Kennedy, and C. M. Spadoni.** 1997. Taxonomic study of aromatic-degrading bacteria from deep-terrestrial-subsurface sediments and description of Sphingomonas aromaticivorans sp. nov., Sphingomonas subterranea sp. nov., and Sphingomonas stygia sp. nov. Int J Syst Bacteriol **47:**191-201.
4. **Black, J. A., W. J. Birge, A. G. Westerman, and P. C. Francis.** 1983. Comparative aquatic toxicology of aromatic hydrocarbons. Fundam Appl Toxicol. **3:**353-8.
5. **Brennan, M. L., W. Wu, X. Fu, Z. Shen, W. Song, H. Frost, C. Vadseth, L. Narine, E. Lenkiewicz, M. T. Borchers, A. J. Lusis, J. J. Lee, N. A. Lee, H. M. Abu-Soud, H. Ischiropoulos, and S. L. Hazen.** 2002. A tale of two controversies: defining both the role of peroxidases in nitrotyrosine formation in vivo using eosinophil peroxidase and myeloperoxidase-deficient mice, and the nature of peroxidase-generated reactive nitrogen species. J Biol Chem. **277:**17415-27. Epub 2002 Feb 27.
6. **Djomo, J. E., A. Dauta, V. Ferrier, J. F. Narbonne, A. Monkiedje, T. Njine, and P. Garrigues.** 2004. Toxic effects of some major polyaromatic hydrocarbons found in crude oil and aquatic sediments on Scenedesmus subspicatus. Water Res. **38:**1817-21.
7. **Handa, N.** 1966. Examination on the Applicability of the Phenol SulfuricAcid Method to the Determination of Dissolved Carbohydrate in Sea Water. The Journal of Oceanographical Society of Japan **22:**79-86.
8. **Henry, J. A.** 1998. Composition and toxicity of petroleum products and their additives. Hum Exp Toxicol. **17:**111-23.
9. **Kawahara, K., H. Kuraishi, and U. Zahringer.** 1999. Chemical structure and function of glycosphingolipids of Sphingomonas spp and their distribution among members of the alpha-4 subclass of Proteobacteria. J Ind Microbiol Biotechnol. **23:**408-413.
10. **King, R. W.** 1988. Petroleum: its composition, analysis and processing. Occup Med. **3:**409-30.
11. **Liang, F., M. Lu, T. C. Keener, Z. Liu, and S. J. Khang.** 2005. The organic composition of diesel particulate matter, diesel fuel and engine oil of a non-road diesel generator. J Environ Monit. **7:**983-8. Epub 2005 Aug 8.
12. **Liu, Z. P., B. J. Wang, Y. H. Liu, and S. J. Liu.** 2005. Novosphingobium taihuense sp. nov., a novel aromatic-compound-

degrading bacterium isolated from Taihu Lake, China. Int J Syst Evol Microbiol **55:**1229-32.

13. **Mackey, A. P., and M. Hodgkinson.** 1996. Assessment of the impact of naphthalene contamination on mangrove fauna using behavioral bioassays. Bull Environ Contam Toxicol. **56:**279-86.
14. **Mueller, J. G., P. J. Chapman, B. O. Blattmann, and P. H. Pritchard.** 1990. Isolation and characterization of a fluoranthene-utilizing strain of Pseudomonas paucimobilis. Appl Environ Microbiol **56:**1079-86.
15. **Pollock, T. J., and R. W. Armentrout.** 1999. Planktonic/sessile dimorphism of polysaccharide-encapsulated sphingomonads. J Ind Microbiol Biotechnol. **23:**436-441.
16. **Ramos, J. L., E. Duque, M. T. Gallegos, P. Godoy, M. I. Ramos-Gonzalez, A. Rojas, W. Teran, and A. Segura.** 2002. Mechanisms of solvent tolerance in gram-negative bacteria. Annu Rev Microbiol. **56:**743-68. Epub 2002 Jan 30.
17. **Samanta, S. K., O. V. Singh, and R. K. Jain.** 2002. Polycyclic aromatic hydrocarbons: environmental pollution and bioremediation. Trends Biotechnol. **20:**243-8.
18. **Sambrook, J., E. F. Fritsch, and T. Maniatis.** 1989. Molecular Cloning. A Laboratory Manual, 2nd ed. Cold Spring Harbor Laboratory Press, Cold Spring Harbor, New York.
19. **Sawyer, R. F.** 1993. Trends in auto emissions and gasoline composition. Environ Health Perspect. **101:**5-12.
20. **Shimada, T.** 2006. Xenobiotic-metabolizing enzymes involved in activation and detoxification of carcinogenic polycyclic aromatic hydrocarbons. Drug Metab Pharmacokinet. **21:**257-76.
21. **Sikkema, J., J. A. de Bont, and B. Poolman.** 1995. Mechanisms of membrane toxicity of hydrocarbons. Microbiol Rev. **59:**201-22.
22. **Sohn, J. H., K. K. Kwon, J. H. Kang, H. B. Jung, and S. J. Kim.** 2004. Novosphingobium pentaromativorans sp. nov., a high-molecular-mass polycyclic aromatic hydrocarbon-degrading bacterium isolated from estuarine sediment. Int J Syst Evol Microbiol. **54:**1483-7.
23. **Stolz, A.** 2009. Molecular characteristics of xenobiotic-degrading sphingomonads. Appl Microbiol Biotechnol. **81:**793-811. Epub 2008 Nov 11.
24. **Story, S. P., E. L. Kline, T. A. Hughes, M. B. Riley, and S. S. Hayasaka.** 2004. Degradation of aromatic hydrocarbons by Sphingomonas paucimobilis strain EPA505. Arch Environ Contam Toxicol. **47:**168-76.
25. **Wang, Z., M. Fingas, S. Blenkinsopp, G. Sergy, M. Landriault, L. Sigouin, J. Foght, K. Semple, and D. W. Westlake.** 1998. Comparison of oil composition changes due to biodegradation and physical weathering in different oils. J Chromatogr A. **809:**89-107.
26. **Yabuuchi, E., H. Yamamoto, S. Terakubo, N. Okamura, T. Naka, N. Fujiwara, K. Kobayashi, Y. Kosako, and A. Hiraishi.** 2001. Proposal of Sphingomonas wittichii sp. nov. for strain RW1T, known as a dibenzo-p-dioxin metabolizer. Int J Syst Evol Microbiol. **51:**281-92.
27. **Yakimov, M. M., K. N. Timmis, and P. N. Golyshin.** 2007. Obligate oil-degrading marine bacteria. Curr Opin Biotechnol. **18:**257-66. Epub 2007 May 9.

Identification of genes regulated by the MvaT-like paralogs TurA and TurB of *Pseudomonas putida* KT2440

Francesco Renzi, Emanuela Rescalli, Enrica Galli, and Giovanni Bertoni
Department of Biomolecular Sciences and Biotechnology, Università degli Studi di Milano, Milan, Italy.

The genome of the *Pseudomonas putida* strain KT2440 contains five paralogous proteins (TurA, TurB, TurC, TurD and TurE) of the H-NS-like MvaT class of transcription regulators. TurA and TurB belong to groups I and II, respectively, both containing orthologous MvaT proteins that are present in all *Pseudomonadaceae* species. On the contrary, TurC, TurD and TurE belong to group III, which contains species-specific paralogous MvaT proteins. We analyzed the global effects on the *P. putida* KT2440 transcriptome of eliminating the conserved TurA and TurB proteins, which had been identified in our previous studies aimed to search for novel specific co-regulators of the upper TOL operon for toluene biodegradation. While the loss of TurA de-repressed the expression of many genes covering a broad range of functional classes in both mid-exponential and early stationary phases, the absence of TurB brought about a very different outcome. Although the loss of TurB affected also very different functions, the number of genes that changed in the *turB* mutant was five-fold smaller than that of TurA. Furthermore, TurB does not act generally as repressor. Interestingly, the degree of overlap between their mutual regulons is very limited. A closer examination of one case where such overlap clearly occurs (a gene cluster for biosynthesis of lipodepsinonapeptide phytotoxins), revealed that TurA and TurB can act in concert, perhaps by forming a heterodimer. In addition, our results indicate that TurA is the master regulator of TurB as well as of the other paralogs, TurD and TurE.

Pseudomonas putida has long been considered a paradigm of ubiquitous metabolically versatile bacteria and fully deserves the definition of a cosmopolitan nutritional opportunist *par excellence* (Timmis, 2002). Several genomic features found in the KT2440 strain seem to be consistent with ubiquity, metabolic versatility and adaptability of *P. putida* (Martins dos Santos *et al*., 2004). In particular, the broad range of functions mirrors the high diversity of protein families encoded by *P. putida* genome. Moreover, throughout this genetic heterogeneity, there is a large number and variety of small paralogous families, whose members can encode distinct functions (Martins dos Santos *et al*., 2004). Therefore, it seems that the selection for environmental versatility has also favored the functional diversification within family members (Martins dos Santos *et al*., 2004) as previously suggested from *P. aeruginosa* genome analysis (Stover *et al*., 2000). High degree of paralogy in *P. putida* also characterizes almost 10% of the genes in the *P. putida* genome involved in the response to environmental cues by signal transduction and gene regulation (Martins dos Santos *et al*., 2004). The families of paralogous regulatory proteins range from very large (e.g. 110 members of LysR transcriptional regulator family) to very restricted (e.g. 3 members of the *lacI* family).

One small paralogous family of regulators in *P. putida* KT2440 comprises the TurA (PP1366) and TurB (PP3765) proteins, which have been identified in our previous

---

Running title. *P. putida* genes regulated by the MvaT-like paralogs TurA and TurB

Keywords. *Pseudomonas putida*, MvaT-like proteins, microarray analysis

studies aimed to search for novel co-regulators of the *Pu* promoter of the TOL plasmid *upper* operon (Rescalli *et al*., 2004), along with other three highly similar proteins encoded by the *loci* PP0017, PP3693, and PP2947. From now on, these will be referred to as TurC, TurD and TurE, respectively. The five Tur proteins belong to the MvaT class of H-NS like proteins restricted to the members of the *Pseudomonadaceae* family (Tendeng *et al*., 2003). Intriguingly, the size of paralogous MvaT families varies depending on the *Pseudomonadaceae* species and even on strains of the same species. For instance, *P. fluorescens* has four and three MvaT members in strains PfO-1 and Pf5, respectively; four members are present in the *P. syringae* pv. *tomato* strain DC3000 while three are found in both *P. syringae* pv. *syringae* B728a and *P. syringae* pv. *phaseolicola* 1448A; only two members are present in *P. aeruginosa*. Phylogenetic studies have split the MvaT proteins into three distinct groups, I, II and III, respectively (Baehler *et al*., 2006). Members of both groups I and II are orthologous proteins present in all *Pseudomonadaceae* species. On the contrary, members of group III are paralogous proteins characteristic of only the *Pseudomonadaceae* subfamily comprising *P. fluorescens, P. syringae* and *P. putida*.

Studies performed on group I and II members in *P. aeruginosa* and *P. fluorescens* have shown their broad regulatory role. MvaT (PA4315; group I) (Diggle *et al*., 2002) and its paralog MvaU (PA2667; group II) (Vallet-Gely *et al*., 2005) were shown to regulate numerous genes (Castang *et al*., 2008; Vallet *et al*., 2004; Westfall *et al*., 2006) in *P. aeruginosa*, including genes encoding for virulence factors and proteins associated with the cell surface, some of which are involved in biofilm formation and multidrug efflux. In the root-associated *P. fluorescens* strain CHA0, MvaT (group I) and MvaV (group II) act together as regulators of genes involved in biocontrol activity (Baehler *et al*., 2006). On the contrary, no information was obtained in *P. putida* KT2440 on the extent of the regulatory role of TurA (group I) and TurB (group II), beyond the TOL plasmid *upper* operon and the ability to co-purify with TurA, respectively (Rescalli *et al*., 2004).

For this reason, this study analyzes the global effects of eliminating TurA and TurB on the *P. putida* KT2440 transcriptome, in both the mid-exponential and in the early stationary phases. We show that the TurA regulon is about five-fold larger than that of TurB, with a limited degree of overlap between them. In the event of regulon interception, our results indicate that TurA and TurB can act in concert, as shown for group I and II members in *P. aeruginosa* and *P. fluorescens*. In addition, our results strongly indicate that the expression of TurB, along with that of other two paralogs, TurD and TurE, is under control of TurA.

MATERIALS AND METHODS

***P. putida* strains, mutants and growth conditions.** The *P. putida* strain KT2442 (Franklin *et al*., 1981) is a rifampicin-resistant derivative of the reference strain *P. putida* KT2440 (Regenhardt *et al*., 2002), a plasmid-free derivative of *P. putida* mt-2 (Nakazawa, 2002), the original isolate of *P. putida* host harbouring the archetypal TOL plasmid pWW0. KT2442 *turA*::Km^R and KT2442 *turB*::Km^R knock-out mutant strains, carrying a Km^R cassette insertion in the PP1366 *locus* (*turA* gene) and in the PP3765 *locus* (*turB* gene) respectively, were constructed by allelic exchange with a Km^R-inserted allele as described previously (Rescalli *et al*., 2004). The KT2442 *turA*::Km^R *turB*:: Km^R double knock-out mutant strain was generated by allelic exchange with a Km^R-inserted allele in the PP1366 *locus* in KT2442 *turB*::Km^R strain. *P. putida* strains were cultured in M9 minimal medium (Miller, 1972) supplemented with 20 mM succinate at 30°C.

Plasmid construction. Plasmids pJP80 and pJP81 were constructed by cloning the 348 bp intergenic region (KT2440 genome coordinates 4308245-4308593) between the operons PP3775-3780 and PP3781-3790 into the reporter plasmid pJAMA8 (Jaspers *et al*., 2000) upstream *luxAB* as follows. To test the activity of P_{3780}, the promoter region of PP3775-3780 cluster, the intergenic

region was first amplified by PCR using the direct primer 5'-ACATGCATGC(*Sph*I)TAGCGCGCACGCG AC-3' and the reverse primer 5'-GCTCTAGA(*Xba*I)CTGAGCGTCAGGCTGC-3' and then cloned into pJAMA8. For the activity test of P_{3781}, the promoter region of PP3781-3790 cluster, the same intergenic region, amplified by PCR using the direct primer 5'-ACATGCATGC(*Sph*I)CTGAGCGTCAGGCTGC and the reverse primer 5'-GCTCTAGA(*Xba*I)TAGCGCGCACGCGAC-3', was cloned into pJAMA8 in the opposite orientation. Plasmid p*JPturB* was constructed to test the activity of P_{turB}, the promoter region upstream *turB* gene, by cloning into pJAMA8 the 350 bp intergenic region (KT2440 genome coordinates 4295370-4295720) between the *loci* PP3764 and PP3765 (*turB*), amplified by PCR using primer pairs 5'-ACAT GCATGC(*Sph*I)TCCAGAATGAAGACGAG-3' and 5'-GCTCTAGA(*Xba*I) CTGTAATCACTCCTGTAC-3'. Recombinant DNA manipulations were carried out according to published protocols (Sambrook and Russell, 2001). All cloned inserts were verified before use by automated sequencing (MWG Biotech).

Luciferase assays. Luciferase assays were performed on overnight cultures of *E. coli* JM109 carrying the promoter reporter plasmids described above and either pVLT31 (de Lorenzo *et al*., 1993) or the TurA-expressing pVLT31 derivative pVLT31-*turA* (Rescalli *et al*., 2004), grown at 37°C in LB supplemented with 100 μg/ml ampicillin, 20 μg/ml tetracycline and 1 mM IPTG. Culture samples were first adjusted to an OD_{600} of 0.1 in PBS buffer and then 5 μl tested for luciferase activity by adding 500 μl of PBS containing 2 nM n-decanal. Measurement of relative light units (RLU) was conducted in a Turner BioSystems Luminometer by a 2 s pre-measurement delay followed by a 5 s measurement after addition of the substrate. Results are expressed as RLU per OD_{600}.

RNA isolation. Total RNA was prepared from cell samples (about 10^9 cells) growing at 30°C in 50 ml of M9 mineral medium supplemented with 20 mM succinate in a 250-ml flask vigorously shaken. After sampling, the cells were mixed with Qiagen RNAprotectTM Bacteria reagent for stabilization and total RNA was purified using Qiagen RNeasy Mini kits including DNase I treatment. Residual DNA was removed from RNA preparations by further treatment with RNase-free DNase I (Ambion) at 37°C for 15 min, followed by DNaseI inactivation with 2.5 mM EDTA at 65 °C for 10 min. The quality of the RNA was assessed on agarose gel electrophoresis while its concentration was measured spectrophotometrically.

Hybridization and processing of microarrays. The DNA microarrays used in this work, the procedures for the generation of fluorescently-labelled cDNA for microarray hybridization, the microarray hybridization conditions and scanning have been described in detail previously (Yuste *et al*., 2006). For transcriptome comparison, differentially-labeled samples from *wt* and either *turA* or *turB* mutant in the same growth stage (mid-exponential phase: OD_{600} of 0.3; early stationary phase: OD_{600} of 1.2) were mixed and hybridized to microarray. For each transcriptome comparison, a minimum of three independent biological replicas, each analyzed on one microarray, were performed. Data cleansing and statistical analysis were carried out using Genespring GX 7.3 (Academic) software package (Agilent Tech., CA). Data were subjected to intensity dependent (LOWESS) normalization, per spot and per microarray. Statistical analysis included the *P* value adjustment for multiple testing as described (Benjamini and Hochberg, 1995) to control the false discovery rate. Categorization was performed using the Role List from http://cmr.jcvi.org.

Real-time RT-PCR analyses. cDNA was generated by incubating 1 μg of RNA with Superscript II Reverse Transcriptase (RT) (Invitrogen), 100 pg of random primers (Invitrogen) in buffer supplied by the manufacturer for 50 min at 42°C. RT was inactivated by incubation at 70°C for 15 min. As a control of DNA contamination in the subsequent quantitative RT-PCR (qRT-PCR) analysis, reactions were also run without RT. qRT-PCR amplifications were performed in triplicate reactions of 25 ml in 96-well microplates prepared with iQ™ SYBR Green Supermix (Bio-Rad) and 300 nM of each primer (see below) and run in an iCycler Real-Time PCR machine (Bio-Rad) as follows: 1 cycle at 95°C for 10 min, 50 cycles at 95°C for 15 s and 60°C for 40 s. The calculation of the relative expression of the different genes in the KT2442 *turA*, KT2442 *turB* and KT2442 *turA*

turB double mutant *vs* the *wt* strain was performed as described by the $2^{-\Delta\Delta Ct}$ method (Livak and Schmittgen, 2001), normalizing first mRNA amounts to 16S ribosome RNA (ΔCt) and then relating the ΔCt in the mutant to the *wt* ($\Delta\Delta Ct$). Statistical analysis of relative expression results was performed by the software tool REST (Pfaffl *et al*., 2002). Preliminary to quantitative analysis, standard curves relating *C*t to the amounts of specific cDNA were generated. To confirm PCR specificity, the PCR products were subjected to melting curve analysis in a temperature range spanning 55–95°C with 1 cycle at 55°C for 50 s and 80 cycles at 55°C for 10 s set with 0.5°C increments after the first cycle.

The primer pairs used for qRT-PCR were:
16S: 5'-TGTCGTCAGCTCGTGTCGTGA-3'/5'-ATCCCCACCTTCCTCCGGT-3'
turA: 5'-CCAATCTGTCGCAGGATGACA-3'/5'-CACGTCGCCGCCCCAAGT-3'
turB:5'-GCGGGTGGTCAAGGTCTATC-3'/ 5'-CGGCCCCATACTGTTCTTTCC-3'
turC:5'-GCCAAGTGGTGCTGATCCTC-3'/5'-TCCGCTGTGTGGATTCTTGTAG-3'
turD: 5'-GTCTGGCCGAATTCCGCAAG-3'/5'-CCCATACTCAGCAAGGAGGTTC-3'
turE: 5'-GATATCATCAACATCCTGGATCC-3'/5'-GTTCTTGTACTGCTTCACTTGC-3'
PP3779: 5'-GTCCCAGCCAACGATAAGCC-3'/5'-CTGACCTTCTCGCGCAGTC-3'
PP3781: 5'-GCCGTTGTCACCCCTACAG-3' /5'GTGGGCTACGCGAGTAGG-3'
PP3779/3780: 5'-GCAACGTGCGATCAGCCG-3'/5'-CCGTTCCAGTGATCATGATCG-3'
PP3781/3782: 5'-GATTTGGCCCGCGCGTTC-3'/5'-GGCATGTGGGTCGAATACCG-3'

DNA binding assays. The preparation of DNA fragments used in the DNA binding assays was as follows. The 312-bp DNA fragment carrying the *Pu* promoter was excised from pEZ9 (de Lorenzo *et al*., 1991) by *Eco*RI-*Bam*HI digestion. The 346-bp DNA fragment carrying the P_{tet} promoter was excised from pACYC184 (Chang and Cohen, 1978) by *Hind*III-*Bam*HI digestion. The DNA fragments carrying $P_{3780\text{-}3781}$ and P_{turB}, respectively were obtained by PCR amplification with the primers used for the construction of pJP80 and pJ*PturB*, respectively, followed by digestion with *Xba*I. The 285-bp DNA fragment carrying P_{turA} was obtained by PCR amplification with the primer pair 5'-ACATGCATGCTGAATGAGACTCCAGAAC-3'/5'-GCTCTAGATGGAGTGTT CCTTAATGCG-3' followed by digestion with *Xba*I. All DNA fragment were end-labeled by in-filling with [α-^{32}P]dATP and the Klenow enzyme.

Binding reactions were performed in a total volume of 25 µl of buffer containing 20 mM Tris-HCl, pH 7.5, 150 mM NaCl, and 5% glycerol. Labeled fragments, added at a final concentration of 5 nM, were incubated at 30 °C for 30 min with purified TurA at the concentrations indicated. Binding reactions were subjected to electrophoretic separation in non-denaturing 5% polyacrylamide gel (polyacrylamide-bis ratio, 40:1) in TBE 0.5x buffer (45 mMTris-borate pH 8.3, 0.1 mM EDTA, 5 mM $MgCl_2$) dried and visualized by scanning in a TyphoonTM 8600 variable mode Imager (GE Healthcare BioSciences). TurA was purified as described previously (Rescalli *et al*., 2004).

Results

Transcriptome analysis for the detection of TurA- and TurB-regulated genes. In order to identify both TurA- and TurB-regulated genes, we performed comparative transcription profiling of KT2442 *vs* either KT2442 *turA* or KT2442 *turB* knock-out mutants by DNA microarrays as described previously (Yuste *et al*., 2006). The use of KT2442, a rifampicin-resistant derivative of KT2440, was not expected to affect our analysis since the alteration of RNA polymerase was shown not to have pleiotopic effects (Hervas *et al*., 2008). For each *wt vs* mutant strain comparison, we purified total RNAs from cell samples, taken both at mid-exponential (ME; A_{600} of 0.3) and early stationary phase (ES; A_{600} of 1.2) in M9 mineral medium supplemented with 20 mM succinate. For each of the two growth stages, a minimum of three independent RNA preparations were analyzed at least twice as described previously (Yuste *et al*., 2006). The microarray procedure and the statistical analysis are detailed in Materials and Methods. Genes were considered differentially expressed when they showed an expression fold change of ≥ 1.5 or ≤ -1.5 and an adjusted *P* value of ≤ 0.05.

244 genes which resulted differentially expressed in the *turA* mutant were grouped

into the role categories defined in the Comprehensive Microbial Resource (Peterson *et al*., 2001) (Fig. S1). Of the 134 genes differentially expressed in the ME phase, 133 genes were up-regulated and 1 gene was down-regulated. Many of them (56) are categorized as hypothetical, uncharacterized, or unknown. The rest are found in most functional categories (Fig. S1). In the ES phase, of 110 genes differentially expressed, 102 genes were up-regulated and 8 genes down-regulated. As in the ME phase, many of them (50) are categorized as hypothetical, uncharacterized, or unknown. The rest are found in most functional categories (Fig. S1). Remarkably, numerous role categories, both in ME and ES phase, were "energy metabolism", "regulatory functions" and "transport and binding proteins".

As shown in Fig. 1 and Table S2, only about 5% of the up-regulated genes in the *turA* mutant overlap between ME and ES phases. This would suggest that TurA regulates two quasi-independent sets of genes depending on the growth stage. Interestingly, the group of 10 genes (Fig. 1 and Table S2) that appeared to be deregulated both in the ME and ES phases in the *turA* mutant included the paralogs, *turB*, *turD*, and *turE* (Table 1).

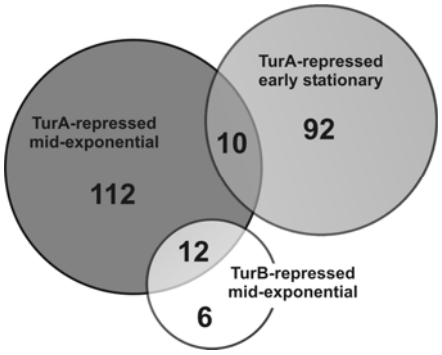

Fig. 1. Venn diagram showing the overlaps between theTurA-regulated genes in mid-exponential and early stationary phases, and TurA/TurB-coregulated genes in mid-exponential phase.

Altogether, 54 genes resulted differentially expressed in the *turB* mutant. Both in the ME and ES phases, the deregulated genes are found in most functional categories (Fig. S2). Of 23 genes differentially expressed in the ME phase in the *turB* mutant, 18 genes were up-regulated and 5 genes down-regulated. In the ES phase, of 31 genes differentially expressed, 16 genes were up-regulated and 15 genes down-regulated. Only two genes, PP3328 and PP5294, overlapped between the ME and ES phases. Therefore, as in the case of TurA, TurB appeared to regulate substantially independent sets of genes depending on the growth stage.

Finally, a set of 12 genes (Fig. 1 and Table S1) showed up-regulation both in *turA* and in *turB* mutant in the ME phase. As a result, we detected an intersection between the regulatory roles of TurA and TurB.

Transcription regulation of Tur paralogs by TurA. As mentioned above, *turB*, *turD*, and *turE* showed up-regulation in the *turA* mutant (Table 1), suggesting a negative regulatory role of TurA on its paralogs. To address this issue, we performed a real-time RT-PCR assessment of the levels of transcription for each paralog and the transcription level changes in the *turA* mutant relative to *wt*. These analyses were performed under the same conditions as described above, namely growth at 30°C in M9 mineral medium with succinate as a sole carbon source and cell sampling at ME (A_{600} of 0.3) and ES (A_{600} of 1.2) phases. As shown in Fig. 2A, mRNA levels of *turA* were the highest of the all paralogs in the ME phase, and decreased about 5 fold in the ES phase. On the contrary, mRNA levels of *turB* were 8.5 fold lower than *turA* ME phase, and increased to about 5 fold in the ES phase. The rest of the paralogs showed no (*turC* and *turE*) or much lower (*turD*) dependence of mRNA

levels from the growth phase. As shown in Fig. 2B and C, using real-time RT-PCR we reconfirmed the up-regulation observed in the microarray analysis (Table 1) of *turB*, *turD*, and *turE* in the *turA* mutant, both in the ME and ES phases. Furthermore, using real-time RT-PCR we re-evaluated the influence of TurB on the transcription of the other paralogs. As shown in Fig. 2B, in the *turB* mutant none of the other paralogs was influenced in the ME phase; however a modest degree of deregulation was visible in the case of *turC*, *turD* and *turE* in the ES phase (Fig. 2C). Therefore, these results indicated a predominant regulatory role of TurA on its paralogs.

In order to assess whether such control was mediated by direct TurA binding and not the TurA-mediated regulation of another transcription factor, we focused on the DNA region upstream of the *turB* gene, expected to carry the P_{turB} promoter.

This region was cloned in a plasmid in front of the reporter *luxAB,* and the luciferase activity was tested in *E. coli* both in the absence and the presence of TurA expressed from another plasmid. Furthermore, the same DNA fragment was end-labeled and the TurA binding tested by band-shift assay. The cloning of the DNA upstream of the *turB* gene in front of *luxAB* increased about 600-fold the luciferase activity elicited by the reporter plasmid without any insert. Therefore, this region clearly demonstrated promoter activity.

As shown in Fig. 6A, TurA expression could repress the luciferase activity expressed from P_{turB} by 2-fold.

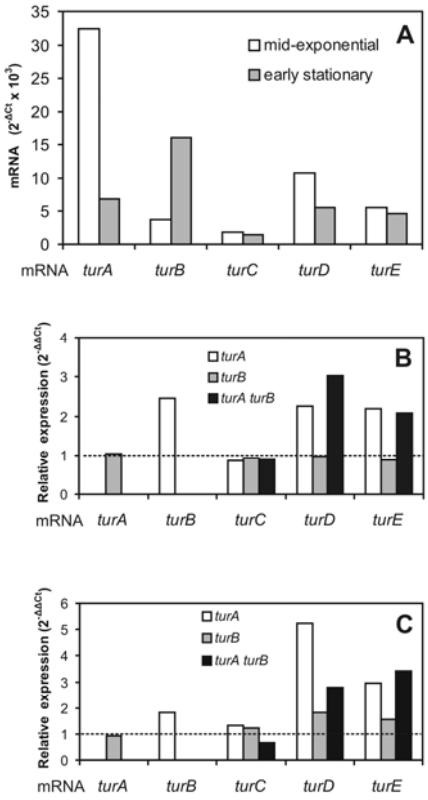

Fig. 2. Analysis by real-Time RT-PCR of *tur* genes expression in *wt* and in *turA, turB, and turA turB* double mutant. (A) represents mRNA levels, displayed graphically as $2^{-\Delta CT}$ values, of each *tur* gene determined in cell samples taken at mid-exponential (A_{600} of 0.3) and early stationary phases (A_{600} of 1.2) in M9 mineral medium supplemented with 20 mM succinate. (B) and (C) correspond to the calculation of the relative expression, displayed graphically as $2^{-\Delta\Delta Ct}$, of the different *tur* genes in the KT2442 *turA*, KT2442 *turB* and KT2442 *turA, turB* double mutant *vs* the *wt* strain, performed on cell samples taken at mid-exponential (A_{600} of 0.3) and early stationary phases (A_{600} of 1.2), respectively. The values represent the average of three independent experiments.

Table 1. Expression fold changes determined by microarray analysis of the *tur* paralogs in both *turA* and *turB* mutants.

TIGR ID	Gene name	Fold change			
		***turA* mutant**		***turB* mutant**	
		ME phase	**ES phase**	**ME phase**	**ES phase**
PP1366	*turA*	-	-	1	1
PP3765	*turB*	1.67	1.93	-	-
PP0017	*turC*	1	1	1	1
PP3693	*turD*	3.04	2.12	1	1.28
PP2947	*turE*	2.62	1.96	1	1

In addition, the test of direct binding (Fig. 3, lanes 4-6) showed that TurA has a certain degree of affinity to the DNA fragment carrying P_{turB}. In this binding test, we used the DNA region upstream of the *turA* gene as well. As shown in Fig. 3 (lanes 1-3), TurA also showed affinity for the DNA region upstream of the *turA* gene. This strongly suggests an autoregulatory activity of TurA.

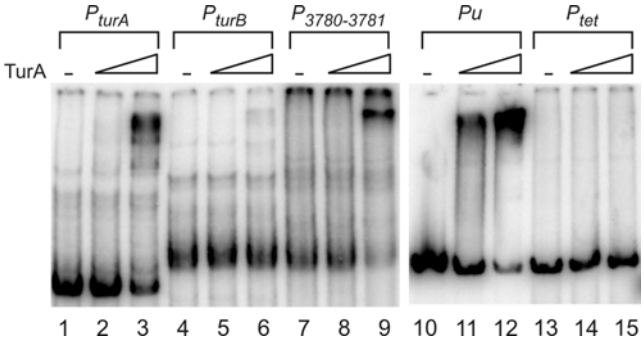

Fig. 3. Analysis *in vitro* of the DNA binding of TurA to selected promoter regions. Band-shift assay on increasing amount of TurA (0, 50, 100 nM, respectively) mixed with end-labeled fragments containing the promoter regions indicated on the top. Positive and negative controls of specific binding are fragments carrying the *Pu* promoter of the TOL *upper* operon (Ruiz *et al*., 2004) and the promoter of a tetracycline resistance cassette, respectively.

Evidence that TurA and TurB can act in concert. A set of genes which showed significant up-regulation in the *turA* mutant in the ME phase clustered into two divergently transcribed operons, PP3780-3775 and PP3781-3790, respectively, within one of the 105 genomic islands with atypical GC contents and/or oligonucleotide signature that most likely were acquired from exogenous sources (Weinel *et al*., 2002) (Fig. 4 and Table S3). The left PP3780-3775 *loci* encode for a cluster of enzymes presumably involved in aminoacid biosynthesis and modification and a transcription regulator of the LysR family, while the right PP3781-3790 *loci* are related to genes for biosynthesis of lipodepsinonapeptide class phytotoxins, like syringomycin and barbamide (Bender *et al*., 1999; Martins dos Santos *et al*., 2004; Nelson *et al*., 2002; Weinel *et al*., 2002). The coherent up-regulation of both the right and left clustered genes in the *turA* mutant (Table S3) strongly reinforced the view that they assembled in the same transcriptional units, respectively. Indeed, we assessed the co-transcription of PP3781 with PP3782, and of PP3780 with PP3779 by RT-PCR (data not shown).

Interestingly, the majority of the right operon genes also showed coherent up-regulation in the *turB* mutant (Table S3). On the contrary, the combined TurA/TurB effect was not so evident for the left operon. In order to confirm microarray data, we performed quantitative real-time RT-PCR experiments analyzing mRNA levels at ME of

both PP3779 and PP3781, as representatives of PP3780-3775 and PP3781-3790 operons, respectively. As shown in Fig. 5, this analysis confirmed the deregulation of PP3781 both in the *turA* and *turB* mutant, and that of PP3779 in the *turA* mutant alone.

To assess further what effects the combined absence of TurA and TurB had on the expression of both operons, we quantified the transcripts in the double mutant *turA turB* in the ME phase. As shown in Fig. 5, the combined loss of TurA and TurB produced higher levels of PP3781 mRNA than the loss of either TurA or TurB alone. Therefore, these results strongly indicate that TurA and TurB can act in concert at the same promoter region. Unexpectedly, in the case of PP3779 the mRNA levels were lower in the double *turA turB* than in the single *turA* mutant. This effect could reflect a functional tradeoff by one or more of the other *tur* paralogs, in the event of simultaneous loss of Tur A and TurB.

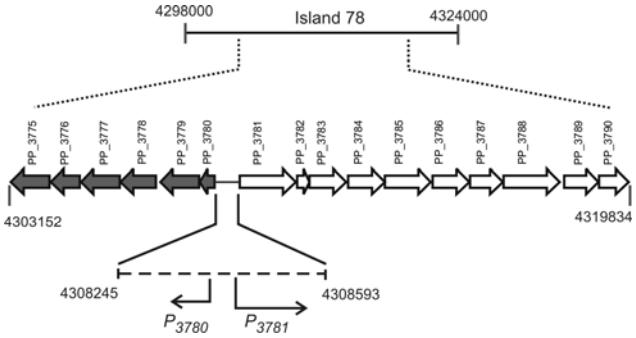

Fig. 4. Schematic diagram showing two divergent transcriptional units regulated by TurA and TurB. The two operons comprise the *loci* PP3780-3775 and PP3781-3790, respectively and belong to the genomic island 78 (from coordinates 4298000 and 4324000 of *P. putida* genome), one of the 105 genomic islands with atypical GC contents and/or oligonucleotide signature that most likely were acquired from exogenous sources (Weinel *et al*., 2002). Gene annotations are listed in Table 1. The left PP3780-3775 *loci* encode for a cluster of enzymes presumably involved in aminoacid biosynthesis and modification and a transcription regulator of the LysR family, while the right PP3781-3790 *loci* are related to operons for the biosynthesis of secondary metabolites, such as phytotoxin peptides and antibiotics, respectively. The coordinates of the intergenic region between the two operons and the putative cognate promoters are also indicated.

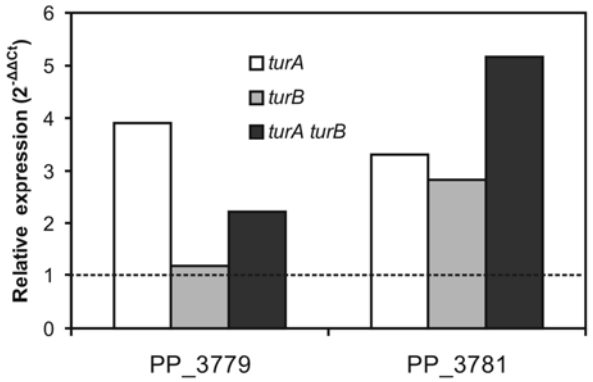

Fig. 5. Analysis by real-Time RT-PCR of the expression of the operons PP3780-3775 and PP3781-3790 in *wt* and in *turA, turB, and turA turB* double mutant. The mRNA levels of PP3779 and PP3781 were taken as representatives of PP3780-3775 and PP3781-3790 operons, respectively. The calculation of the relative expression, displayed graphically as $2^{-\Delta\Delta Ct}$, in the KT2442 *turA*, KT2442 *turB* and KT2442 *turA turB* double mutant *vs* the *wt* strain, was performed on cell samples taken at mid-exponential (A_{600} of 0.3) in M9 mineral medium supplemented with 20 mM succinate. The values represent the average of three independent experiments.

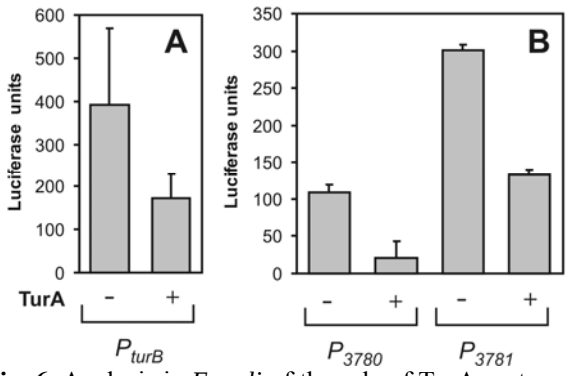

Fig. 6. Analysis in *E. coli* of the role of TurA on target promoters. (A) corresponds to luciferase activities determined on JM109 (pJ*PturB*) (P_{turB}), transformed either with with pVLT31 (- TurA) or pVLT31-*turA* (+ TurA) and grown in LB medium supplemented with 1 mM IPTG. (B) represents luciferase activities determined on JM109 (pJP80) (P_{3780}) and JM109 (pJP81) (P_{3781}), both transformed either with pVLT31 (- TurA) or pVLT31-*turA* (+ TurA) and grown as in (A).

In order to assess whether the tight control of the two operons by TurA was exerted by direct binding, the PP3780-PP3781 intergenic DNA region, which was expected to carry the divergent promoters, P_{3780} and P_{3781}, of left and right operon, respectively, was cloned in both the orientation in front of the *luxAB* reporter genes and the luciferase

activity tested in *E. coli* in the absence and the presence of TurA. Furthermore, the same DNA fragment was end-labeled and the TurA binding tested by band-shift assay. As shown in Fig. 6B, both orientations showed promoter activity, with the increase of luciferase activity compared to that of the reporter plasmid without any insert being about 150- and 500-fold for P_{3780} and P_{3781}, respectively. TurA expression reduced the luciferase activity expressed from P_{3780} and P_{3781} by 5- and 2.5- fold, respectively. In addition, the test for direct binding (Fig. 3A, lanes 7-9) showed that TurA can interact with the PP3780-PP3781 intergenic DNA region.

Discussion

Phylogenetic analyses of MvaT proteins resolve their sequences into three well-supported groups (Fig. S3). Groups I and II both contain orthologous sequences from the *P. aeruginosa/P. stutzeri* and *P. fluorescens/P. syringae/P. putida* subfamilies, consistent with an origin from an ancient gene duplication event. Group III contains multiple paralogous sequences from members of the *P. fluorescens/P. syringae/P. putida* subfamily, presumably resulting from a series of gene duplication events occurring after the separation of the two lineages. The lack of information regarding the position of the root of the tree means that a loss of group III sequences from the *P. aeruginosa/P. stutzeri* subfamily cannot be completely excluded.

However, as suggested by the comparison of the *P. putida* and *P. aeruginosa* genomes, most lineage specific-genes are expansions of paralogous genes families. For instance, about 500 open reading frames in the KT2440 genome were identified as putative duplications that arose after *P. putida* diverged from common evolutionary lineage with *P. aeruginosa* (Martins dos Santos *et al*., 2004). We can speculate that the emergence and maintenance of multiple MvaT paralogs in the *P. fluorescens/P. syringae/P. putida* subfamily were positively selected as they promoted regulatory expansion and consequently higher adaptability to the habitats in which these species thrive. For instance, the group III proteins may act as ecoparalogs (Sanchez-Perez *et al*., 2008), functioning as regulators of the same target genes as group I and II proteins under different environmental conditions. Alternatively, instead of giving rise to an environmental response expansion, group III proteins may regulate sets of genes different to those of groups I and II and may indirectly expand the regulons of these latter proteins. However, whatever the nature of the regulatory expansion, it may have retained a certain degree of functional redundancy. The simultaneous loss of the two group I and II paralogs MvaT proteins encoded by the *P. aeruginosa* genome, MvaT and MvaU, respectively, results in cell death. On the contrary, for both *P. fluorescens* and *P. putida* the simultaneous loss of group I and II paralogs, MvaU/MvaV (Baehler *et al*., 2006) and TurA/TurB (this work), does not affect cell viability. This difference might reflect a functional tradeoff of group III paralogs on the other two groups.

In this study, we aimed to evaluate the extent of the regulatory role in *P. putida* KT2440 relative to its groups I and II MvaT proteins, TurA and TurB, respectively, and the degree of interception between the corresponding regulons. Our results indicated that TurA acts prevalently as repressor of many genes belonging to a broad range of functional classes in both the ME and ES phases. Therefore, TurA seems to play a global regulatory role not only during balanced and unrestricted growth but also in environmentally relevant transitions to scenarios of nutrient limitation and occurrence of stressors such as the entry into the stationary phase. Remarkably, the regulation by TurA in the ES phase of several transcription factors, signal transduction proteins, and the *rpoD* gene for the vegetative sigma factor σ^{70} might also be relevant to this role. It is interesting to note that the mRNA levels of *rpoD* decrease threefold as *P. putida*

cells enter into the ES phase (Yuste *et al*., 2006). TurA might be instrumental in this repression.

Likewise, TurB acts both in the ME and ES phases on genes belonging to a broad range of functional classes. However, the number of TurB-regulated genes apparently was about 5-fold lower than TurA. Furthermore, the proportion of down-regulated genes in the *turB* mutant was higher than the *turA* mutant. Thus, unlike TurA, TurB may not act prevalently as repressor.

Surprisingly, our microarray analyses indicate that there is limited overlap between the TurA and TurB regulons. In fact, only in the ME phase, we detected a narrow set of genes whose expression is affected both by *turA* and *turB* inactivation. This scenario appears to be completely different from that described recently in *P. aeruginosa*, where MvaT and MvaU, TurA and TurB orthologous, respectively, were shown to bind to the same chromosomal regions and function coordinately in the regulation of a large set of about 350 genes (Castang *et al*., 2008). In this case, coordinate activity of MvaT and MvaU is thought to bring about the integration of multiple environmental signals. This would be achieved through differential affinities of the various homomers and heteromers of MvaT and MvaU for promoters DNA and regulation of the *mvaT* and *mvaU* genes in response to different environmental signals (Castang *et al*., 2008). As mentioned above, in the case of *P. putida*, the integration of multiple environmental signals for the fine-tuning of the TurA and/or TurB regulons could have been achieved by the process of ecoparalogization which gave rise to the group III paralogs TurC, TurD and TurE. Differential gene regulation among the five Tur paralogs, promiscuity in heteromers formation and distinct affinities for promoters DNA of the various homomers and heteromers could have further enhanced the environmental signal integration.

Irrespective of which signal modulates the expression of each Tur paralog (e.g. growth phase; see Fig. 2A), our results strongly indicated that the expression of TurB, TurD and TurE is submitted to TurA. Furthermore, since binding to its own promoter region, it is very likely that TurA auto-regulates. On the contrary, TurB would appear to play no role in the transcription regulation of either TurA or the group III paralogs. Therefore, we can speculate that TurA levels act as a switch superimposed to the regulatory network governing this family of paralogs and the response of the target genes.

In this study, we also produced evidence that TurA and TurB can act in concert at the same promoter region. In fact, the transcription of the PP3781-3790 operon is clearly under negative control of both TurA and TurB (Fig. 5 and Table S3). In addition, the loss of both TurA and TurB gives rise to further up-regulation of the operon (Fig. 5). The mechanism underlying this simultaneous and addictive regulation could be similar to that proposed for the coordinate activity of MvaT and MvaU in *P. aeruginosa* (Castang *et al*., 2008), i.e. differential affinities for target DNA sites of the various homomers and heteromers (see above). Interestingly, only TurA seems to act also on the divergently transcribed operon PP3780-3775 represented by PP3779 (Fig. 5). However, the loss of both TurA and TurB results in partial repression. This effect could reflect a functional tradeoff by one or more of the other *tur* paralogs, in the event of simultaneous loss of Tur A and TurB. Such an effect could also explain the partial repression of *turD* gene in the ES phase (Fig. 2C).

The PP3781-3790 *loci* are related to genes for the biosynthesis of lipodepsinonapeptide phytotoxins (e.g syringomycin). Besides being phytotoxic, this class of compounds has fungicidal activity against a broad spectrum of filamentous fungi and yeasts (Bender *et al*., 1999). Therefore, the expression of PP3781-3790 operon might have activity of biocontrol against competitors (Martins dos Santos *et al*., 2004).

Interestingly, it was shown that MvaT and MvaV, TurA and TurB orthologous, in the *P. fluorescens* CHA0 strain respectively, act together as global regulators of biocontrol activity (Baehler *et al*., 2006). Therefore, our results suggest a convergence of the regulatory roles of group I and II MvaT proteins between *P. putida* and *P. fluorescens*.

Finally, since PP3781-3790 *loci* are located in a genomic island with atypical sequence features and most likely acquired from exogenous sources (Weinel *et al*., 2002), the repression by TurA and TurB appears to be reminiscent of the xenogeneic silencing activity attributed to the protein H-NS, due to the distinct preference for the AT-rich regions of DNA (Navarre *et al*., 2007) and, more recently, to MvaT and MvaU of *P. aeruginosa* for analogous DNA binding properties (Castang *et al*., 2008).

ACKNOWLEDGMENTS

We are grateful to G. Pea for the support in the microarrays data analysis, D. Horner and C. Gissi for phylogenetic analyses and G. Pavesi for microarrays database analysis. This work was funded by *Ministero dell'Istruzione, dell'Università e della Ricerca, Roma* (PRIN 2007 grant 20077MY8M9_004 to E.G.) and by European Commission (grant TARPOL, FP7-KBBE-2007-1, contract number 212894).

REFERENCES

1. **Abascal, F., Zardoya, R., and Posada, D.** 2005. ProtTest: selection of best-fit models of protein evolution. Bioinformatics **21:** 2104-2105.
2. **Baehler, E., de Werra, P., Wick, L.Y., Pechy-Tarr, M., Mathys, S., Maurhofer, M., and Keel, C.** 2006. Two novel MvaT-like global regulators control exoproduct formation and biocontrol activity in root-associated *Pseudomonas fluorescens* CHA0. Mol Plant Microbe Interact **19:** 313-329.
3. **Bender, C.L., Alarcon-Chaidez, F., and Gross, D.C.** 1999 *Pseudomonas syringae* phytotoxins: mode of action, regulation, and biosynthesis by peptide and polyketide synthetases. Microbiol Mol Biol Rev **63:** 266-292.
4. **Benjamini, B. and Hochberg, Y.** 1995. Controlling the false discovery rate: a practical and powerful approach to multiple testing. J R Stat Soc Ser B **57:** 289-300.
5. **Castang, S., McManus, H.R., Turner, K.H., and Dove, S.L**. 2008. H-NS family members function coordinately in an opportunistic pathogen. Proc Natl Acad Sci U S A **105:** 18947-18952.
6. **Chang, A.C. and Cohen, S.N.** 1978. Construction and characterization of amplifiable multicopy DNA cloning vehicles derived from the P15A cryptic miniplasmid. J Bacteriol **134:** 1141-1156.
7. **de Lorenzo, V., Eltis, L., Kessler, B., and Timmis, K.N.** 1993. Analysis of *Pseudomonas* gene products using *lacI*^{q}/*Ptrp-lac* plasmids and transposons that confer conditional phenotypes. Gene **123:** 17-24.
8. **de Lorenzo, V., Herrero, M., Metzke, M., and Timmis, K.N.** 1991. An upstream XylR- and IHF-induced nucleoprotein complex regulates the sigma 54-dependent *Pu* promoter of TOL plasmid. EMBO J **10:** 1159-1167.
9. **Diggle, S.P., Winzer, K., Lazdunski, A., Williams, P., and Camara, M.** 2002. Advancing the quorum in *Pseudomonas aeruginosa*: MvaT and the regulation of N-acylhomoserine lactone production and virulence gene expression. J Bacteriol **184:** 2576-2586.
10. **Franklin, F.C., Bagdasarian, M., Bagdasarian, M.M., and Timmis, K.N.** 1981. Molecular and functional analysis of the TOL plasmid pWWO from *Pseudomonas putida* and cloning of genes for the entire regulated aromatic ring meta cleavage pathway. Proc Natl Acad Sci U S A **78:** 7458-7462.
11. **Guindon, S., Lethiec, F., Duroux, P., and Gascuel, O.** 2005. PHYML Online--a

web server for fast maximum likelihood-based phylogenetic inference. Nucleic Acids Res **33:** W557-W559.

12. **Hervas, A.B., Canosa, I., and Santero, E.** 2008. Transcriptome analysis of *Pseudomonas putida* in response to nitrogen availability. J Bacteriol **190:** 416-420.
13. **Jaspers, M.C., Suske, W.A., Schmid, A., Goslings, D.A., Kohler, H.P., and van der Meer, JR.** 2000. HbpR, a new member of the XylR/DmpR subclass within the NtrC family of bacterial transcriptional activators, regulates expression of 2-hydroxybiphenyl metabolism in *Pseudomonas azelaica* HBP1. J Bacteriol **182:** 405-417.
14. **Livak, K.J. and Schmittgen, T.D**. 2001. Analysis of relative gene expression data using real-time quantitative PCR and the 2-Delta Delta CT. Method. Methods **25:** 402-408.
15. **Martins dos Santos, V.A.P., Heim, S., Moore, E.R., Stratz, M., and Timmis, K.N.** 2004. Insights into the genomic basis of niche specificity of *Pseudomonas putida* KT2440. Environ Microbiol **6:** 1264-1286.
16. **Miller,J.H.** 1972. *Experiments in Molecular Genetics*. Cold Spring Harbor, NY: Cold Spring Harbor Laboratory Press.
17. **Nakazawa, T.** 2002. Travels of a *Pseudomonas*, from Japan around the world. Environ Microbiol **4:** 782-786.
18. **Navarre, W.W., McClelland, M., Libby, S.J., and Fang, F.C.** 2007. Silencing of xenogeneic DNA by H-NS-facilitation of lateral gene transfer in bacteria by a defense system that recognizes foreign DNA. Genes Dev **21:** 1456-1471.
19. **Nelson, K.E., Weinel, C., Paulsen, I.T., Dodson, R.J., Hilbert, H., Martins dos Santos, V. *et al.*** 2002. Complete genome sequence and comparative analysis of the metabolically versatile *Pseudomonas putida* KT2440. Environ Microbiol **4:** 799-808.
20. **Peterson, J.D., Umayam, L.A., Dickinson, T., Hickey, E.K., and White, O.** 2001. The Comprehensive Microbial Resource. Nucleic Acids Res **29:** 123-125.
21. **Pfaffl, M.W., Horgan, G.W., and Dempfle, L.** 2002. Relative expression software tool REST. for group-wise comparison and statistical analysis of relative expression results in real-time PCR. Nucleic Acids Res **30:** e36.
22. **Regenhardt, D., Heuer, H., Heim, S., Fernandez, D.U., Strompl, C., Moore, E.R., and Timmis, K.N.** 2002. Pedigree and taxonomic credentials of *Pseudomonas putida* strain KT2440. Environ Microbiol **4:** 912-915.
23. **Rescalli, E., Saini, S., Bartocci, C., Rychlewski, L., de, L., V, and Bertoni, G.** 2004. Novel physiological modulation of the Pu promoter of TOL plasmid: negative regulatory role of the TurA protein of *Pseudomonas putida* in the response to suboptimal growth temperatures. J Biol Chem **279:** 7777-7784.
24. **Ruiz,R., Aranda-Olmedo, M.I., Dominguez-Cuevas,P., Ramos-Gonzalez, M.I., and Marques, S.** 2004. Transcriptional regulation of the toluene catabolic pathways. In *Pseudomonas vol. 2 - Virulence and Gene Regulation*. Juan-Luis Ramos ed.. New York: Kluwer Academic/Plenum Publishers, 509-537.
25. **Sambrook, J. and Russell, J.W.** 2001. *Molecular cloning: a laboratory manual*. Cold Spring Harbor Laboratory Press.
26. **Sanchez-Perez, G., Mira, A., Nyiro, G., Pasic, L., and Rodriguez-Valera, F. 2008.** Adapting to environmental changes using specialized paralogs. Trends Genet **24:** 154-158.
27. **Stover, C.K., Pham, X.Q., Erwin, A.L., Mizoguchi, S.D., Warrener, P., Hickey, M.J. *et al.*** 2000. Complete genome sequence of *Pseudomonas aeruginosa* PA01, an opportunistic pathogen. Nature **406:** 959-964.

28. **Tendeng, C., Soutourina, O.A., Danchin, A., and Bertin, P.N.** 2003. MvaT proteins in *Pseudomonas* spp.: a novel class of H-NS-like proteins. Microbiology **149:** 3047-3050.
29. **Thompson, J.D., Higgins, D.G., and Gibson, T.J.** 1994. CLUSTAL W: improving the sensitivity of progressive multiple sequence alignment through sequence weighting, position-specific gap penalties and weight matrix choice. Nucleic Acids Res **22:** 4673-4680.
30. **Timmis, K.N. 2002.** *Pseudomonas putida*: a cosmopolitan opportunist par excellence. Environ Microbiol **4:** 779-781.
31. **Vallet, I., Diggle, S.P., Stacey, R.E., Camara, M., Ventre, I., Lory, S. *et al.*** 2004. Biofilm formation in *Pseudomonas aeruginosa*: fimbrial cup gene clusters are controlled by the transcriptional regulator MvaT. J Bacteriol **186:** 2880-2890.
32. **Vallet-Gely, I., Donovan, K.E., Fang, R., Joung, J.K., and Dove, S.L**. 2005. Repression of phase-variable cup gene expression by H-NS-like proteins in *Pseudomonas aeruginosa*. Proc Natl Acad Sci U S A **102:** 11082-11087.
33. **Weinel, C., Nelson, K.E., and Tummler, B.** 2002. Global features of the *Pseudomonas putida* KT2440 genome sequence. Environ Microbiol **4:** 809-818.
34. **Westfall, L.W., Carty, N.L., Layland, N., Kuan, P., Colmer-Hamood, J.A., and Hamood, A.N.** 2006. *mvaT* mutation modifies the expression of the *Pseudomonas aeruginosa* multidrug efflux operon mexEF-oprN. FEMS Microbiol Lett **255:** 247-254.
35. **Yuste, L., Hervas, A.B., Canosa, I., Tobes, R., Jimenez, J.I., Nogales, J. *et al.*** 2006. Growth phase-dependent expression of the *Pseudomonas putida* KT2440 transcriptional machinery analysed with a genome-wide DNA microarray. Environ Microbiol **8:** 165-177.

SUPPLEMENTAL MATERIAL

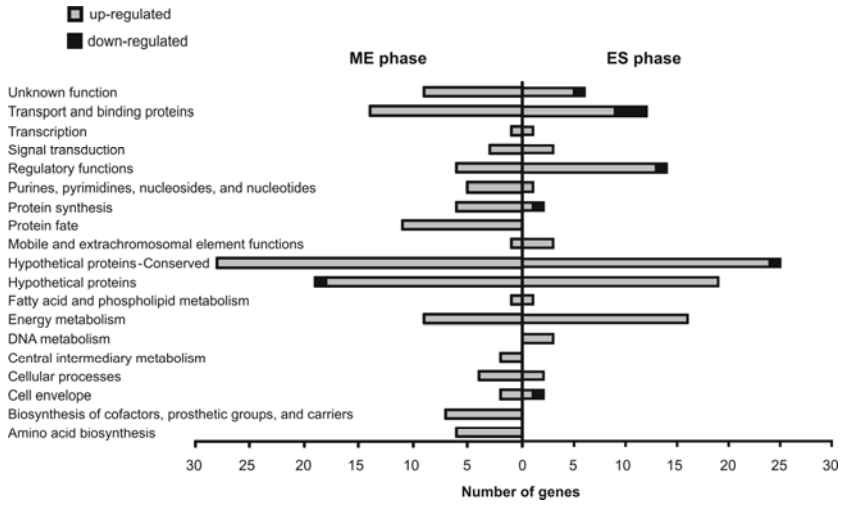

Fig. S1. Breakdown of role categories of the TurA-regulated genes. Each bar indicates the type of role category and the number of genes whose expression increased (up-regulated) or decreased (down-regulated) in the *turA* mutant either in ME or ES phases.

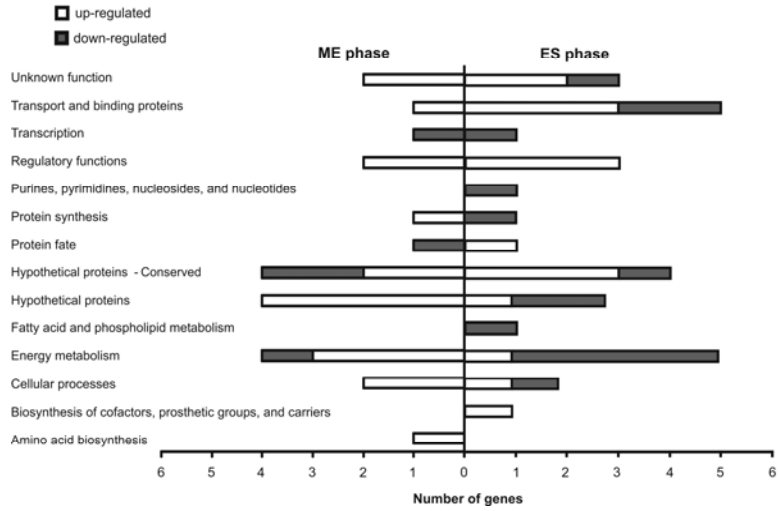

Fig. S2. Breakdown of role categories of the TurB-regulated genes. Each bar indicates the type of role category and the number of genes whose expression increased (up-regulated) or decreased (down-regulated) in the *turB* mutant either in ME or ES phases.

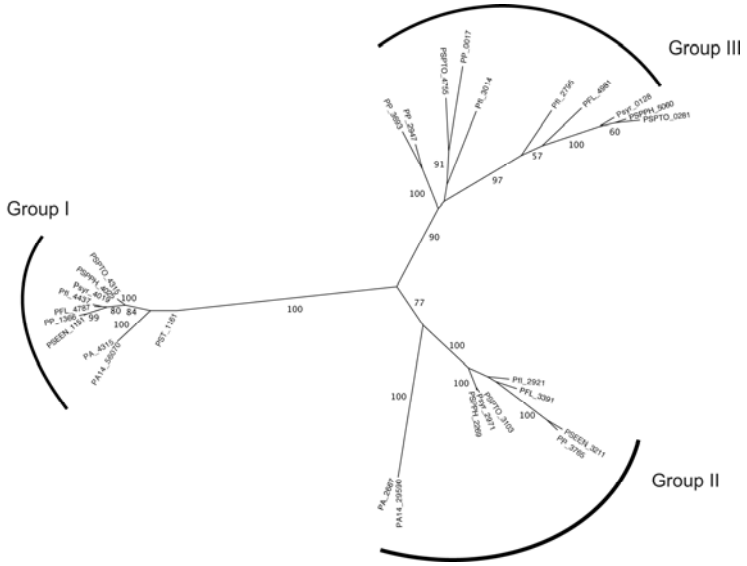

Fig. S3. Phylogenetic tree of the MvaT proteins. MvaT protein sequences were aligned using ClustalW (Thompson *et al*., 1994), resulting in a dataset consisting of 129 positions from 29 sequences. The Dayhoff model plus invariant sites and a gamma distribution for rate heterogeneity across sites (+Γ) was selected as the model best fitting to the data, using ProtTest v1.3 and the Akaike information criterion (Abascal *et al*., 2005). Phylogenetic reconstruction within the framework of Maximum Likelihood were performed using the PhyML online service (Guindon *et al*., 2005), setting the invariant site frequency and the alpha value as calculated by ProtTest (0.19 and 1.29, respectively). Bootstrap analyses were carried out on 100 replicates. The 29 MvaT protein included in the analyses are indicated by the *locus* tag in the Comprehensive Microbial Resource (Peterson *et al*., 2001).

TABLE S1. TurA/TurB-regulated genes in Mid-Exponential phase

TIGR ID	Gene name	Description	Fold change	
			turA mutant	*turB* mutant
PP_3328		ring-cleaving dioxygenase	1,8	2,13
PP_3775		sarcosine oxidase	3,73	1,56
PP_3778	*pro-C*	pyrroline-5-carboxylate reductase	4,38	1,67
PP_3781		oxygen-independent Coproporphyrinogen III oxidase family protein	5,99	1,84
PP_3782		hypothetical protein	6,05	2,02
PP_3783		conserved hypothetical protein	6,02	1,9
PP_3785		hypothetical protein	5,56	2,1
PP_3786		aminotransferase	4,97	1,72
PP_3787		hypothetical protein	5,61	1,67
PP_3788		non-ribosomal peptide synthetase	5,05	1,71
PP_3789		efflux transporter	4,72	1,63
PP_3798		conserved hypothetical protein	1,79	1,51

TABLE S2. TurA repressed genes in both Mid-Exponential and Early Stationary growth phase

TIGR ID	Gene name	Description	Fold change	
			Mid-exponential phase	Early stationary phase
PP_2947	*turE*	transcriptional regulator MvaT, P16 subunit, putative	2,62	1,96
PP_3693	*turD*	transcriptional regulator MvaT, P16 subunit, putative	3,04	2,12
PP_3765	*turB*	transcriptional regulator MvaT, P16 subunit, putative	1,67	1,93
PP_3106		conserved hypothetical protein	2,29	1,59
PP_3107		conserved hypothetical protein	2,48	1,60
PP_3536		hypothetical protein	1,91	1,69
PP_3707		hypothetical protein	2,13	1,69
PP_3779		transcriptional regulator, LysR family	3,46	1,57
PP_3780		hypothetical protein	4,44	1,71
PP_5063	*betB*	betaine aldehyde dehydrogenase	2,01	2,00

TABLE S3. Expression fold changes determined by microarray analysis of operons PP3780-3775 and PP3781-3790 in *turA* and *turB* mutants in ME phase.

TIGR ID	Gene name	Description	Fold change	
			***turA* mutant**	***turB* mutant**
PP3775		Sarcosine oxidase	3.73	1.56
PP3776	*rarD3*	RarD protein	4.26	1
PP3777		Conserved hypothetical protein	2.89	1
PP3778	*proC*	Pyrroline-5-carboxylate reductase	4.38	1.67
PP3779		Transcriptional regulator, LysR family	3.46	1
PP3780		Hypothetical protein	4.44	1
PP3781		Oxygen-independent Coproporphyrinogen III oxidase family protein	5.99	1.84
PP3782		Hypothetical protein	6.05	2.02
PP3783		Conserved hypothetical protein	6.02	1.9
PP3784		Conserved domain protein	4.75	1
PP3785		Hypothetical protein	5.56	2.1
PP3786		Aminotransferase	4.97	1.72
PP3787		Hypothetical protein	5.61	1.67
PP3788		Non-ribosomal peptide synthetase	5.05	1.71
PP3789		Efflux transporter	4.72	1.63
PP3790		Diaminopimelate epimerase, putative	3.99	1

Cloning of new bacterial oxygenases from PAH degrading bacteria

IvanVaghi, Rossella Giachetta, Luca Bianchi, Cristina Zonca, Roberta Orlandi, Viviana Orlandi, and Paola Barbieri

Department of Structural and Functional Biology – University of Insubria – Varese

Bacterial oxygenases are non eme metal-enzymes able to catalyze the oxidation of many aromatic compounds, including some PAH. These enzymes are particularly interesting because of their potential biotechnological applications, that is the introduction of hydroxyl group(s) into non-natural substrates. Aim of this work was the isolation and the preliminary characterization of new bacterial oxygenase from PAH-degrading bacterial strains. We focused on two naphthalene degrading *Pseudomonas* sp. strains and a phenanthrene degrading *Sphingobium* sp. Naphthalene dioxygenase (NDO) encoding genes of the two *Pseudomonas* strains were amplified, cloned in pGEMTEasy and sequenced. Both clusters displayed high homology with NDOs from *P. aeruginosa* and *P. stutzeri* strains. The sequence of a generic dioxygenase conserved region amplified from *Sphingobium* showed homology with the genes *bphA1f* and *bphA2f* coding for the terminal hydroxylase of the phenantrene dioxygenase of *Novosphingobium aromaticivorans*. The primers designed using the sequences available in the data bases allowed to amplify the genes of interest, that were cloned in pGEM and/or pET vectors. In Sphingomonads, the oxygenase encoding genes are not clustered: the genes coding for the electron transport subunits are physically separated from those coding for the two subunits of the hydroxylating subcomplex . Thus, we also cloned the genes for the electron transport subunits, in order obtain the sequences encoding for the entire enzymatic complex in a single vector. We also replaced the genes for the hydroxylase with a second copy also cloned from the same organism. Functional analyses of the cloned genes are under way.

Polycyclic aromatic hydrocarbons (PAHs) are hydrophobic organic compounds consisting of two or more combined benzene rings in linear, angular or cluster arrangements. There are more than 100 diverse PAH compounds, and most of them persist in the ecosystem for many years owing to their low aqueous solubility and their absorption to solid particles (1).

Numerous bacteria have been found that degrade PAHs, and some can utilize low-MW PAHs as their sole carbon source. Biodegradation mechanisms require the presence of molecular oxygen to initiate the enzymatic attack of PAH rings (2). The starting reactions in PAHs metabolism in bacteria involve oxygenases, that play a key role because of their ability in introducing oxygen onto the PAHs compounds. In the initial step, dioxygenase-catalyzed oxidation of arenes generally takes place in aerobic bacterial systems to yield vicinal cis-dihydrodiols as the early products by a multicomponent enzyme system. These dihydroxylated intermediates may then be cleaved by intradiol or extradiol ring-cleaving dioxygenases through either an ortho-cleavage pathway or a meta-cleavage pathway, leading to central intermediates such as protocatechuates or catechols that are further converted to tricarboxylic acid (TCA) cycle intermediates (3).

Dioxygenases responsible for the formation of cis-dihydrodiols appear to be ubiquitous in bacteria and have been classified accordingly to the range of carbon

Running title. PAH oxygenases

Keywords. Naphthalene, phenanthrene, oxygenase, *Pseudomonas*, *Sphingobium*

substrate, e.g. toluene (TDO), naphtalene (NDO) and biphenyl (BPDO). For lager PAHs, both NDO and BPDO are capable of catalyzing dihydroxilation, with only the latter enzyme capable of metabolizing tetracyclic or larger compounds (4).

The multicomponent naphthalene dioxygenase system has been extensively investigated especially in *Pseudomonas* strains (5), such as the archetype *Pseudomonas putida* G7, possessing the naphthalene catabolic plasmid NAH7 (6, 7), and *P. stutzeri* AN10 possessing the naphthalene-dissimilatory genes in the chromosome (8). Their naphthalene-degrading genes are organized in two operons: the upper pathway operon (*nah* operon) coding for the enzymes involved in the conversion of naphthalene to salicylate (*nahAaAbAcAdBFCED*) and the lower pathway operon (*sal* operon) coding for the conversion of salicylate to tricarboxylic acid cycle intermediates through the meta-cleavage pathway enzymes (*nahGTHINLOMKJ*) (9).

It has been observed that a high proportion of the PAH-degrading isolates in soil belong to the Sphingomonads; members of the genus *Sphingomonas* and related organisms are able to degrade a wide range of natural and xenobiotic compounds such as biphenyl, naphtalene, fluorene, phenantrene and different herbicides and pesticides (9). Sphingomonads which degrade aromatic compounds very often possess several pairs of genes coding for the large and small subunits of the ring-hydroxylating subcomplex. Different hydroxylating subcomplexes seem generally interact with only a single set of the electron transport subunits, consisting of a ferredoxin and a ferredoxin reductase. This has been initially demonstrated for the naphthalene-, biphenyl-, and toluene-degrading organism *S. yanoikuyae* B1 which contains at least seven sets of putative ring-hydroxylating subcomplexes (XylXY, BphA1a2a, BphA1b2b, BphA1c2c,BphA1d2d, BphA1e2e, and BphA1f2f) but only one copy each of the genes coding for the ferredoxin (*bphA3*) and the ferredoxin reductase (*bphA4*) (11, 12). Similar observations were also reported for the relevant genomic regions of *S. aromaticivorans* F199 (which degrades a similar range of compounds as strain B1) and of *Sphingobium* (formerly *Sphingomonas*) sp. P2 (11).

Aim of this work was the isolation and the preliminary characterization of new bacterial oxygenase from PAH-degrading bacterial strains. Attention was focused on two naphthalene degrading *Pseudomonas* sp. strains and a phenanthrene degrading *Sphingobium* sp. strain.

MATERIALS AND METHODS

Cultural conditions. The strains were grown at 30°C under shaking in mineral M9 medium supplemented with the appropriate C sources: naphthalene (400 μg/ml) was supplied as crystals; phenanthrene, at increasing concentrations, was dissolved in M9:dibutylphthalate 1:10. Growth was monitored by viable count technique or by biomass evaluation (OD 600 nm). Biofilms were obtained diluting 1:100 a 48 hr culture, grown in M9 supplemented with 5 mM glucose, in 1 ml of M9 in 12 well microplate previously coated with increasing concentrations of phenanthrene dissolved in ethanol. After 24 h of incubation at 30°C without shaking, biofilm formation was quantified by crystal violet staining: after removing the planktonic cells, the biomass was stained with 0.1% crystal violet for 15 min, washed three times with deionized water and then dissolved with 96% ethanol before determining the OD at 600 nm (13). Biofilm formation was normalized to planktonic growth by means of biofilm index (BI), which was calculated as OD of the biofilm x (OD inoculum/ OD of planktonic fraction) (14).

Molecular methods. DNA extractions were performed as indicated by SIGMA and Qiagen kits. PCR amplifications were carried out using the primers listed in Table 1. Different amplification programs were used according to annealing temperatures of each primer pair. The

Table 1. *Primers used in the present work*

Primer	Sequence	Target
NahAcF NahAcR	5'-TGGGCATGAAGAACTTTTCC-3' 5'-AACGTACGCTGAACCGAGTC-3'	*nahA* internal fragment
NahAc7F NahAc7R	5'-TGGCGATGAAGAACTTTTCC-3' 5'-AACGTACGCTGAACCGAGTC-3'	*nahA* conserved region
NDOF NDOR	5'-GAGCTCATGGAACTTCTCGTACTACCG-3' 5'-CTCGAGTCACATAAAGATCATCACATTGTGCGT-3'	*nahAabcd*
Phn321F Phn671R	5'-TTCTCGGTCGGGACTTCCAA-3' 5'- GGCAACCAGATCTGTCATG –3'	*bphA1f* conserved region
Phn2F Phn2R	5'-TTAAGCTT(HindIII)ATGAATGGATCGGCGGCACTC -3' 5'- TTGAGCTC(SacI)TTATACAAAGAAATAGAGATTCTTGTC-3'	*bphA1fA2f*
FdF FdR	5'-TTTCTAGA(XbaI)ATGTCAAACAAATTGCGACTCTGT-3' 5'-TTGGTACC(KPNI)TCATGCTGCTCCTTCGGG-3'	*bphA3*
FdRF FdRR	5'-TTGGTACC(KpnI)ATGAAATCGATAGCCGTGGTC-3' 5'-TTAAGCTT(HindIII)CTAACCAGCCTGCTTGAGGATTTC-3'	*bphA4*

entire gene clusters or each single gene were then cloned in pGEM vectors and, when required, transferred to pET vectors. *E. coli* JM109 (15) and ER2566 (New England Biolabs, USA) were used as host strains. Transformations were performed by electroporation and recombinant strains were selected on LB agar plates supplemented with ampicillin 100 μg/ml or kanamycin 50 μg/ml. Analyses of gene product were performed by SDS-PAGE after induction with 1 mM IPTG. Indole functional assays were performed with resting cells as previously reported (16).

Results and discussion

Strain characterization. Three bacterial strains, previously isolated from a polluted soil for their ability to use PAHs as the sole C and energy sources, were considered in this work and tentatively identified by 16S rDNA analysis. The two strains isolated in the presence of naphthalene (designated N1 and N2) belong to the *Pseudomonas* genus, the one isolated on phenanthrene (PhS) belongs to the genus *Sphingobium*.

Both *Pseudomonas* sp. N1 and N2 displayed a quite abundant planktonic growth on naphthalene (Fig. 1). Both strains were unable to use fluorene and phenanthrene as the sole C and energy sources, but the appearance in the cultural broth of a brown colour, becoming blackish with time, suggested a partial oxidation of these compounds.

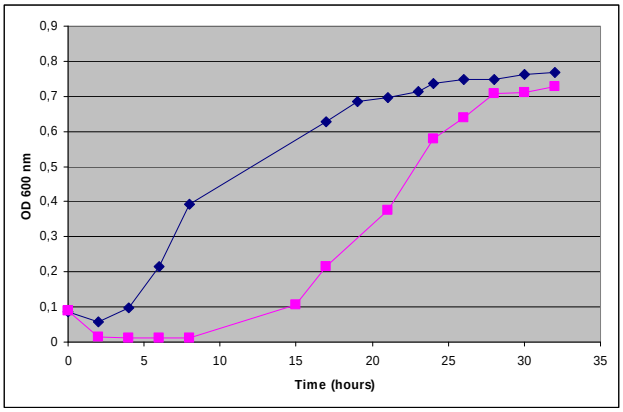

Fig. 1. Growth curves of *Pseudomonas* sp. N1 (♦) and N2 (■) in the presence of naphthalene.

Sphingobium sp. PhS displayed a phenanthrene dose-dependent growth in biphasic system: 1 mM was the tested dose that determined the higher increase in cells concentration after 3 days of incubation (Fig. 2).

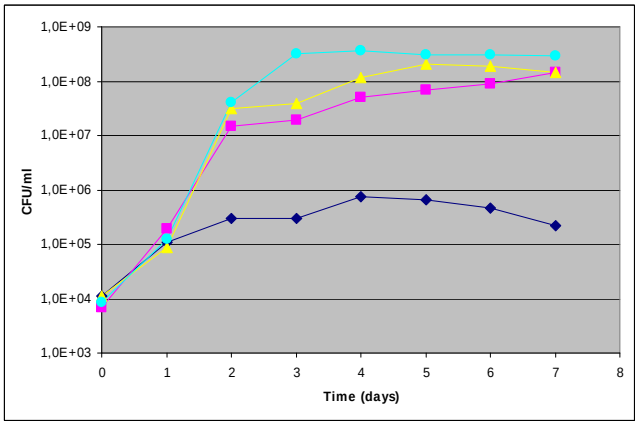

Fig. 2. Growth curves of *Sphingobium* sp. PhS in biphasic cultures without (♦) or with phenanthrene 1 mM (●), 0.5 mM (■) or 0.25 mM (▲).

Substrates range showed a good catabolic versatility of *Sphingobium* sp. PhS: phenantrene and naphthalene determined a biomass growth more evident than toluene, anthracene and fluorene ones. Among the mechanisms by which microorganisms *in vivo* may increase the bioavailability of hydrophobic substrates there are the biofilm formation and the production of cell-bound emulsifiers (17). A preliminary approach was made in order to evaluate the ability of this strain to construct biofilm. The growth in adherent form was dose-dependent: phenanthrene 4 mM determined the highest yield in biofilm formation after five days of static incubation (BI= 2) than phenanthrene 2 mM (BI= 1) and phenanthrene 1 mM (BI=0.9). A chemotactic behaviour enhances the ability of motile bacteria to locate and degrade low concentrations of toxic, but metabolizable, compounds present in contaminated environments. Preliminary soft agar plate assay showed a chemoctatic response of *Sphingobium* sp. PhS to phenanthrene.

Cloning of oxygenase encoding genes. The general strategy to clone oxygenase encoding genes from the strains cited above proceeded through the amplification and the sequencing of a small conserved region of the large subunit of the hydroxylating subcomplex, the design of new primers based on the sequences of the oxygenase showing the highest degree of homology, amplification and cloning of the amplification product.

Primers NahAcF and NahAcR allowed to amplify from strain N1 a region of approx. 1000 bp, which showed 100% homology with the one of the *nah* genes of a *P. aeruginosa* strain. An amplification product from N2 was instead obtained using the primers NahAc7F and NahAc7R; the amplicon (136 bp) showed 98% homology with the corresponding region of a *P. stutzeri* strain. Thus the NDO encoding sequences of *P. aeruginosa* and *P. stutzeri* were aligned and compared with those from other *Pseudomonas* strains in order to design primers (NDO F and NDO R) for the amplification of the entire gene cluster. The 3.5 kb amplicon was then cloned in

pGEM-T easy and sequenced. The presence of 4 ORFs highly similar to those of other *Pseudomonas* NDOs was confirmed. Preliminary functional assays, using the generic substrate indole, revealed that both enzymes are expressed and functional.

A similar strategy was used to clone peripheral oxygenases from *Shingobium* sp. PhS. The approx. 300 bp fragment, amplified with the primers Phn321F and Phn 617R, displayed a high degree of homology with the *bphA1f* gene of *N. aromaticivorans*. On these bases we could assume all the genes of *bph* series could show a similar homology. We therefore designed our primers on *bphA1fA2f* (hydroxylating subcomplex f), *bphA1aA2a* (hydroxylating subcomplex a), *bphA3* (ferredoxin) and *bphA4* (ferredoxin reductase) published sequences of *N. aromaticivorans*. We obtained amplified fragments showing a high homology (95% to 98%) with the analogous *N. aromaticivorans* genes. As the dioxygenase complex genes lay scattered on *Sphingobium* genome, so we had to clone each single gene in succession. Thanks to proper restriction sites we cloned the fragments obtained step by step into pGEM 3Z or pGEM 7Z vectors, to obtain pSG6 (*bphA3A4A1fA2f*) and pRO2 (*bphA3A4A1aA2a*) plasmids, each thus carrying the genes potentially coding for an entire enzymatic complex. The two fragments were then excised and transferred to vectors of pET series for a better protein expressions. We obtained pRO3 (*bphA3A4A1fA2f*) and pRO4 (*bphA3A4A1aA2a*) plasmids, used for expression and biotransformation experiments (Fig. 3).

However, neither the gene product analyses, nor preliminary phenanthrene biotransformation assays gave satisfactory results when pRO3 and pRO4 were transformed in *E. co*li ER2566. A detailed analysis of the sequences cloned in these two plasmids did not revealed any fault that could compromise their expression

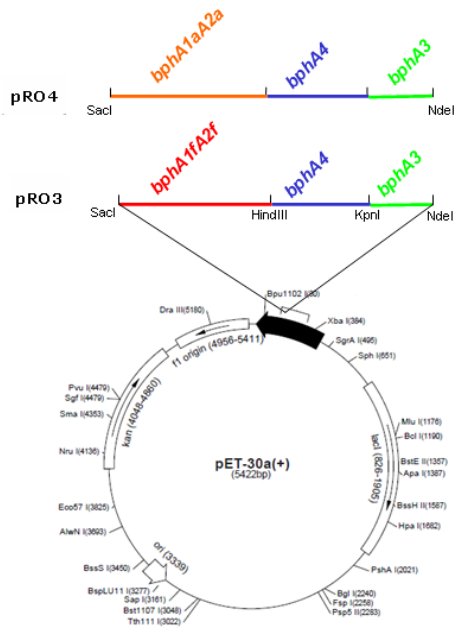

Fig. 3. Maps of pRO3 and pRO4. See text for further details.

Conclusions

The strategy exploited to clone peripheral oxygenases from PAH degrading microorganisms allowed to isolate the genes coding for two naphthalene dioxygenases highly similar to other NDOs isolated from *Pseudomonas* and two putative oxygenases potentially involved in the first step of phenanthrene catabolism. Although NDOs have been largely studied under a genetic and structural viewpoint, little information are available about their ability to oxidize substrates larger than naphthalene. Further work will thus be focused on this topic.

As regards the *Shingobium* oxygenases, till now little information is available about their expression and biochemical features. As also our attempts to express the *Shingobium* genes failed, we are now transferring both pRO3 and pRO4 in other *E. coli* strains better suited for expression and functional studies.

ACKNOWLEDGMENTS

This work was supported by grants from the Ministry of University and Research (PRIN/2007).

REFERENCES

1. **Volkering F, AM Breure, A Sterkenburg and van JG Andel**. 1992. Microbial degradation of polycyclic aromatic hydrocarbons: effect of substrate availability on bacterial growth kinetics. Appl Microbiol Biotechnol **36**: 548-552.
2. **Peng RH, AS Xiong, Y Xue, XY Fu, F Gao, W Zhao, YS, and Tian, QH Yao**. 2008. Microbial biodegradation of polyaromatic hydrocarbons. FEMS Microbiol Rev. **32**:927-55.
3. **Gibson DT and RE Parales.** 2000**.** Aromatic hydrocarbon dioxygenases in environmental biotechnology. Curr Opin Biotechnol. **11**(3):236-43.
4. **Boyd DR, ND Sharma , NI Bowers , H Dalton , MD Garrett , JS Harrison and GN Sheldrake** . 2006. Dioxygenase-catalysed oxidation of disubstituted benzene substrates: benzylic monohydroxylation versus aryl cis-dihydroxylation and the meta effect. Org Biomol Chem. **7**:3343-9.
5. **Yen KM and CM Serda.** 1988. Genetics of naphthalene catabolism in pseudomonads. Crit Rev Microbiol.**15**:247-68.
6. **Dunn NW and IC Gunsalus**. 1973. Transmissible plasmid coding early enzymes of naphthalene oxidation in *Pseudomonas putida*. J. Bacteriol. **114** :974-9.
7. **Yen KM and IC Gunsalus** 1982. Plasmid gene organization: naphthalene/salicylate oxidation. Proc Natl Acad Sci U S A. **79**:874-8.
8. **Bosch, R., E Garcia-Valdes and ER Moore,** 1999. Genetic characterization and evolutionary implications of a chromosomally encoded naphthalene-degradation upper pathway from *Pseudomonas stutzeri* AN10. Gene **236**, 149–157.
9. **Schell, M.A. and P.E Wender**. 1986. Identification of the *nahR* gene product and nucleotide sequences required for its activation of the *sal* operon. J. Bacteriol. **166**,9–14.
10. **Basta T., S. Buerger and A. Stolz** . 2005. Structural and replicative diversity of large plasmids from sphingomonads that degrade polycyclic aromatic compounds and xenobiotics. Microbiology. **151**: 2025-37.
11. **Zylstra GJ, E Kim and Goyal AK.** 1997**.** Comparative molecular analysis of genes for polycyclic aromatic hydrocarbon degradation. Genet Eng (N Y). **19**:257-69
12. **Chadhain SMN, EM. Moritz, E K,Gerben and J. Zylstra** 2007**.** Identification, cloning, and characterization of a multicomponent biphenyl dioxygenase from *Sphingobium yanoikuyae* B1. J Ind Microbiol Biotechnol (2007) **34**:605–613
13. **Christensen, G.D., W.A Simpson,., J.J. Younger, L.M Baddour, F.F. Barrett, D.M. Melton and E.H. Beachey,** 1985. Adherence of coagulase-negative staphylococci to plastic tissue culture plates: a quantitative model for the adherence of staphylococci to medical devices. J. Clin. Microbiol. **22**, 996–1006.
14. **Fabretti, F., C.Theilacker, L. Baldassarri, Z.Kaczynski, A.Kropec, O.Holst, and J**. **Huebner.** 2006. Alanine esters of enterococcal lipoteichoic acid play a role in biofilm formation and resistance to antimicrobial peptides. Infect Immun **74**, 4164–4171.
15. **Yanish-Perron C., J.,Vieira and Messing J**. 1982. The pUC plasmid and M13mp7 derived system for insertion mutagenesis and sequencing with synthetic universal primers. Gene **19**:259-268.
16. **Bertoni G., F. Bolognese, E. Galli, and P. Barbieri.** 1996. Cloning of the Genes

for and characterization of the early stages of toluene and o-xylene catabolism in *Pseudomonas stutzeri* OX1. Appl. And Env. Microbiol. **62** (10):3704-3711

17. **Johnsen AR, Y.Wick Lukas and Harms Hauke**. 2005. Principles of microbial PAH-degradation in soil. Environmental Pollution. **133**:71-84